MULTI-LAYER TRAFFIC ENGINEERING IN OPTICAL NETWORKS UNDER PHYSICAL LAYER IMPAIRMENTS

A DISSERTATION

SUBMITTED TO THE DEPARTMENT OF ELECTRICAL AND

ELECTRONICS ENGINEERING

AND THE INSTITUTE OF ENGINEERING AND SCIENCE

OF BİLKENT UNIVERSITY

IN PARTIAL FULFILLMENT OF THE REQUIREMENTS

FOR THE DEGREE OF

DOCTOR OF PHILOSOPHY

By

Namık Şengezer

August 2010

I certify that I have read this dissertation and that in my opinion it is fully adequate, in scope and in quality, as a dissertation for the degree of doctor of philosophy.

Assoc. Prof. Dr. Ezhan Karaşan(Supervisor)

I certify that I have read this dissertation and that in my opinion it is fully adequate, in scope and in quality, as a dissertation for the degree of doctor of philosophy.

Prof. Dr. Erdal Arıkan

I certify that I have read this dissertation and that in my opinion it is fully adequate, in scope and in quality, as a dissertation for the degree of doctor of philosophy.

Assoc. Prof. Dr. Nail Akar

I certify that I have read this dissertation and that in my opinion it is fully adequate, in scope and in quality, as a dissertation for the degree of doctor of philosophy.

Assist. Prof. Dr. İbrahim Körpeoğlu

I certify that I have read this dissertation and that in my opinion it is fully adequate, in scope and in quality, as a dissertation for the degree of doctor of philosophy.

Assist. Prof. Dr. Altan Koçyiğit

Approved for the Institute of Engineering and Science:

Prof. Dr. Levent Onural
Director of Institute of Engineering and Science

ABSTRACT

MULTI-LAYER TRAFFIC ENGINEERING IN OPTICAL NETWORKS UNDER PHYSICAL LAYER IMPAIRMENTS

Namık Şengezer

Ph.D. in Electrical and Electronics Engineering

Supervisor: Assoc. Prof. Dr. Ezhan Karaşan

August 2010

We study Traffic Engineering (TE) in Multiprotocol Label Switching (MPLS)/Wavelength Division Multiplexing (WDM) networks and propose a multi-layer TE method. MPLS provides powerful TE features for IP networks and is widely deployed in backbone networks. WDM can increase the transmission capacity of optical fibers to tremendous amounts, therefore it has been the dominant multiplexing technology used in the optical layer.

The proposed multi-layer TE solution facilitates efficient use of network resources where the TE mechanisms in the MPLS and WDM layers coordinate. We consider a static WDM layer and available traffic expectation information. The TE problem arising in the considered scenario is the Virtual Topology Design (VTD) problem, which involves the decision of WDM lightpaths to be established, calculation of MPLS Label Switched Paths (LSPs) on the resulting virtual topology, and calculation of the routes and wavelengths in the physical topology that correspond to the lightpaths in the virtual topology. We assume a daily traffic pattern changing with the time of day and aim to design a static

virtual topology that satisfies as much of the offered traffic as possible, over the whole day.

In our proposed solution, the multi-layer VTD problem is solved by decomposing it into two sub-problems, each involving in a single layer. The decomposition approach is used in the thesis due to the huge computational burden of the combined solution for real-life networks. The sub-problem in the MPLS layer is the design of the lightpath topology and calculation of the LSP routes on this virtual topology. This problem is known to be NP-complete and finding its optimum solution is possible only for small networks. We propose a Tabu Search based heuristic method to solve two versions of this problem, resource oriented and performance oriented. Integer Linear Programming (ILP) relaxations are also developed for obtaining upper and lower bounds. We show that the gap between the produced solutions and the lower and upper bounds are around 10% and 7% for the resource and performance oriented problems, respectively.

Since the actual traffic can show deviations from the expected values, we also developed an MPLS layer online TE method to compensate the instantaneous fluctuations of the traffic flows. In the proposed method, the LSPs are rerouted dynamically using a specially designed cost function. Our numerical studies show that using the designed cost function results in much lower blockings than using commonly used Widest Shortest Path First and Available Shortest Path First approaches in the literature.

The corresponding sub-problem of the multi-layer VTD problem in the WDM layer is the Static Lightpath Establishment (SLE) problem. Along with the capacity and wavelength continuity constraints, we also consider the Bit Error Rate (BER) constraints due to physical layer impairments such as attenuation, polarization mode dispersion and switch crosstalk. This problem is NP-complete even without the BER constraints. We propose a heuristic solution method and develop an exact ILP formulation to evaluate the performance of the proposed

method for small problem sizes. Our proposed method produces solutions close to the optimum solutions for the cases in which the ILP formulation could be solved to optimality.

Then, these solution methods for the single layer sub-problems are combined in a multi-layer TE scheme to solve the VTD problem in both layers jointly. The proposed TE scheme considers the physical layer limitations and optical impairments. This TE scheme can be applied by keeping each layer's information hidden from the other layer, but our simulations show that it can produce more effective and efficient solutions when the physical layer topology information is shared with the MPLS layer. We also investigate the effect of non-uniform optical components in terms of impairment characteristics. The numerical results show that more traffic can be routed when all the components in the network have moderate impairment characteristics, compared to the case in which some components have better and some have worse impairment characteristics.

Keywords: Traffic Engineering, Optical Networks, MPLS, WDM, Physical Layer Impairments, Virtual Topology Design, Lightpath Establishment Problem

ÖZET

OPTİK AĞLARDA FİZİKSEL KATMAN BOZUKLUKLARI ALTINDA ÇOK KATMANLI TRAFİK MÜHENDİSLİĞİ

Namık Şengezer

Elektrik ve Elektronik Mühendisliği Bölümü Yüksek Lisans

Tez Yöneticisi: Doç. Dr. Ezhan Karaşan

Ağustos 2010

Bu araştırmada Çoklu Protokol Etiket Anahtarlaması (Multiprotocol Label Switching MPLS)/Dalga Boyu Bölüşümlü Çoğullama (Wavelength Division Multiplexing: WDM) ağlarında trafik mühendisliği (Traffic Engineering: TE) incelenmiş ve çok katmanlı bir TE yöntemi önerilmiştir. MPLS, IP ağları için güçlü TE özellikleri sağlamaktadır ve omurga ağlarda yaygın olarak kullanılmaktadır. WDM, optik fiberlerin iletim kapasitesini çok yüksek miktarlara çıkarabilir, bu yüzden optik katmanda kullanılan hakim çoğullama teknolojisidir.

Önerilen çok katmanlı TE çözümü, ağ kaynaklarının MPLS ve WDM katmanlarındaki TE mekanizmalarının eşgüdümlü çalıştığı verimli kullanımına olanak sağlamaktadır. Sabit bir WDM katmani ve trafik beklentisinin önceden mevcut olduğu farzedilmiştir. Ele alınan senaryoda ortaya çıkan TE problemi, Sanal Topoloji Tasarımı (Virtual Topology Design: VTD) problemidir ve kurulacak WDM ışıkyollarının belirlenmesi, MPLS Etiket Anahtarlamalı Yollarının (Label Switched Path: LSP) ortaya çıkan sanal topolojide yönlendirilmesi ve fiziksel topoloji üzerinde sanal topolojıdeki ışıkyollarına karşılık gelen yol ve dalgaboylarının hesaplanmasını içerir. Gün içinde saate göre değişen bir trafik modeli

farzedilmiştir ve amaç tüm gün boyunca sunulan trafiğin mümkün olduğunca çoğunu karşılayan sabit bir sanal topoloji tasarlamaktır.

Önerilen çözümde çok katmanlı VTD problemi, her biri tek bir katmana karşılık gelen iki alt probleme ayrıştırılarak çözülmektedir. Bu tezde kullanılan ayrıştırma yaklaşımının sebebi, birleşik çözümün gerçek ağlar için getirdiği büyük hesaplama yüküdür. MPLS katmanındaki alt problem ışıkyolu topolojisinin tasarımı ve sanal topoloji üzerindeki LSP yollarının hesaplanmasıdır. Bu problemin NP-tam olduğu bilinmektedir ve en iyi çözümünün bulunması yalnızca küçük boyutlu ağlar için olanaklıdır. Bu problemin kaynak yönelimli ve başarım yönelimli olmak üzere iki versiyonunu çözmek için Tabu Araştırmaya dayalı buluşsal bir yöntem geliştirilmiştir. Alt ve üst sınırlar elde etmek için Tamsayılı Doğrusal Programlama (Integer Linear Programming: ILP) gevşetimleri de geliştirilmiştir. Üretilen çözümler ile alt ve üst sınırlar arasındaki farkın kaynak ve başarım yönelimli problemler için sırasıyla %10 ve %7 civarında olduğu gösterilmiştir.

Gerçek trafik beklenti değerlerinden sapmalar gösterebileceği için trafik akımlarındaki dalgalanmaları dengelemek amacıyla MPLS katmanında çalışan bir çevrimiçi TE yöntemi de geliştirilmiştir. Önerilen yöntemde LSP'ler özel tasarlanmış bir gider fonksiyonu kullanılarak dinamik bir şekilde yeniden yönlendirilmektedir. Sayısal sonuçlar, tasarlanan gider fonksiyonunun kullanımının literatürde yaygın olarak kullanılan İlk Önce En Geniş En Kısa Yol ve İlk Önce Uygun En Kısa Yol yaklaşımlarının kullanımından çok daha düşük engellemelere yol açtığını göstermektedir.

Çok katmanlı VTD probleminin WDM katmanına karşılık gelen alt problemi Sabit Işık Yolu Kurulumu (Static Lightpath Establishment: SLE) problemidir. Kapasite ve dalgaboyu sürekliliği kısıtları ile beraber zayıflama, polarize mod saçılımı ve anahtar çapraz girişimi gibi fiziksel katman bozukluklarından kaynaklanan Bit Hata Oranı (Bit Error Rate: BER) kısıtları da göznüne alınmıştır.

Bu problem, BER kısıtları olmadığı durumda bile NP-tamdır. Buluşsal bir çözüm yöntemi önerilmiş ve eksiksiz bir ILP formülasyonu geliştirilmiştir. Önerilen yöntem, en iyi çözümlerin ILP formülasyonu çözülerek bulunabildiği durumlarda en iyi çözümlere yakın çözümler üretmektedir.

Daha sonra, tek katmanlı alt problemler için önerilen bu çözüm yöntemleri, her iki katmandaki problemleri birleşik olarak çözmek için çok katmanlı bir TE tasarımında birleştirilmiştir. Önerilen TE tasarımı, fiziksel katman kısıtlamalarını ve optik bozulmaları göz önünde bulundurmaktadır. Bu TE tasarımı, her katmanın bilgilerini diğer katmandan saklı tutarak uygulanabilmektedir fakat benzetimler göstermektedir ki fiziksel katman bilgisi MPLS katmanıyla paylaşıldığında daha verimli ve etkili çözümler üretebilmektedir. Bozulma özellikleri açısından birörnek olmayan optik bileşenlerin etkisi de incelenmiştir. Sayısal sonuçlar, ağdaki bütün bileşenlerin makul ölçüde bozulma özelliklerine sahip olduğu durumlarda bazı bileşenlerin daha iyi, bazılarının ise daha kötü bozulma özellikleri olduğu duruma gore daha fazla trafiğin yönlendirilebildiğini göstermektedir.

Anahtar Kelimeler: Trafik Mühendisliği, Optik Ağlar, MPLS, WDM, Fiziksel Katman Bozuklukları, Sanal Topoloji Tasarımı, Işıkyolu Kurulum Problemi

ACKNOWLEDGMENTS

I would like to express my sincere thanks to my supervisor Assoc. Prof. Dr. Ezhan Karaşan for his guidance, support, and encouragement during the course of this research.

I would also like to thank Prof. Dr. Erdal Arıkan, Assist. Prof. Dr. İbrahim Körpeoğlu, Assoc. Dr. Nail Akar and Assist. Prof. Dr. Altan Koçyiğit for reading and commenting on the thesis.

Thanks to my dear friends and colleagues Ahmet Serdar Tan, Ayça Özçelikkale Hünerli, Gökhan Bora Esmer, Kıvanç Köse and Mehmet Köseoğlu for their invaluable help.

Finally, I would like to express my deepest gratitude to my family and my wife Duygu for her endless love and patience. I could not succeed without her support.

Contents

List of Figures

List of Tables

List of Abbreviations

ASE   Amplified Spontaneous Emission

ASP   Available Shortest Path

ATM   Asynchronous Transfer Mode

BER   Bit Error Rate

BUTE   Budapest University of Technology and Economics

BXQC   Branch Exchange with Quality of service Constraints

COLD   Collaborative Lightpath Topology Design

CSPF   Constrained Shortest Path First

DCF   Dispersion Compensating Fiber

DRA   Distributed Raman Amplifier

DREAM   Dynamic Rerouting Algorithm

DTAG   Deutsche Telekom AG

E-MB   Exhaustive Minimum BER

E-MMB   Exhaustive Minimum Maximum BER

FEC   Forward Error Correction

FEC   Forwarding Equivalence Class

FFB	First Fit with BER
FWM	Four Wave Mixing
GMPLS	Generalized MPLS
IGP	Interior Gateway Protocol
ILF	IP/MPLS Layer First
ILP	Integer Linear Programming
IP	Internet Protocol
IS1	Interaction Strategy 1
IS2	Interaction Strategy 2
IS3	Interaction Strategy 3
ISI	Inter-Symbol Interference
LAN	Local Area Network
LC	Low-load Cost
LCPF	Least Critical Path First
LDF	Longest Demand First
LERO	Lightpath Establishment without Reordering
LERR	Lightpath Establishment without Rerouting
LLT	Low-Load Threshold
LSP	Label Switched Path
LSR	Label Switched Router
MB	Minimum BER

MC	Medium-load Cost
MILP	Mixed Integer Linear Programming
MIRA	Minimum Interface Routing Algorithm
MMB	Minimum Maximum BER
MPLS	Multiprotocol Label Switching
MVTD	Multi-layer Virtual Topology Design
OLF	Optical Layer First
OSNR	Optical Signal to Noise Ratio
OXC	Optical Cross-Connect
PBR	Profile Based Routing
PLIA	Physical Layer Impairment Aware
PMD	Polarization Mode Dispersion
POLIO	Pre-Ordering Least Impact Offline
QoS	Quality of Service
ROLE	Reordered Lightpath Establishment
RS	Random Search
RSVP	Resource Reservation Protocol
RWA	Routing and Wavelength Assignment
SDF	Shortest Demand First
SLA	Service Level Agreement
SLE	Static Lightpath Establishment

SP	Shortest Path
SPF	Shortest Path First
SPM	Self Phase Modulation
SSMF	Standard Single Mode Fiber
SVTD	Single-layer Virtual Topology Design
SWPF	Shortest Widest Path First
TE	Traffic Engineering
TES-1	Traffic Engineering Strategy-1
TES-2	Traffic Engineering Strategy-2
VTD	Virtual Topology Design
VTDT	Virtual Topology Design Tool
WAN	Wide Area Network
WDM	Wavelength Division Multiplexing
WGT	Wavelength Graph Tool
WRN	Wavelength Routing Node
WRS	Wavelength Routing Switch
WSP	Widest Shortest Path
WSPF	Widest Shortest Path First
XCS	Cross- Connect Switch
XPM	Cross Phase Modulation

Dedicated to My Most Precious Treasure in Life,

My Dear Wife...

Chapter 1

Introduction

Most of the traffic carried in the telecommunication networks today is originated from Internet based services. With the migration of more and more services to the Internet Protocol (IP), Internet traffic is foreseen to increase its dominance in the future networks. However, as the Internet traffic grows day by day, the revenue coming from the Internet services does not increase at the same rate and the revenue per unit traffic decreases. In fact, currently revenue from voice-based services is generally much higher than the revenue from Internet services [1]. The typical approach taken by the telecom operators to accommodate the increasing traffic is the overprovisioning of resources, which is not a cost effective solution. Moreover, if the networks are to be upgraded by adding more bandwidth and infrastructure with the same rate as the traffic increases, the costs will exceed the revenue [2]. The solution to this dilemma is to design cost effective and flexible networks that use resources efficiently, which is achieved by Traffic Engineering (TE).

Traffic engineering is mainly defined as "aspect of Internet network engineering dealing with the issue of performance evaluation and performance optimization of operational IP networks" [3]. Performance optimization can be accomplished by capacity and traffic management. Capacity management involves capacity planning, routing control and resource management. Traffic management includes functions such as admission control, queuing and scheduling and other functions controlling access to the network resources. Different types of TE applications aim performance optimization within different time scales. Capacity planning usually focuses on time scales ranging from days to years. Routing control actions operate at time periods from milliseconds to days. Packet level processing functions such as admission control and queue management act in very small time periods, ranging from picoseconds to milliseconds [3].

TE can be performed in IP networks effectively by deploying Multiprotocol Label Switching (MPLS) under the IP layer [4]. MPLS was introduced to address the shortcomings of the shortest path based IP routing which forwards packets according to the destination address only and uses mostly fixed and traffic characteristic independent routes [5]. With IP routing, links on the shortest paths between certain node pairs may get congested while there are lightly loaded links on other alternative paths, and bottlenecks may be created. MPLS brings explicit routing capability by integrating label swapping forwarding paradigm with network layer routing. Thus, it eliminates the dependency to shortest path routing and allows a more efficient use of network resources. It can also set up bandwidth guaranteed Label Switched Paths (LSPs) to route the traffic, to satisfy the Quality of Service (QoS) requirements stated in customer service-level agreements (SLAs).

The high traffic requirements of IP based services are accommodated in the transport networks by using optical transmission technologies that provide enormous bandwidth. The dominant multiplexing technology used in the transport layer in today's optical networks is the Wavelength Division Multiplexing (WDM). With WDM, by multiplexing different data streams at different wavelengths, the transmission capacity of a single optical fiber can be increased to tremendous values, in the order of several Tb/s. In the first-generation optical networks, WDM layer was used to constitute links between the nodes at the two ends of the fiber optic cables. In this approach, the optical signals at each wavelength are converted into electronic domain at the end of the fiber, using a separate optical transceiver/receiver pair for each wavelength. As the number of wavelengths supported by the fiber optic cables increased, this approach became infeasible due to the high cost and space requirements of the optical transceivers. With the availability of all-optical cross connects (OXCs) and amplifiers, the emerging solution to this problem is setting up all-optical connections between the source and destination nodes of the traffic and bypassing the intermediate nodes. These all-optical end-to-end connections are called lightpaths. However, WDM technology has its own limitations. Lightpaths need to be assigned fixed wavelengths on all the links along their paths, unless very expensive wavelength converters are used. Furthermore, the impairments resulting from the optical components along the route of a lightpath have a cumulative effect and may cause high Bit Error Rates (BERs), making communication through the lightpath infeasible. These limitations need to be taken into account when establishing lightpaths in the WDM layer.

Because of this multi-layered structure of optical networks, requirements and performance criteria arising in each of the layers should be considered when performing TE. The bandwidth capacity of a lightpath is typically much higher than the bandwidth requirements of MPLS Label Switched Paths. Therefore, the lower granularity LSP connections should be 'groomed' into the high capacity

lightpaths. Consequently, the lightpaths of the WDM layer make up the links of the virtual topology seen by the MPLS layer. In a multi-layer traffic engineering scenario covering both MPLS and WDM layers, the TE decisions include the lightpaths that should be established, the routes of the MPLS layer LSPs on the resulting virtual topology and the physical route and wavelength assigned to each of the lightpaths.

With the deployment of all-optical network components more and more widely and use of WDM to establish end-to-end all-optical connections in today's optical networks, the multi-layer aspect of traffic engineering gains more importance. A typical single layer TE approach does not consider the WDM layer requirements when performing capacity planning in the MPLS layer. The assumption of such an approach is that the WDM layer can provide any amount of lightpath connections between any two nodes in the network. However, as lightpaths traverse multiple fibers, wavelength and BER constraints become the limiting factors in the WDM layer. A virtual topology, i.e., the lightpath topology, which is designed without considering wavelength constraints and physical impairments of the WDM layer may not be feasible in the physical layer because of the insufficient number of wavelengths to assign each of the lightpaths, or the high BERs of the lightpaths that should be established. Conversely, if the lightpaths to be established are decided without considering the traffic requirements of the MPLS layer, the resulting virtual topology will not be suitable to accommodate the traffic introduced by the MPLS layer. As a result, both of the MPLS and WDM layers should be considered jointly for a realistic and effective traffic engineering solution. On the other hand, a multi-layer approach also increases the complexity. Consideration of both layers together increases the number of constraints and the decision variables in the TE problem. In addition, control layer communication should be provided between the equipments belonging to different layers.

In this study, we propose a multi-layer solution for traffic engineering in MPLS/WDM networks. The lightpaths to be established and the resulting WDM layer virtual topology are assumed to be static. We assume that the traffic pattern in the network changes with the time of day and that traffic information for each traffic source destination pair is available in the form of expected traffic in each hour. The resulting problem is the multi-hour virtual topology design problem. In the solution method we propose for this problem, the MPLS and WDM layers work interactively to produce feasible solutions that satisfy all the constraints arising in both layers. To cope with the instantaneous variations in the traffic, we also propose a dynamic MPLS layer TE scheme based on LSP reroutings. In the following section, the transport network architecture considered in this thesis is explained.

1.1 Components of Contemporary Transport Networks

In MPLS, the routers with label switching functionality are called Label Switched Routers (LSRs). In an MPLS/WDM network, the packets that are originated from the networks running IP, enter the MPLS core network through the Edge LSRs. Each LSR is connected to an OXC switch. The electronic data is converted into the optical domain through the optical transceivers between LSRs and OXCs and travels along a single lightpath in the optical domain until it is converted back into electronic domain at the OXC at the end of the lightpath. Lightpaths can traverse multiple fibers in the physical layer. Each lightpath in the WDM layer is seen as a single link by the MPLS layer, and the total of lightpaths make up the virtual topology seen by the MPLS layer. Figure 1.1 depicts a typical example of an MPLS/WDM layered transport network.
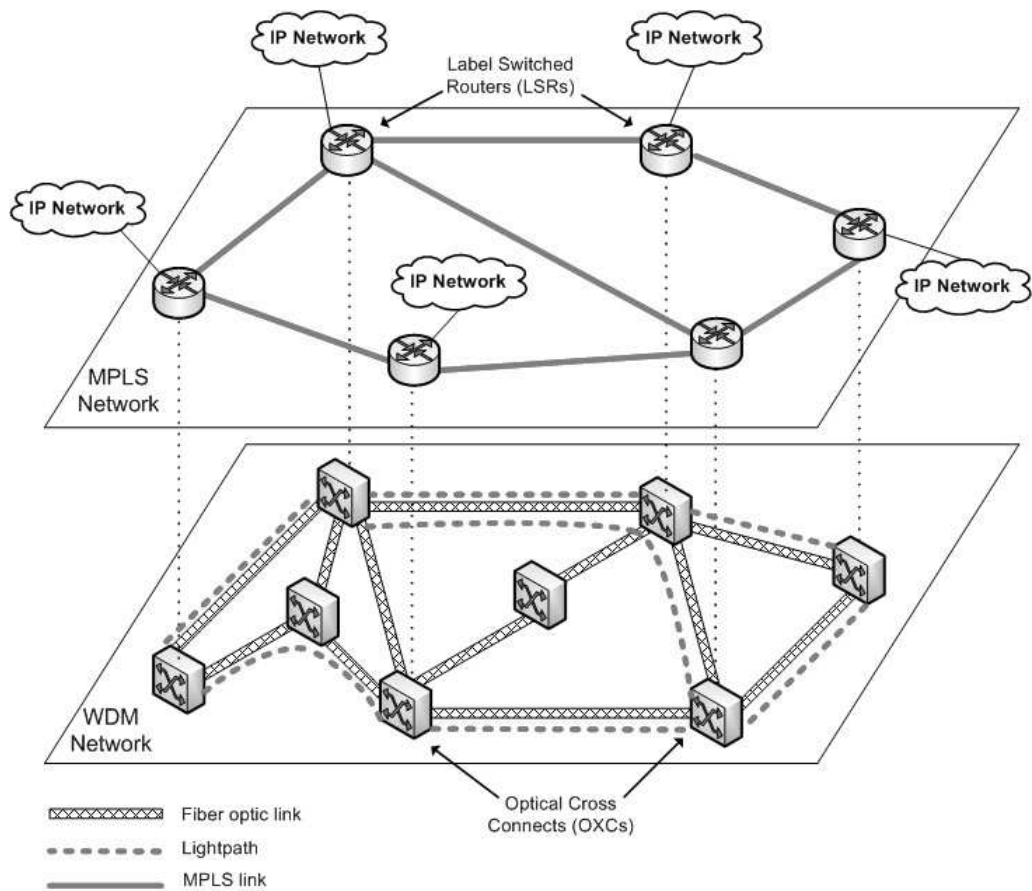
Figure 1.1: An example of MPLS/WDM transport network

1.1.1 Multiprotocol Label Switching (MPLS)

Multiprotocol Label Switching is a forwarding paradigm that integrates network routing with a label swapping frame. As the term 'Multiprotocol' suggests, its techniques are applicable to any network layer protocol, however in this study, being the most dominant network layer protocol, the assumed network layer protocol is IP, as in the most of the literature.

In connectionless network layer protocols, the packets are partitioned into 'Forwarding equivalence classes (FECs)' and each FEC is mapped to a next hop. In the forwarding scheme of IP, the packets are assigned to FECs according to the longest matching prefix of the packet's destination address with the addresses in the routing table. Hence, in an IP router, any two packets with the same destination is assigned to the same FEC. In each of the hops the packet traverses,

6

its destination address is examined and it is assigned to a new FEC. In MPLS, this assignment to a particular FEC is done just once when the packet enters the MPLS network. This assignment is done by LSRs through which the packet enters the MPLS network, by appending it a short fixed length value known as a label. In the consecutive hops, the label is used as index into a table that determines the next hop of the packet and a new label to assign. The old label of the packet is replaced with the new label, and it is forwarded to the next hop [6].

MPLS architecture provides powerful features for TE [4]. The encapsulated IP packets can be routed explicitly along virtual connections called Label Switched Paths. The explicit routing capability in MPLS combined with enhanced link state interior gateway protocols (IGPs) and resource reservation protocol (RSVP), enables the routing of the traffic flows considering both the quality of service and bandwidth requirement of the traffic flows and current network state such as traffic load and available capacity on the links. The extensions to RSVP allow the dynamic updates of the LSP bandwidth and construction of new explicit route before tearing down the old route, which enables LSP reroutings without disrupting traffic flows [7, 8].

1.1.2 Wavelength Division Multiplexing (WDM)

Wavelength Division Multiplexing is a prevailing multiplexing technology for optical communications and is widely used in Wide Area and Metropolitan Area optical networks today. WDM divides the bandwidth capacity of a single fiber into multiple channels and thus increases fiber's transmission capacity greatly. With large number of wavelengths, it is not feasible to equip each node in the network with an optical transceivers for each of the wavelength channels because of the high cost and space requirements of optical transceivers. This problem is

solved using wavelength selective Optical Cross Connect switches, which can optically switch the incoming data at a wavelength channel in an incoming fiber to another channel using the same wavelength in an outgoing fiber. Thus, the need for optical to electronic and back to optical conversion of data is eliminated for the traffic passing through a node. The result is end-to-end optical connections that can traverse multiple fibers, that are called lightpaths.

The WDM technology imposes certain constraints on the lightpaths. A lightpath should occupy the same wavelength in all-optical fibers it traverses. This is called the wavelength continuity constraint. Although wavelength continuity constraint can be removed by using wavelength interchanging OXCs that employ wavelength converters, this usage is prohibitive due to high equipment cost. Any two lightpaths passing through a common optical fiber cannot be assigned the same wavelength. Therefore, the number of lightpaths that can occupy the same wavelength on an optical link is bounded by the number of optical fibers on that link. This rule forms the capacity constraint. The problem of finding a route for a lightpath on the physical topology and assigning it a wavelength that is unoccupied on all the links along this route is called the Routing and Wavelength Assignment (RWA) problem.

Wavelength continuity and capacity constraints are not the only constraints that need to be considered in the WDM layer, when establishing lightpaths. Optical layer is not a perfect transmission medium and there are physical phenomena distorting the optical signal quality as the signal passes through imperfect optical components. These phenomena are called physical layer impairments. Detailed information on physical layer impairments is given in Chapter 5. Due to the physical layer impairments, the BER experienced by the optical communication through a lightpath may rise to a level above the acceptable threshold for successful communication. During RWA, the physical layer impairments should also be considered and the resources should be allocated in a way to guarantee that

the BER along each of the established lightpaths remains within the acceptable limits. This is called the BER constraint. In a realistic solution for the RWA problem, the BER constraint should also be taken into account.

1.1.3 Interoperation Among Layers of Transport Networks

The multi-layered structure of optical networks raises the issues of on which layer traffic engineering should be applied and how. There are three commonly accepted models proposed by IETF for the interoperation of the MPLS and optical layers: overlay, peer and augmented [9]. In the overlay model, the control planes of the MPLS and optical networks are separated. The interaction between these layers is in a client/server relation. MPLS layer requests lightpaths from the optical layer, which make up the virtual topology seen by the MPLS layer. In the peer model, a single control plane is deployed over the MPLS and optical layers and has access to information of and control over both layers. In the third, augmented model, routing on each layer is controlled by the control plane of that layer, but certain information can be shared between the control planes to make better use of the network resources [9].

Having a complete view of both layers, the peer model is more promising in optimization and efficient usage of network resources. However, the control plane needs to collect and manage significantly more information, and problems of interoperability arise in inter-provider scenarios [10]. On the other side, the overlay model has the drawback of not using the network resources as efficient as in the peer model. Nevertheless, separate management and control of MPLS and optical layers can be preferable by the operators to ensure the privacy of each layer, and it is more realistic and easier to implement with today's technology [11].

The traffic engineering scheme we propose can be applied under all of these interoperation models. Nevertheless, as shown in Chapter 6, when applied in the augmented and peer models, significantly better performance can be achieved by sharing the WDM layer connectivity information with the MPLS layer.

1.2   Virtual Topology Design (VTD) Problem

As stated at the beginning of this chapter, since the bandwidth capacity of a lightpath is typically much higher than the bandwidth requirements of LSPs, the LSP connections should be 'groomed' into lightpaths. The lightpaths established in the WDM layer make up the links of the virtual topology seen by the MPLS layer. The problem of designing this virtual topology is referred as the Virtual Topology Design (VTD) Problem. When considered in a multi-layer context, the variables that should be decided in the VTD problem include the lightpaths that should be established, the routes of the MPLS layer LSPs on the resulting virtual topology, and calculation of the routes and wavelengths in the physical topology that correspond to the lightpaths in the virtual topology. Figure 1.2 visualizes two separate virtual topologies constructed on the same physical topology. As
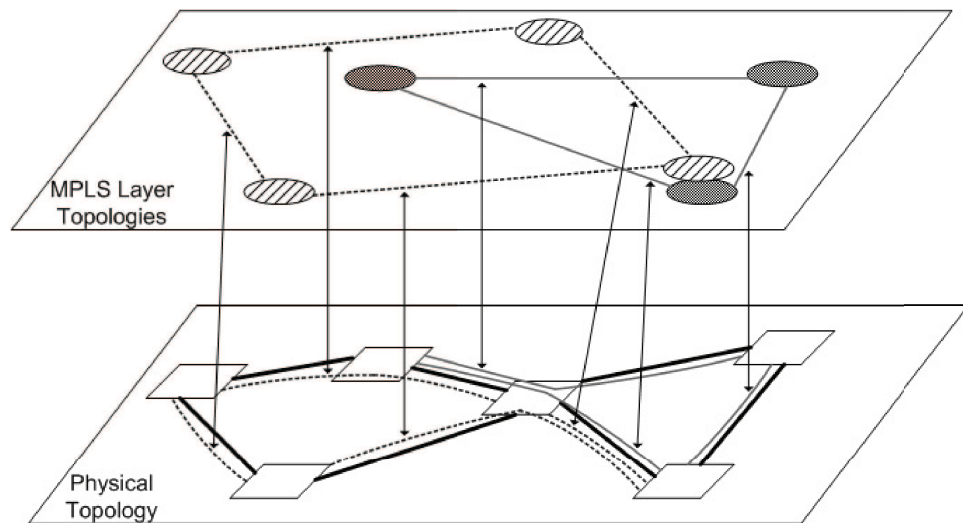
Figure 1.2: Two virtual topologies constructed on the same physical topology (The arrows map the virtual topology links to their routes in the physical layer)

VTD problem involves multiple layers, it can be decomposed into smaller sub-problems each involving a single layer. The problem of deciding the lightpaths to establish and the routes of the LSPs on the lightpaths corresponds to the MPLS layer. To avoid confusion, in the rest of this thesis, the decomposed problem will be referred as the Single layer VTD (SVTD) problem, and the complete VTD problem involving multiple layers will be referred as the Multi-layer VTD (MVTD) problem. The problem corresponding to the WDM layer is the establishment of the lightpaths of the designed virtual topology. This problem is referred as the Static Lightpath Establishment (SLE) problem. SVTD and SLE problems need to be solved together to produce a feasible solution to the MVTD problem.

The traffic in a network changes substantially in time. This change displays a pseudo-periodic behavior in different time scales (daily, weekly, monthly, etc.) [12, 13]. On the daily basis, there may be large differences between the traffic in different hours of the day; and the resulting daily traffic pattern is relatively similar for different days [13, 14, 15]. Based on this pseudo-periodic behavior of the traffic, the network operator can predict the offered traffic in different time periods during the day and use this information for a more efficient management of the network [12]. In local area networks (LANs), the busy hours for the traffic flows (aggregated traffic between two nodes) coincide and network management can be done according to the most busy hour traffic. For wide area networks (WANs), networks that are spread over a large geographical area, the busy hours will depend on the time zones of the nodes generating traffic and it is likely that one traffic flow will be in its busiest period, while another is in a more 'quiet' period [16]. Using this fact, it is possible to design a single configuration that will enable the network operator to satisfy the offered traffic using fewer resources compared to a pessimistic design based on the most busy hours [16, 17].

We assume a daily traffic pattern in our study and aim to design a static virtual topology that satisfies as much of the offered traffic during whole day, as possible. The term 'static' is used in the sense that the virtual topology will stay fixed during larger time periods compared to the considered time scale, e.g., at least weeks or months for a daily time scale. This problem is referred as the Multi-hour VTD problem in the literature (multi-hour, virtual topology design and flow routing). Changes in the traffic pattern in larger time scales are out of the scope of this study. Nevertheless, these changes can be treated as a change in the traffic expectations and our solution can be used to design a new virtual topology based on the new expectations.

In the scenario we consider in this thesis, the designed lightpath topology (i.e., virtual topology) remains fixed for large periods of time. Our assumption is that, the WDM layer is not able to provide dynamic lightpath connections that can be set up and torn down on demand in very small periods of time (in the order of milliseconds), which is consistent with today's technological conditions. There has been considerable research on dynamic lightpath establishment over recent years [18, 19, 20, 21]. Today, although dynamic establishment of lightpaths has been realized in laboratory conditions and on test networks for experimental purposes, a fully dynamic global lightpath topology is not possible [22].

Even in a scenario in which the whole network is deployed with a technology that can provide 'instant' lightpath connections, the benefits of using dynamic lightpaths over using static lightpaths are controversial. Studies comparing the two approaches directly [23, 24, 25, 26] report contradictory results since the results depend on the specific topologies, architectures and traffic characteristics [27]. It is stated in [23, 26, 27] that, the advantages of dynamic lightpath establishment (in terms of cost) are observed only for low loads and sparsely connected networks. [24] and [25] report that static establishment that make use of priori known traffic matrices needs less network resources to satisfy all the connections,

when compared with a dynamic lightpath establishment case, in which routing decisions are done dynamically based on the instantaneous situation of network.

In the case of availability of dynamic lightpath establishment, another solution approach to multi-hour VTD problem would be designing different topologies for different time periods and periodically reconfiguring the virtual topology. However, in such an approach, the traffic will be disrupted in the reconfiguration instances and the transitions from one configuration to another will raise another problem, since it will not be acceptable to tear down all the lightpaths and establish them according to the new configuration. Furthermore, some studies show that, the cost savings of such an approach is minimal and using the knowledge of the traffic matrices and with a careful planning, it is possible to design a static topology achieving almost the same performance with a reconfigurable one [12, 16, 17]. Our findings that are reported in the Section 4.1 also show that, even if instant reconfiguration of the virtual topology without disrupting the traffic flows is assumed to be possible, the same performance can be achieved on a static virtual topology using about 12% more network resources. In addition, the charging policies for static and dynamic lightpaths should be expected to be different and it is reasonable to assume that the per hour price of a static lightpath connection would be lower than the price of a dynamic one [28]. Therefore, even using less network resources, the cost effectiveness of a reconfigurable virtual topology is disputable from the MPLS layer operator's point of view. As a result, it can be concluded that static virtual topology design will remain as an important traffic engineering problem even in the availability of fully dynamic lightpaths.

1.3 Contributions of the Thesis

In this thesis, we develop a multi-layer TE scheme for MPLS/WDM networks. The most important contribution of the proposed scheme is that, it considers requirements of both layers and satisfies the constraints in each of the layers, while aiming to optimize the overall network performance. If the WDM layer wavelength constraints and physical layer impairments are not considered in planning of the MPLS layer links and their capacities, it may not be possible the establish the resulting virtual topology in the physical layer. The impact of these constraints becomes more significant as more multi-hop lightpath connections are established in today's networks; and ignoring or relaxing these constraints may result in infeasible solutions. Therefore, an effective and applicable TE solution should satisfy the requirements of multiple layers, and the network operators need to consider both layers jointly when performing TE.

Another significant feature of our proposed TE scheme is that, it responds to traffic changes in different time scales. While the virtual topology is designed in a multi-layer and offline fashion with the consideration of the daily traffic pattern, a dynamic MPLS layer TE method is proposed to compensate the instantaneous traffic fluctuations, since MPLS allows reconfiguration of the traffic flow routes without disrupting the remaining traffic flows.

To the best of our knowledge, this is the first study that solves the Multi-hour VTD problem while satisfying the wavelength continuity and BER constraints of the WDM layer. Previous studies on Multi-hour VTD problem either assume full wavelength conversion capability at every node [12] or assume unlimited number of wavelengths and relax the constraints in the WDM layer [29], or completely ignore the limitations of the underlying optical layer [17]. There are very few works studying the VTD problem in the presence of physical layer impairments, and they assume a static traffic pattern and a single traffic matrix. In these

studies, physical layer impairments are modeled as a constraint on the physical length of the established lightpaths [30, 31] or as a fixed cost component for each of the fiber links [32]. These approaches simplify the problem but exclude the impairments resulting from the interaction of wavelength channels and depend on the allocation of resources, such as crosstalk. Our proposed TE scheme considers the aggregate effect of all physical impairments also including node crosstalk, and produces solutions that are fully feasible according to the assumed physical layer model. It can be applied under both overlay, augmented and peer interoperation models, but has a better performance under augmented and peer models.

Because of its complexity, the multi-hour VTD problem is solved by decomposing it into smaller sub-problems, even in the simplified versions that do not consider physical layer constraints [33]. In our solution methodology, we decompose the problem into two sub-problems, each involving a single layer. First we study the Single layer VTD (SVTD) problem and propose Tabu Search based topology design algorithms for two versions of the problem, as resource oriented and performance oriented. We also develop Integer Linear Programming (ILP) formulations to evaluate the performance of the proposed algorithms. In this phase, since the WDM layer constraints are not considered and it is assumed that the WDM layer will be able to construct any virtual topology that is designed, this is a single layer approach involving the MPLS layer. Comparing their solutions with the upper bounds produced by solving the ILP formulations, we show that our heuristic algorithms have quiet good performance. The gap between the produced solutions and the lower bounds is around 10% for the resource oriented problem; the gap between the produced solutions and the upper bounds are around 7% for the performance oriented problem.

In a realistic scenario, the traffic flows may not fit to the expected values exactly and exhibit some amount of deviation. To cope with these deviations we propose an online TE mechanism, Dynamic Rerouting Algorithm (DREAM),

based on rerouting of MPLS layer LSPs. DREAM can be applied with a distributed fashion and the traffic flows will not be disrupted by the use of 'make before break' function provided by MPLS. We develop a dynamic cost function to use when calculating the LSP routes. We show that use of this cost function results in lower blocking ratios than the Available Shortest Path First (ASP) approach and the Widest Shortest Path First (WSP) approach that is reported to have a good performance, in the literature.

Then, we address the corresponding problem of MVTD in the WDM layer, Static Lightpath Establishment problem. We propose a polynomial time heuristic solution for the SLE problem: ReOrdered Lightpath Establishment (ROLE). We investigate the performance of ROLE and compare it with a recently proposed heuristic algorithm Pre-Ordering Least Impact Offline-RWA (POLIO-RWA), which is shown to perform better than previously proposed heuristic solutions [34]. We also develop an ILP formulation for the SLE problem subject to physical layer impairments. In the developed formulation, the aggregated effect of physical impairments is considered and hard constraints are imposed to guarantee that BERs along established lightpaths are below the chosen threshold. This ILP formulation is used as a performance benchmark for ROLE on smaller size networks, and for providing upper bounds even when the ILP model cannot be solved to optimality, for larger topologies.

Our numerical studies show that ROLE can establish up to 14% more lightpaths than POLIO-RWA algorithm. In our comparisons with ILP solutions, the number of lightpaths that can be established by ROLE is close to the optimum solutions for all the problem sets, for which the optimum solution can be obtained. In the ILP formulation solutions, longer lightpath demands have considerably higher blocking probabilities than shorter lightpaths. ROLE can produce solutions with a more fair blocking distribution according to lightpath demand lengths, in which longer lightpaths have a higher probability of being

established, compared with the ILP formulation solutions. We also investigated the effect of switch crosstalk ratio on the produced solutions. According to the results, for values smaller than -35 dB, the switch crosstalk ratio has a small effect on the number of established lightpaths and at -25 dB it reaches its maximum effect.

After that, we develop a Multi-layer TE scheme, Collaborative Lightpath Topology Design (COLD), for the joint solution of the corresponding sub-problems of the MVTD problem in the MPLS and WDM layers. If SVTD and SLE problems are solved separately, the virtual topology designed by the MPLS layer may not be feasible in the physical layer. In such a case, significant traffic losses will occur since some of the traffic flows are planned to be routed on lightpaths that could not be established by the WDM layer. There may be sufficient resources in the physical layer to prevent these losses by establishing other lightpaths, but this cannot be realized without interaction between the solution methods. In our proposed solution, we solve the MVTD problem iteratively by providing interaction between the solution methods used for SVTD and SLE problems.

In the COLD scheme, a Tabu Search based heuristic algorithm algorithm is run in the MPLS layer. This algorithm produces the final virtual topology iteratively by updating the virtual topology step by step. At each iteration, the feasibility of the virtual topology at that iteration is verified by communicating with the WDM layer. The WDM layer solves the SLE problem for the requested topology using the ROLE algorithm and replies the MPLS layer on whether the topology is feasible or not. As a result, the virtual topology generated by COLD is completely feasible in the physical layer according to the assumed physical layer model. COLD can be applied under different interoperation models since the only necessary communication between layers is the request of a virtual topology and a positive or negative answer to that request. However, we show that if physical

layer connectivity information is shared between the layers, better solutions are produced in terms of routed lightpaths and resource usage.

1.4 Organization of the Dissertation

The rest of the dissertation is as follows. In the following Chapter, we give a review of the proposed TE methods in the literature. In Chapter 3, we study the SVTD problem in the MPLS layer and introduce our proposed solutions. We also introduce our proposed online TE mechanism in the MPLS layer, DREAM. Chapter 4 presents comparative investigations of TE mechanisms with static and reconfigurable WDM layer virtual topologies, based on joint studies conducted with partners from different universities. In this Chapter, the TE mechanism we propose in Chapter 3 is used with the static virtual topology, and the TE mechanisms used with the dynamic virtual topology are based on approaches previously proposed by our partners. In Chapter 5, the SLE problem in the WDM layer is studied and the proposed solution, ROLE algorithm, is introduced. In Chapter 6, we introduce our proposed solution for the MVTD problem, COLD and investigate its application under different interoperation models and physical layer scenarios.

Chapter 2

Traffic Engineering: Literature Review

Traffic engineering (TE) applications can be classified basically in two categories as being static or dynamic according to assumed traffic conditions. In static TE applications, the connection demands are known beforehand and the problem is an optimization problem of allocating the network resources to the demands in the most efficient way to satisfy certain constraints. The objective can be performance based (e.g. minimizing the total delay or maximizing throughput) or resource based (minimizing the cost of a certain network resource such as the number of wavelengths or transceivers) or combination of both. In dynamic TE problems, the connection requests arrive one at a time in a random order and the aim is to serve the arriving request, considering the current state of the network.

TE applications also differ according to the layer where TE decisions take place. Some TE applications are performed solely in the MPLS layer, by allocating/reallocating the MPLS layer resources to connection demands arriving to, or that has already been served in the MPLS layer, with no consideration of the underlying WDM layer resources. TE applications involving only the WDM

layer takes the connection requests incoming to the WDM layer (i.e., the light-path requests) and routes them on top of the physical topology by allocating the wavelength resources accordingly. Another approach is to consider both layers jointly in terms of both performance criteria and resource allocation. This last approach requires the case of a single administrative unit controlling both layers or separate but collaborating network control planes.

In the rest of this chapter, we give an overview of the some of the recent and significant TE approaches from the literature by classifying them according to the assumed traffic condition and the layers involved.

2.1 Static Traffic Engineering

2.1.1 Static TE in the MPLS Layer

Static traffic engineering in the MPLS layer can be seen as a subproblem of the more general virtual topology design problem, focusing on the MPLS layer, without the consideration of WDM layer constraints. A set of LSP connection requests with certain bandwidth requirements are given and traffic engineering may involve deciding between which node pairs to establish the lightpaths, the routes of the LSPs on the lightpath topology, whether to route or reject an LSP connection request depending on the total resources and the priority of the re-quests. Since WDM layer resources and constraints are not considered, mapping of the lightpaths onto the physical topology is out of the scope of this prob-lem. The simplest approach for the solution of this problem is assigning a single lightpath for each connection request, but this would be an excessively expensive solution and a waste of WDM layer resources since the bandwidth requirements of the LSPs are usually much smaller than the capacity of a single lightpath. Therefore, the general approach is either to consider the established lightpaths

as cost components in the objective function [17, 35] or in the constraints; or to put strict constraints on the total number of established lightpaths or number of lightpaths between two node [33]. This problem can be formulated using integer linear programming and is shown to be NP-complete [35].

The authors of [35] proposes an Mixed Integer Linear Programming (MILP) formulation for a more general case of this problem. Available virtual links of different capacities are assumed. The number and type of the virtual links between each node pair and the routes of the LSPs are determined by solving the flow based formulation. The objective is to minimize the total cost associated with the virtual links.

An ILP formulation minimizing the maximum congestion on any lightpath (i.e., virtual link) is presented in [33]. A single lightpath is allowed between each node pair. A propagation delay is associated with each possible lightpath, and a constraint imposing an upper bound on the propagation delay is introduced for each node pair. The maximum number of lightpaths that can emanate from a node is also bounded by a constraint.

A multi-hour version of the aforementioned virtual topology design problem for a traffic pattern changing with the time of the day is studied in [17]. It is assumed that the virtual topology is static, but the routes of LSPs can be reconfigured in time periods, in which the traffic shows significant changes. The aim is to determine number and places of the virtual topology links and the routes of LSPs on that virtual topology for each considered time period with the objective of minimizing the capacity cost and routing all the offered traffic. The problem is formulated as an MILP using a path based approach. The candidate paths are generated using k-shortest paths algorithm. A decomposition algorithm using Lagrangean relaxation with duality and subgradient optimization is proposed for the solution of the problem.

In [2], the authors assume dynamic packet traffic and develop a model for calculating the number of lightpath connections required between a source and destination node to achieve a given upper bound on the blocking probability. Then, they propose a heuristic algorithm that designs the virtual topology aiming to minimize the number of lightpaths. The algorithm sorts the demands in a decreasing order. It starts establishing direct lightpaths between the source and destination nodes of the demands at the top of the list. At each iteration, if there is sufficient residual capacity in the lightpaths established so far, it routes the current demand on those lightpaths, otherwise it establishes new lightpaths between the source and the destination of the demand.

Another problem arising in the MPLS layer TE is investigated in [36] and [37]. As the LSPs arrive and are served one by one, or as the traffic or network conditions change, the routes of the LSPs may need to be re-optimized. In the re-optimization process, not only the new routes of the LSPs but the rerouting scheduling also becomes important when going from one configuration the the other. In [36], it is assumed that the optimized new routes of the LSPs are given and the studied problem is finding the best rerouting sequence. The capacities of the links are not exceed at any instant during reroutings, and to ensure this some LSPs may be deallocated temporarily. The aim is to find the rerouting sequence that causes minimum amount of deallocations. Four greedy heuristics are proposed for the solution of this problem and evaluated under different traffic conditions.

LSP connections of different QoS classes are assumed in [37]. The high class connections cannot be rerouted; medium class ones can be rerouted only with make before break function, after setting up the new route; and the low class ones can be reallocated to reroute the higher class connections. The objective is to calculate the new routes of the LSPs and the rerouting sequence, such that the number of reroutings is minimized while the QoS specifications are not violated.

By analyzing its complexity and showing that its linear relaxation is very weak, the problem is shown to be very difficult to solve. Some theoretical results are obtained and simple heuristics are defined for rerouting of different classes of connections.

2.1.2   Static TE in the WDM Layer

The end-to-end connections in the WDM layer are lightpaths, therefore when TE is performed purely in the WDM layer, the connection requests (i.e., demands) that need to be satisfied are in terms of lightpaths. The corresponding TE problem involves deciding which of the offered lightpath demands to satisfy and assigning a route and a wavelength to each of the lightpath demands that will be established. This problem is referred as the Lightpath Establishment Problem, and as Static Lightpath Establishment Problem, when the lightpath demands are static. The problem of finding a route and assigning a wavelength to the lightpath that will be established is known as the Routing and Wavelength Assignment problem, which can be thought as a subproblem of the lightpath establishment problem. In some of the studies in the literature both terms may be used to refer to the same problem.

RWA problem has been investigated in a numerous number of studies in the last decades [38, 39]. For the NP-complete offline (i.e., static) version of the problem, Linear Programming formulations and heuristic search algorithms applying meta-heuristics are proposed. A review of the RWA problem and various proposed solutions in the literature can be found in [39]. When establishing a lightpath, to find a route with a free wavelength is not the only constraint that needs to be considered. As the optical signal propagates over a lightpath, it will experience quality degradation due to physical impairments in various components. This signal quality degradation is cumulative and when the signal reaches the receiver, the resulting Bit Error Rate may be above the acceptable

value for successful communication through the lightpath. As a result, in the lightpath establishment (or RWA) problem, keeping the BER along the lightpath below the acceptable threshold is one of the constraints, when physical layer impairments are taken into account. The model we use in this study includes physical layer impairments, therefore we are going the focus on the studies on RWA, that considers physical layer impairments.

RWA problem under physical layer impairments has been recently subject to increasing attention in the literature. Among the proposed solutions, there are linear programming formulations [40, 41, 42], applications of metaheuristics such as Tabu Search [43], genetic algorithms [44, 45] and heuristic algorithms [34, 46, 47, 48, 49]. The authors of [50] presents a comprehensive literature survey on the Physical Layer Impairment Aware (PLIA) RWA solutions for both offline and online versions of the problem. As stated in [34] and [42], most of the studies in the literature focus on online PLIA RWA and the more difficult offline version is rather less investigated. Below, a brief review of recent studies and various solution approaches on offline PLIA RWA problem is given.

A number of studies propose linear programming based solutions for the PLIA RWA problem. In [41], a cost is assigned to links for each type of impairment. Then, the total flow cost in the network is minimized by using linear programming. Impairment effects depending on the interference of lightpaths, such as crosstalk, are neglected in that phase. In the next phase, BERs of the lightpaths to be established are calculated and if some BERs violate the minimum threshold, RWA is redone. Linear programming formulations are proposed also in [40] and [42]. These studies consider the aggregated effect of different types of impairments and takes the interference among the lightpaths into account. In [40], the physical layer impairments are incorporated by adding surplus variables in the objective function, instead of using hard constraints. The aggregate effect of the physical layer impairments is included as a hard constraint in [42]. In both

studies, ILP formulations are solved using linear programming relaxations with a piecewise linear cost function designed to produce integer solutions without integrality constraints. This method is reported to yield integer solutions in most of the investigated problems. The formulation in [42] is compared with a non-PLIA RWA formulation and another formulation assuming worst case scenario for lightpath interference, and shown to perform better than both in terms of blocking ratio and the number of wavelengths needed to satisfy the connection requests.

Another approach for solving the PLIA RWA problem is use of meta-heuristics. The authors of [45] propose a multi objective optimization strategy. To constraint the physical layer impairments, parameters such as mean number of common hops, mean path length and mean number of common edges are included in the objective function and genetic algorithms are used for solution.

There are also studies applying heuristic RWA algorithms with a specific order. A sequential algorithm based on Random Search (RS) is proposed in [46]. The lightpath demands are considered one by one in a predefined order and served with using alternate routing with k shortest paths and first fit wavelength assignment scheme, without the consideration of physical layer impairments. This process is repeated with random orderings of the demands and the order with the minimum number of blocked lightpath demands is chosen. After the RWA phase, a BER test is applied to each of the lightpaths in the solution set and a regenerator is placed along the lightpaths failing the test.

In the POLIO-RWA algorithm proposed in [34], the lightpath demands are sorted according to the lengths of the shortest paths between their sources and destinations in an increasing order and served in that order. For each lightpath, the route and wavelength is chosen to maximize the minimum Q factor among the active lightpaths. POLIO-RWA is compared with the solutions proposed in [41] and [46], and shown to have a lower blocking rate.

2.1.3 Multi-layer Static TE

When parameters of the underlying physical layer topology are given, multi-layer static traffic engineering is the equivalent of the virtual topology design problem. This problems includes deciding between which nodes to open the lightpaths and the routes of the LSPs on the virtual topology (i.e., lightpath topology) and solving the routing and wavelength assignment problem for the lightpaths to be established. A detailed description of the problem and a survey on the ILP formulations proposed for different versions of the problem in terms of the imposed constraints and the objective function is presented in [51]. Some heuristics proposed in the literature for the solution of this problem are also reviewed. Since virtual topology design problem involves deciding how to 'groom' the lower capacity LSPs into higher capacity lightpaths, it is also referred as the 'traffic grooming' problem in the literature. [52] and [53] provide reviews of the traffic grooming problem, along with the proposed models and solution approaches in the literature, mainly focusing on ring networks. Below, we summarize some of the important and recent studies in the literature, on multi-layer virtual topology design.

In [54], the authors propose an ILP formulation with the objective of minimizing the average MPLS layer hop distance. A constraint is imposed on the maximum lightpath length. Assuming full wavelength conversion at every node, wavelength assignment problem is not considered. Since the formulation can be solved only on topologies of a few nodes, they propose two heuristics for solving problems of larger size. The first heuristic minimizes the single hop traffic, the second maximizes the single hop traffic.

Another study investigating the virtual topology design problem in case of full wavelength conversion is [12]. A multi-hour traffic pattern is used; and the lightpaths and LSP routes are considered as permanent. The problem is formulated as an MILP problem with the objective of minimizing a total cost including

the number of wavelengths used, the length of the wavelength paths and the average queuing delay while routing all the traffic flows. A space reduction heuristic using a set of candidate paths obtained by the k-shortest paths algorithm and a decomposition heuristic is utilized to solve the MILP problem.

The authors of [30] study a special case of the virtual topology design problem with constraints from both layers. Constraints are imposed on the number of LSRs traversed by the LSPs in the MPLS layer for QoS issues, and on the length of the lightpaths in the WDM layer to reduce the transmission quality impairments. In the investigated problem, not all the nodes are placed LSRs and the objective is to determine the locations of LSRs and the lightpath routes. The network cost to minimize involves installation of LSRs and setting up lightpaths. It is assumed that the lightpaths are routed along the shortest paths on the physical topology, and the wavelength assignment problem is not considered. An MILP formulation is proposed for the problem and a heuristic is proposed which is derived from decomposing the problem into two simpler MILP problems and solving them one by one.

The aim in the virtual topology design problem investigated in [55] is to minimize electronic layer resource usage, by using direct lightpaths to route the demands, as much as possible. Constraints on the WDM layer resources such as the number of wavelengths and physical links are considered. A 'wavelength graph model' and an ILP formulation using this model is developed. Three heuristics are also proposed for the solution of the problem. First is a sequential shortest path algorithm that serves the demands on the shortest paths on an auxiliary graph, one by one with different sorting orders. Second is a parallel shortest path algorithm that calculates the shortest paths for a block of demands in parallel. Third heuristic is used to improve the obtained results by replacing some of the used paths by shorter ones.

Another exact ILP formulation for the virtual topology design problem is presented in [56]. The objective is to minimize the maximum load on the any of the lightpaths. The lightpaths to be established, their routes on the physical layer and wavelengths, and the routes of the LSPs on the virtual topology are the variables to decide. A constraint is imposed on the maximum hop counts of the lightpaths. For the solution of the formulation, a heuristic approach is proposed. First, the integer relaxed version is solved, then a feasible solution is obtained by applying rounding algorithms.

2.2   Dynamic Traffic Engineering

In dynamic TE, the connection requests are not known beforehand and arrive one by one randomly and on a dynamic basis. If TE application involves only the MPLS layer, the arriving traffic demands are electronic layer demands which should be routed along LSPs. Then, the TE actions may include deciding whether to admit an incoming LSP request or not, updating the bandwidth of an LSP, tearing down an already established LSP, routing a newly arriving LSP and allocating the required resources, and in the case of a dynamic WDM layer, requesting establishment of a new lightpath (the establishment of the lightpath in the WDM layer will be out of the scope of the TE application).

Dynamic TE applications involving the WDM layer assume a dynamic WDM layer that is reconfigurable in a reasonable amount of time, without disrupting the traffic flows for a long period. If only the WDM layer is involved, the considered traffic demands are in terms of lightpath connections. Then, the aim is to serve the lightpath connection demand by assigning it a route and an available wavelength, while utilizing the WDM layer resources in an efficient way and satisfying certain constraints.

In case of multi-layer TE, both WDM and MPLS layers are involved. The TE decisions may include whether to route the arriving request on the current WDM layer topology or to establish a new lightpath; and how to route the LSPs on the WDM layer topology and the lightpaths on the physical topology.

2.2.1 Dynamic TE in the MPLS Layer

Most of the studies on dynamic TE in the MPLS layer, investigate the problem of how to route the incoming LSP requests while using the MPLS layer resources efficiently in order to be able to accommodate the requests that will arrive later. One of the most influential ones among the recent studies is [57]. In this study, an MPLS layer TE scheme is proposed using Minimum Interface Routing Algorithm (MIRA) to dynamically route the incoming LSPs. In MIRA, minimum interference paths are chosen by avoiding 'critical links'. Critical links are defined as following: when an LSP is routed along a critical link, the max-flow values of one or more other LSPs decrease. The problem of detecting critical links is formulated as an integer programming problem and shown to be NP-hard and a linear relaxation of the problem is solved.

Inspired by [57], the authors of [58] develop another MPLS layer TE strategy, Profile Based Routing (PBR). In PBR, using SLAs or by monitoring, a prediction of the future traffic distribution is obtained. Using this prediction, the paths are chosen in an online fashion and admission control is applied by rejecting the LSP requests if they will cause possible blockings of future LSPs with a high probability.

Another dynamic LSP routing algorithm is proposed in [5]. Along with the concept of the 'critical links' introduced in [57], the residual capacities of the links

and the hop lengths of the paths are also considered. The LSPs are routed by using shortest path routing with link weights that take into account the mentioned factors.

The authors of [59] state that, the performance of MIRA decreases significantly when the network state information is highly inaccurate. They introduce the concept of 'criticality threshold', which supplies a thorough characterization of link critically. Based on this concept, they propose the Least Critical Path First (LCPF) algorithm, which is shown to perform better than MIRA when the network state information is not accurate.

2.2.2 Dynamic TE in the WDM Layer

In dynamic RWA problem, since the decisions need to be carried out dynamically in very short time periods, fast heuristics are widely proposed. An overview of the classical RWA problem without considering physical layer impairments and solution approaches in the literature can be found in [39]. We focus on the RWA problem in case of physical layer impairments, which is a more contemporary topic. [50] provides a comprehensive survey and classification of the PLIA RWA solutions in the literature. In some of the proposed solution approaches, physical layer impairment are considered in the routing phase and wavelength assignment is carried out separately, on the chosen route [60]. Another approach is to calculate the route without consideration of the physical layer impairments, and consider physical layer impairments in the wavelength assignment phase [61, 62]. In some of the studies, the two problems are solved jointly, taking the physical layer impairments into account [63, 64].

In the PLIA solution proposed in [65], RWA is carried out without considering the physical layer impairments, first. Then, the signal quality for the calculated route and wavelength is estimated. If it is below the acceptable value, RWA

algorithm searches for another route and wavelength. It is stated that, even this simple method can provide a 30% reduction in the blocking probability compared with a non-PLIA approach.

In [60], the physical impairments are modelled as noise whose variance can be predicted. Physical layer impairments are not considered in the wavelength assignment process. The proposed solution searches wavelengths one by one and if it finds an available wavelength, it calculates the shortest path for that wavelength using noise variances as link weights.

The solution proposed in [61] considers physical impairments in the wavelength assignment phase, using shortest path fixed routing. The wavelengths are separated and sorted according to their place in the spectrum. The separation and sorting is done in a way to reduce the effects of Four Wave Mixing and Cross Phase Modulation. The algorithm tries wavelengths in the given order. Another study investigating PLIA wavelength assignment is [62]. Fixed shortest path routing is assumed also in this study. The proposed approach mainly focuses on crosstalk as physical layer impairment. A special wavelength ordering is applied, according to this ordering the consecutive wavelengths in the list have the maximum frequency separation.

Routing and wavelength assignment problems in case of physical layer impairments, are considered jointly in [63]. Searching all the paths and wavelengths, the path, wavelength combination giving maximum Optical Signal to Noise Ratio (OSNR) is selected. A simplified model is used for OSNR calculation. The static noises depending on the physical layer parameters are calculated beforehand. The dynamic components depending on the current connections are approximated. Authors of [64] also consider routing and wavelength assignment problems jointly in the presence of physical impairments. They propose two fast heuristics. The first algorithm performs shortest path routing with link weights determined by the available wavelengths along the links, the physical lengths of the links and

the number of established connections at the end nodes of the links. Consideration of the link lengths in the weight function aims to reduce the impairment effects along the fiber and consideration of the connections at the end nodes aims to reduce the crosstalk effect. The second algorithm calculates a route for each wavelength, minimizing the crosstalk effect and chooses the route, wavelength combination with the lowest crosstalk effect. The crosstalk minimizing algorithm is shown to have a better performance in terms of blocking ratio.

2.2.3   Multi-layer Dynamic TE

In a dynamic multi-layer TE scheme, the arriving traffic demands can be served using the already available MPLS layer resources, or by providing new resources to the MPLS layer by opening new lightpaths in the underlying WDM layer. The strategy of preferring the first approach is referred as IP/MPLS Layer First (ILF) and preferring the second is referred as Optical Layer First (OLF) [66, 67, 68, 69, 70]. In the ILF strategy, the MPLS layer tries to route an incoming LSP request on the virtual topology and if no available path is found, it requests a direct lightpath between the source and destination from the WDM layer. OLF aims to make use of the physical layer resources as much as possible, as it tries to route each LSP on a direct lightpath between the source and destination. If the WDM layer cannot provide the requested lightpath, it searches for a multi-hop path on the virtual topology.

[66] compares these two strategies and show that OLF has a lower blocking ratio. It also investigates the effect of the number of add/drop ports of the OXCs. [67] presents two routing algorithms using the ILF and OLF strategies with three different adaptive route selection schemes in the MPLS layer. It also reports that OLF approach has a lower blocking ratio.

In [68], the authors present multi-layer routing schemes using ILF and OLF strategies. They also propose a communication protocol between the Constrained Shortest Path First (CSPF) engine and the Generalized MPLS (GMPLS) controller, which are used to implement these routing schemes, and demonstrate an experiment using this protocol [69].

An adapted ILF type routing algorithm is proposed in [70]. It is stated that requesting a new lightpath when there is no available path for an LSP request is ineffective since the current LSPs are already congesting the network using long routes. The proposed algorithm measures the congestion in the MPLS layer and requests a lightpath if it is above the determined threshold.

In [71], the authors make use of the fact that each of the ILF and OLF approaches can be more advantageous than the other under certain traffic conditions. The proposed hybrid routing strategy defines resource usage indexes for both layers using the link loads and chooses to use one of ILF or OLF schemes according to the values of these indexes.

In the OLF strategy and in the ILF strategy when there's not sufficient resources in the MPLS layer, a direct lightpath between the source and destination nodes of the incoming LSP is requested from the WDM layer. There may be cases in which there is no available route in the MPLS and optical layers, but the LSP can be routed on a concatenation of MPLS and WDM layer paths. This type of solutions are missed in these strategies. The authors deal with this problem in [11] with application of the saturated cuts method. In this method, MPLS layer sends the information of nodes that are connected to the source and the destination nodes with the sufficient residual capacity to route the LSP. The optical layer calculates the shortest path from any two nodes from these sets and opens the lightpath between the corresponding nodes. The same problem is addressed in [72] with a different solution. The MPLS layer receives the information of the nodes which are three or less hops away from the source or the destination in the

33

physical layer. If an MPLS or WDM layer path cannot be established between the source and the destination, MPLS layer tries to establish a concatenation of MPLS and WDM layer paths through these nodes.

Another common approach is to construct a joint, auxiliary topology whose links consist of the available wavelengths and the already established lightpaths with their residual capacities. Then, a routing algorithm is run on the resulting topology with the defined costs to route the incoming LSP requests [73, 74, 75, 76, 77]. The TE scheme proposed in [73] performs routing on such a topology with a load-based cost function for the already established lightpaths. Available but unopened lightpaths are also included in the topology with a specific cost.

The algorithm proposed in [74] routes the LSPs on a joint topology assigning a lower cost to the already established lightpaths. Another algorithm using the joint topology approach is presented in [75]. This algorithm aims to keep the open capacity between these nodes at maximum. In the resulting graph, the links in the minimum cut sets of the ingress and egress nodes are defined as the critical links and assigned high costs. In [76], while the residual capacity of the established lightpaths are included in the auxiliary graph, an extra cost is defined for the grooming of these lightpaths.

In [77], the authors consider different types of node architecture that can perform single/multi-hop partial/full grooming. Nodes with each architecture are represented differently in the auxiliary graph and the LSP's are routed on the shortest paths in terms of number of fiber links traversed.

Several studies in the literature propose TE mechanisms that monitor the traffic load in both layers and update the WDM layer topology accordingly [78, 79, 80]. In [78], lightpath loads are monitored, when a load imbalance is encountered, the virtual topology is reconfigured to compensate it by adding or deleting one lightpath at a time. This is achieved by formulating the problem as

MILP and using an MILP solver. In [79] and [80], IP layer traffic load is measured and the virtual topology is optimized with an extended version of Branch Exchange with Quality of service Constraints (BXQC), originally proposed for multi-layer Asynchronous Transfer Mode (ATM) networks.

In the next chapter, our proposed solution for MPLS layer TE is introduced. The proposed solution consists of a virtual topology design algorithm that is run offline, and an online mechanism based on dynamic rerouting of LSPs.

Chapter 3

Traffic Engineering in MPLS Layer

In this chapter, traffic engineering in the MPLS layer is investigated. MPLS provides connections called Label Switched Paths (LSPs) which can be used to route traffic by providing bandwidth guarantee. It also enables explicit routing of LSPs for traffic engineering purposes, so the routes of the LSPs can be determined to optimize the throughput of the network, according to the instantaneous traffic and network state. In this thesis, we assume that the traffic flows are routed in the MPLS layer through bandwidth guaranteed LSPs.

As explained in Section 1.2, the links of the virtual topology seen by the MPLS layer consists of lightpaths established by the WDM layer. We assume that WDM layer is static and that traffic demand matrix representing the traffic expectation information is available beforehand. In the considered scenario, the main part of the TE problem is the optimum design of the virtual topology, using the traffic information.

In the considered traffic model, a daily, i.e., changing with the time of the day, traffic pattern is used. The pattern of the traffic flow between two nodes depends

on the traffic generation rates of the nodes and the time zones of the nodes. The details of the used traffic model are explained in Section 3.1. The objective is to design a static virtual topology optimized for the whole 24-hour period. This problem is referred as "Multi-hour Virtual Topology Design Problem" in the literature [17]. In this chapter, we focus on the MPLS layer and do not consider the constraints in the WDM layer while setting up the lightpaths. Therefore, to prevent confusion with the multi-layer version of the Virtual Topology Design (VTD) problem, this problem will be referred as Single Layer VTD (SVTD) problem.

In Section 3.2, two different versions of the problem are studied: resource oriented and performance oriented. ILP formulations are introduced and Tabu Search based heuristic algorithms are developed for each version. The ILP formulations are used for evaluating the performances of the proposed heuristic algorithms for small problem sets.

The virtual topology seen by the MPLS layer is designed according to the expected values of the traffic flows for each time period, and the routes of the LSPs carrying traffic flows on the virtual topology are also calculated along with the topology. However, the actual instantaneous traffic may exhibit deviations from the expected values and these deviations may result with traffic loss if the LSPs are routed using the routes calculated according to the expected values of the traffic flows. To compensate these deviations and to reduce and if possible prevent traffic losses, the routes of the LSPs should be updated dynamically according to the instantaneous traffic loads on the links of the virtual topology. In Section 3.3.1, an online traffic engineering mechanism called Dynamic Rerouting AlgorithM (DREAM), which uses such a dynamic rerouting approach, is proposed. DREAM is compared with rerouting approaches using routing algorithms that are commonly used in the literature and shown to outperform these approaches.
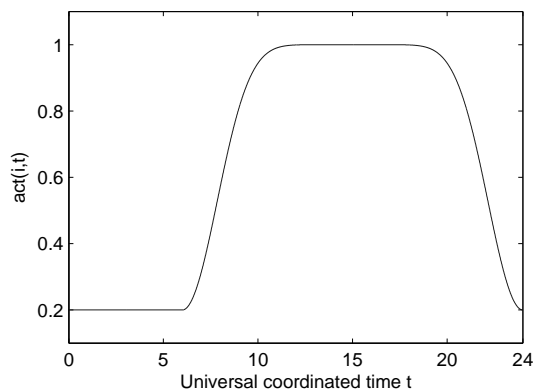
Figure 3.1: Activity function

3.1 Traffic Model

Internet traffic exhibits a traffic characteristic changing with the time of the day depending on the user and provider activities. Factors such as user populations, provider sites and their geographical locations also influence the traffic characteristics. The model that is proposed in [16] addresses all these issues, and therefore we chose this model to use in our work. This model is suitable for generating the traffic when the nodes are spread over a large geographical area. In this model, for each node i, a time zone offset τ_i and a traffic generation rate $tgen_i$ are defined. $tgen_i$ represents the expected maximum instantaneous traffic generated by node i, which depends on the population associated with node i, i.e., population of the cities surrounding the geographical location of the node. An activity function $act(i, t)$ depending on these values is defined as

$$act(i,t) = \begin{cases} 0.2 & \text{if } t_{\text{local}}(i,t) \in [0:00; 6:00) \\ 1 - 0.8 \left(\cos \left(\frac{(t_{local}(i,t)-6)\pi}{18} \right) \right)^{10} & \text{if } t_{\text{local}}(i,t) \in [6:00; 24:00) \end{cases}$$

(3.1)

In this formula, t is the coordinated universal time in hours and the function $t_{\text{local}}(i,t)$ is defined as, $t_{\text{local}}(i,t) = (t + \tau_i + 24) \bmod 24$. The activity function is illustrated in Fig. 3.1 for a node i which belongs to the universal time zone.

38

For a node pair (i, j), the expected instantaneous traffic between these nodes at time t is calculated as

$$T_{\text{expected}}(i, j, t) = tgen_i \times act(i, t) \times tgen_j \times act(j, t) \qquad (3.2)$$

The actual instantaneous traffic between nodes i and j is obtained by adding a zero mean Gaussian random variable to this expected value, in order to model the uncertainty in the traffic predictions. The standard deviation of the Gaussian random variable is given by k times the expected traffic i.e.,

$$T_{\text{actual}}(i, j, t) = T_{\text{expected}}(i, j, t) + N(0, k \times T_{\text{expected}}(i, j, t)) \qquad (3.3)$$

The parameter k will be referred as the 'traffic unpredictability parameter'. It is the measure of the deviation of the actual traffic from its estimate and will be used for evaluating the performances of the implemented TE mechanisms in Section 3.3. The traffic generation rate $tgen_i$ is assumed to be uniform for all the nodes in the network. This rate will be referred as $tgen$, through the rest of this chapter. The lightpath capacities will be expressed as the ratio of the lightpath bandwidth to unit traffic between two nodes, which is represented by $tgen^2$.

3.2 WDM Layer Virtual Topology Design

When designing the virtual topology, both the network resources (number of interfaces, lightpaths, etc.) and the network performance (throughput, blocked traffic, etc.) need to be considered. One approach is to optimize the performance while satisfying certain constraints on the used network resources, and another approach is to minimize the usage of network resources while satisfying a constraint on the performance. A third approach is be to develop a metric that

consists of both resource usage and performance parameters and to optimize this metric. However, this last approach is rather difficult to apply because the considered parameters are from different domains and there are no certain rules to make a fair comparison between them, i.e., the cost of setting up an additional lightpath in the network and the cost of rejecting some amount of a customer's traffic depend on several factors making any comparison very difficult. Therefore, the general approach is to optimize either resource or performance metrics while imposing certain constraints on the other. We investigated both the resource oriented approach and the performance oriented approach. In the first approach, the objective is to minimize the total number of lightpaths as the network resource, while routing all the offered traffic. In the second approach, the objective is to maximize the performance metric, which is the total amount of routed traffic in the considered multi-hour time period, by setting up a fixed number of lightpaths.

In the investigated problem, the traffic expectation information is available for each node pair and for each hour, in terms of a traffic matrix. For a demand d between two nodes, the maximum expected traffic in hour h is denoted by T_{dh}.

3.2.1 Resource Oriented Virtual Topology Design

The considered resource metric to minimize is the total number of lightpaths. All traffic requests in the given traffic matrices should be satisfied. We also consider nodal interface constraints and apply an upper bound on the maximum nodal degree in the resulting topology. We developed an ILP formulation and also implemented a heuristic for the solution of this problem. This problem is NP-complete. Multiple time periods are considered and the number of decision variables increases linearly with the number of considered time periods. As a result, the optimum solution can be reached using ILP only for small size networks. Therefore, we assumed splittable LSP flows in the ILP formulation,

and the produced solutions provide a lower bound for the problem to evaluate the performance of the proposed heuristic.

Mixed Integer Linear Programming (MILP) Formulation

The exact solution of the ILP formulation for multi-hour SVTD problem is computationally difficult. In the following formulation, we make some simplifying assumptions for the ILP formulation so that we can obtain a lower bound on the exact solution of the problem. Specifically, we assume that traffic between each node pair can be split, so that integer routing variables can be relaxed. The aim is to obtain a lower bound on the minimum number of lightpaths required to accommodate multi-hour traffic pattern. The mixed Integer Linear Programming formulation is as follows:

Sets:

D: Set of demands.

H: Set of hours.

N: Set of nodes.

Constants:

T_{dh}: Volume of demand d at time h

C: Capacity of a single link

U_{max}: Maximum utilization ratio ($U_{max} = 0.9$ means the flow through a link will not exceed 90% of the capacity of that link)

O_{max}: : Maximum nodal degree allowed in the logical topology (optical interface constraints of label switched routers)

Decision variables:

x_{ij}^{dh}: Continuous decision variable representing the amount of routed flow from

node i to node j, belonging to demand d at time h.

y_{ij}: Integer decision variable representing the number of established lightpaths between nodes i and j.

Objective Function:

$$Minimize \sum_{i \in N, j \in N} y_{ij} \tag{3.4}$$

Subject to:

$$\sum_{j \in N} x_{ij}^{dh} - \sum_{j \in N} x_{ji}^{dh} = \begin{cases} T_{dh}, & \text{if } i \text{ is the source of demand } d \\ -T_{dh}, & \text{if } i \text{ is the destination of demand } d \\ 0, & \text{otherwise} \end{cases}$$

$$\text{for } i = 1, 2, ..., |N|; \ d = 1, 2, ..., |D|; \ h = 1, 2, ..., |H| \tag{3.5}$$

$$\sum_{d \in D} x_{ij}^{dh} + \sum_{d \in D} x_{ji}^{dh} \leq y_{ij} \cdot C \cdot U_{max}$$

$$\text{for } i = 1, ..., |N|; \ j = 1, ..., |N| \ (i \neq j); \ h = 1, ..., |H| \tag{3.6}$$

$$\sum_{j \in N} y_{ij} \quad \leq \quad O_{max} \quad \text{for} \quad i \quad = \quad 1, ..., |N|; (i \quad \neq \quad j) \tag{3.7}$$

The objective function is to minimize the number of established lightpaths. (3.5) represents the flow constraints, guaranteing that all the offered traffic is routed. (3.6) corresponds to the capacity constraints, which implies that the traffic routed through a lightpath cannot exceed the lightpath capacity multiplied by the maximum utilization ratio. The third type of constraints (3.7) are the optical interface constraints, which impose an upper bound on the number of lightpaths that can emanate from a node.

The number of variables in this formulation increases exponentially with the network size and the optimum solution may not be obtained even for reasonably sized networks because of the time and memory requirements of the ILP solvers. We use this formulation for quantifying the performance of the heuristic multi-hour logical topology design algorithm, which utilizes Tabu Search procedure.

Tabu Search Based Heuristic Algorithm

Tabu Search is an iterative local search procedure utilizing adaptive memory. It is first proposed by Glover and has been being used to solve a variety of optimization problems including resource planning, telecommunications, VLSI design, financial analysis, etc [81]. Tabu Search is widely used in network design and planning problems. It is reported to produce better solutions than Simulated Annealing and Genetic Algorithms in routing [82], logical topology design [83] and various telecommunication network optimization problems [84]. Therefore, we utilized the Tabu Search metaheuristic in our heuristic solution for the VTD problem.

In Tabu Search procedure, starting from an element of the solution space, the solution space is explored by moves from one solution to another to find the solution giving the best objective value. Its distinguishing feature from other search procedures is that, non-improving moves are also allowed to escape local optima and adaptive memory is used to avoid entrapments in cycles.

The basic strategy is to declare each visited solution tabu by adding it to a tabu list and forbid it for a number of iterations. The entries in the tabu list are assigned "tenures" that expire over a number of iterations. The solutions with expiring tenures are removed from the tabu list. At each iteration, among the possible moves that do not result to a tabu solution, the one giving the best objective value is chosen.

In our algorithm, the search space consists of all the logical topologies that can support the given LSP traffic matrix on every hour under the utilized routing algorithm. An offline routing algorithm based on the shortest path approach is run to check if a topology is an element of the search space. For a single hour h of the traffic demand matrix, the LSPs are sorted according to their bandwidth demands where the LSP with the largest demand is in the first place. For a lightpath between nodes i and j, the link weight $(W_{i,j})$ is calculated as $W_{i,j} = 1/Cres_{i,j}$, where $Cres_{i,j}$ is the remaining available capacity of the lightpath if the current LSP is routed on that lightpath. The LSP is routed along the minimum cost path which is calculated by using the Dijkstra's algorithm with the defined link weights. Each LSP is routed one by one and if all of the LSPs can be routed successfully, then the topology is said to support the traffic demand matrix for hour h. A topology which supports the traffic matrix for each hour, is an element of the search space.

The initial solution is generated randomly. A topology generator algorithm which places the lightpaths in a random manner is run until a topology supporting the LSP traffic matrix is generated. At each run, the number of lightpaths to be placed is increased. When a suitable topology is generated, it is used as the initial topology in the tabu search topology design algorithm. There are four types of moves defined to visit the elements of the search space which are illustrated in Figure 3.2:

Type-1 Move: This type of move consists of tearing down an established lightpath in the current topology.

Type-2 Move: Let n_1, n_2 and n_3 be three nodes and (n_1, n_2) and (n_1, n_3) two established lightpaths in the current topology. Then, a type-2 move involving nodes n_1, n_2 and n_3 is defined as tearing down (n_1, n_2) and (n_1, n_3), and establishing a new lightpath (n_2, n_3). Since multiple lightpaths between
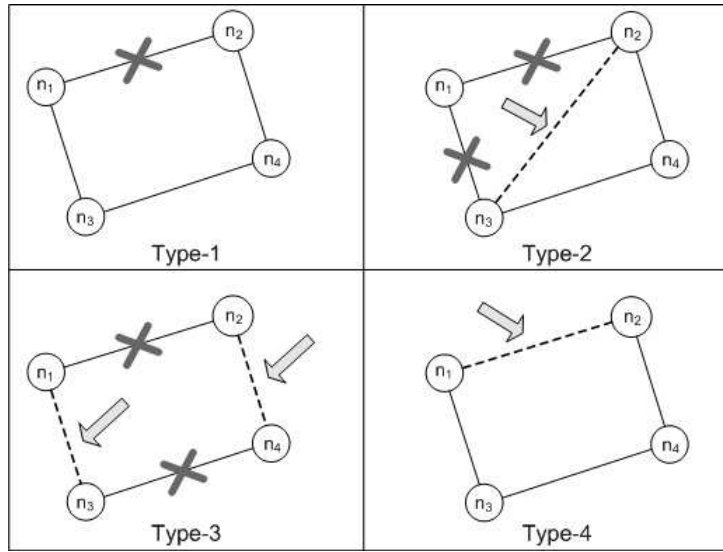
Figure 3.2: Move types in tabu search based algorithm

nodes are allowed in the logical topology, there may already exist a lightpath between the the nodes n_2 and n_3.

Type-3 Move: Let n_1, n_2, n_3 and n_4 be any four nodes with the lightpaths (n_1, n_2) and (n_3, n_4) established. Then, a type-3 move is defined as tearing down the lightpaths (n_1, n_2) and $((n_3, n_4)$, and establishing two new lightpaths, (n_1, n_3) and (n_2, n_4).

Type-4 Move: A type-4 move is simply establishing a new lightpath in the existing topology.

The objective criteria to minimize is the number of lightpaths needed to satisfy all the LSP demands for each hour. Since type-1 and type-2 moves decrement the number of lightpaths, they have a higher priority than type-3 and type-4 moves, by this way the algorithm tends to decrease the value of the objective criteria. Type-3 moves do not change the number of lightpaths, therefore they have a higher priority then type-4 moves which increment the number of lightpaths on the network topology.

The flowchart of the algorithm is given in Figure 3.3. The algorithm starts with the logical topology generated by the random topology generator algorithm. All valid moves (the moves which are not in the tabu list and lead to a topology that supports the traffic for each hour without violating the degree constraints) of type-1 and type-2 are calculated. If there are one or more such moves, the next move is randomly chosen among these moves. If there are no valid type-1 or type-2 moves, then the algorithm calculates the set of valid type-3 moves. The next move is chosen among the elements of this set if it is not empty, otherwise the next move is a randomly chosen type-4 move. Since the current topology is an element of the solution space, i.e., it supports the traffic demands for each hour, a type-4 move cannot result in a topology which does not support the traffic, therefore every type-4 move which is not in the tabu list and do not violate the degree constraints is valid.

After making the chosen move, the move is added to the tabu list with the current topology. A tabu tenure value is chosen randomly from a predetermined interval and assigned to that tabu list entry. The tenures of each entry in the list are decremented by one and the entries with expiring tenures are removed from the list. The stopping condition of the algorithm is no improvement in the objective function, which is the number of lightpaths, for a specified number of iterations. If this condition occurs, the algorithm stops and records the best topology found so far as the solution.

We tested the performance of this tabu search based algorithm on a sample network with 10 nodes. To obtain solutions of the ILP formulation in a reasonable amount of time, we considered a 10-hour time interval. The time zone information of the nodes are given in Table 3.1. All nodes are assumed to have an equal amount of population, so $tgen$ is the same for all nodes and chosen to be 2 $(Gbits/sec)^{1/2}$. The capacity of a single lightpath is 10 Gbits/sec, which can be expresses as $2.5tgen^2$. Maximum lightpath utilization (U_{max}) is chosen
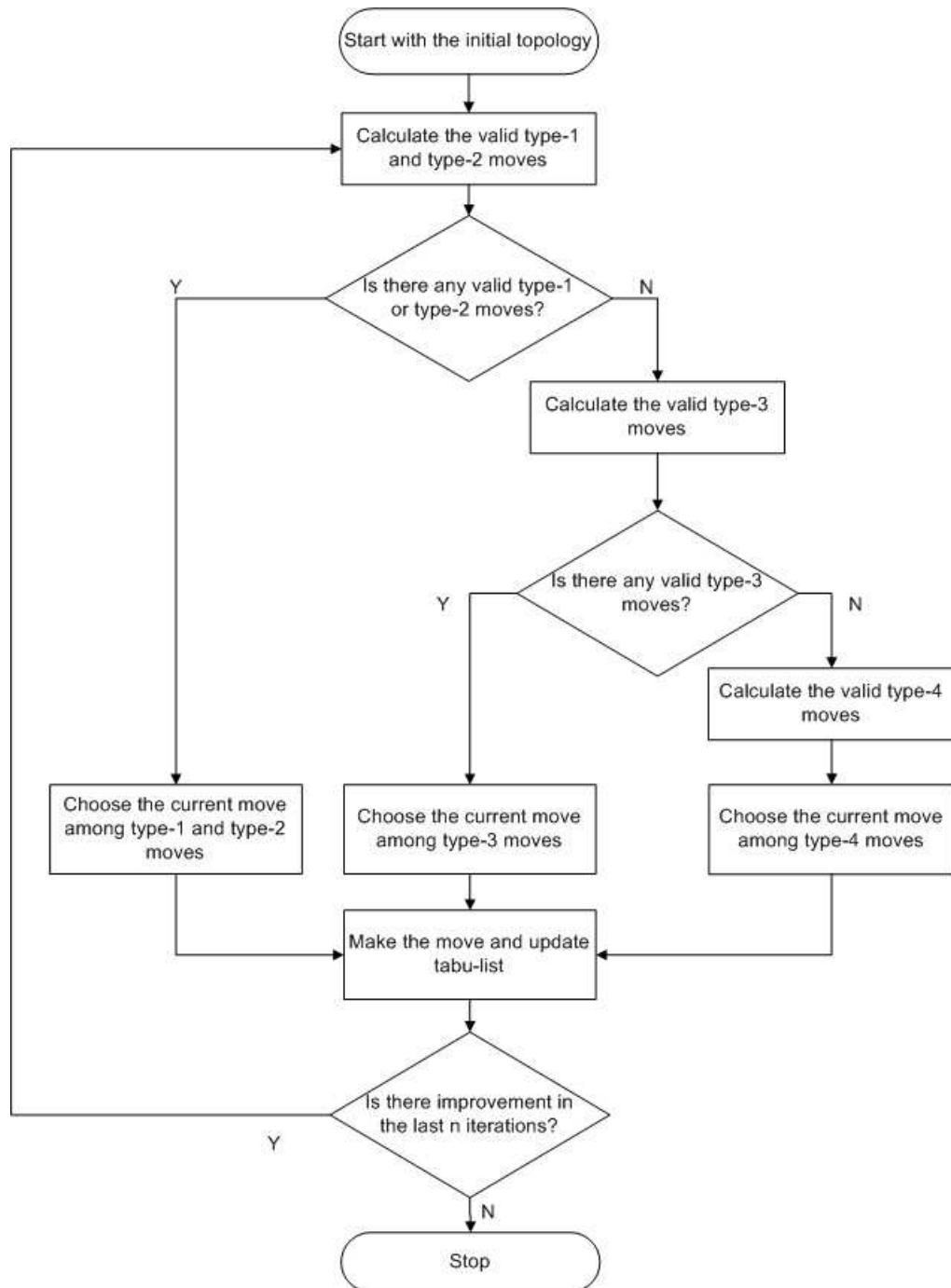
Figure 3.3: Flowchart of the resource oriented tabu search based algorithm

Table 3.1: Time zone information of the nodes

Node ID	1	2	3	4	5	6	7	8	9	10
Time Zone	0	0	2	2	2	4	4	4	6	6

Table 3.2: Number of Lightpaths (LP) in Single and Multi-Hour (MH) LTD solutions of the Tabu Search (TS) algorithm and Lower Bounds (LB) obtained with ILP, and optimality gaps

Hour		1	2	3	4	5	6	7	8	9	10	MH
Number	TS	21	20	21	17	14	12	12	13	15	18	22
of LP	LB	19	18	19	16	13	12	12	12	15	16	20
Gap (%)		10.5	11.1	10.5	6.2	7.7	0	0	8.3	0	12.5	10

to be 0.8, so each single lightpath is allowed to carry a maximum amount of 8 Gbits/sec traffic. Maximum nodal degree (O_{max}) is 6.

We compared the solutions with the lower bounds obtained from the solutions of the ILP formulation given above. The results are given in Table 3.2 together with the single hour topology design solution results for each hour. The tabu search algorithm produced solutions with a 10% performance gap compared with the lower bound on the optimum solution. In the ILP solutions, the flows are allowed to be split in order to reduce the number of integer variables in the formulation, while in the tabu search algorithm each LSP is routed on a single path. The results are quite satisfactory when this fact is taken into consideration. Splitting the traffic flows, i.e., dividing a single flow into multiple sub-flows and routing them on different paths, may cause other problems in the network layer. It may not be possible to split the flows with the same amount as in the produced solutions because of the packet sizes. Moreover, in some transport protocols such as TCP, if the packets belonging to the same session are transmitted on different routes, that may cause out of order packet arrival.

3.2.2 Performance Oriented Virtual Topology Design

The considered performance metric to maximize is the total amount of routed traffic from the given traffic matrix. The total number of lightpaths ($|L|$) is given. Nodal interface constraints are also considered as in resource oriented optimization. We developed an ILP formulation and also implemented a heuristic for the solution of this problem.

Mixed Integer Linear Programming (MILP) Formulation

As in the previous section, we make the simplifying assumption that traffic between each node pair is splittable so that integer routing variables can be relaxed. The resulting formulation gives us an upper bound on the objective function.

The sets are the same as in the ILP formulation proposed in Section 3.2.1. The decision variables x_{ij}^{dh} and y_{ij} are also the same as in the previous formulation. A new decision variable, z_d^h, which represents the amount of routed traffic belonging to demand d in hour h, is introduced. The rest of the formulation is as follows:
Objective Function:

$$Maximize \sum_{h \in H} \sum_{d \in D} z_d^h \tag{3.8}$$

Subject to:

$$\sum_{j \in N} x_{ij}^{dh} - \sum_{j \in N} x_{ji}^{dh} = \begin{cases} z_{dh}, & \text{if } i \text{ is the source of demand } d \\ -z_{dh}, & \text{if } i \text{ is the destination of demand } d \\ 0, & \text{otherwise} \end{cases}$$

$$\text{for } i = 1, 2, ..., |N|; \ d = 1, 2, ..., |D|; \ h = 1, 2, ..., |H| \tag{3.9}$$

$$\sum_{d \in D} x_{ij}^{dh} + \sum_{d \in D} x_{ji}^{dh} \leq y_{ij} \cdot C \cdot U_{max}$$

$$\text{for } i = 1, ..., |N|; \ j = 1, ..., |N| \ (i \neq j); \ h = 1, ..., |H| \quad (3.10)$$

$$\sum_{j \in N} y_{ij} \quad \leq \quad O_{max} \quad \text{for} \quad i \quad = \quad 1, ..., |N|; (i \quad \neq \quad j) \quad\quad\quad (3.11)$$

$$z_d^h \quad \leq \quad T_{dh} \quad\quad\quad \text{for} \quad d \quad = \quad 1, ..., |D|; \quad h \quad = \quad 1, ..., |H| \quad\quad (3.12)$$

$$\sum_{i \in N} \sum_{j \in N} y_{ij} = L \quad\quad\quad\quad (3.13)$$

The objective function is to maximize the amount of routed traffic from the demand set D. Eq. (3.10),(3.10) and (3.11) are the flow, capacity and optical interface constraints, respectively; similar to the constraints used in the ILP formulation presented in Section 3.2.1. (3.12) implies that the amount of routed traffic belonging to a demand cannot exceed the total traffic offered by that demand. The last type of constraints (3.13) state that the total number of established lightpaths should be equal to the predefined value.

Even this simplifying formulation takes a considerable amount of time (up to several weeks depending on the number of nodes and the number of lightpaths) to solve using the commercial ILP solver CPLEX.We use the solution of this relaxed formulation as an upper bound to evaluate the performance of our proposed heuristic algorithm.

Tabu Search Based Heuristic Algorithm

In this algorithm, the search space consists of moves that satisfy the nodal interface constraints. The traffic matrix is input to the algorithm and the objective function is the amount of traffic that can be routed on the current topology over all $|H|$ hours. A move is defined as tearing down an existing lightpath and setting up a new lightpath between two nodes. A valid move is defined as a move that is not in the tabu list and results in a topology that satisfies the interface constraints. The initial solution is generated by a random topology generator algorithm. This algorithm places the lightpaths randomly between the nodes without violating the nodal interface constraints. If the generated topology is not connected, the algorithm is run from the beginning until a connected topology is generated. The flowchart of the algorithm is given in Figure 3.4.

The Tabu Search algorithm starts from the initial solution. At each iteration, the set of valid moves (M) are calculated. For each move m in M, the resulting objective function, i.e. the amount of traffic that can be routed on the resulting virtual topology, is calculated.

To calculate the objective function, an offline routing algorithm based on the shortest path approach is run with the traffic matrix for each hour. For a single hour h, the traffic flows are sorted according to their traffic rate in a decreasing order and they are served in that order. The link weight $(W_{i,j})$ for the lightpath between nodes i and j is calculated dynamically as $1/Cres_{i,j}$ where $Cres_{i,j}$ is the residual capacity of the lightpath, if the LSP is routed on that lightpath. If a lightpath does not have sufficient capacity to carry the current flow, it is assigned a predetermined extremely high cost.

The flows are routed along the minimum cost path, calculated by using the Dijkstra's algorithm. The total amount of routed traffic is calculated as the sum of the all the routed traffic in each hour. Among the moves in M, the one resulting
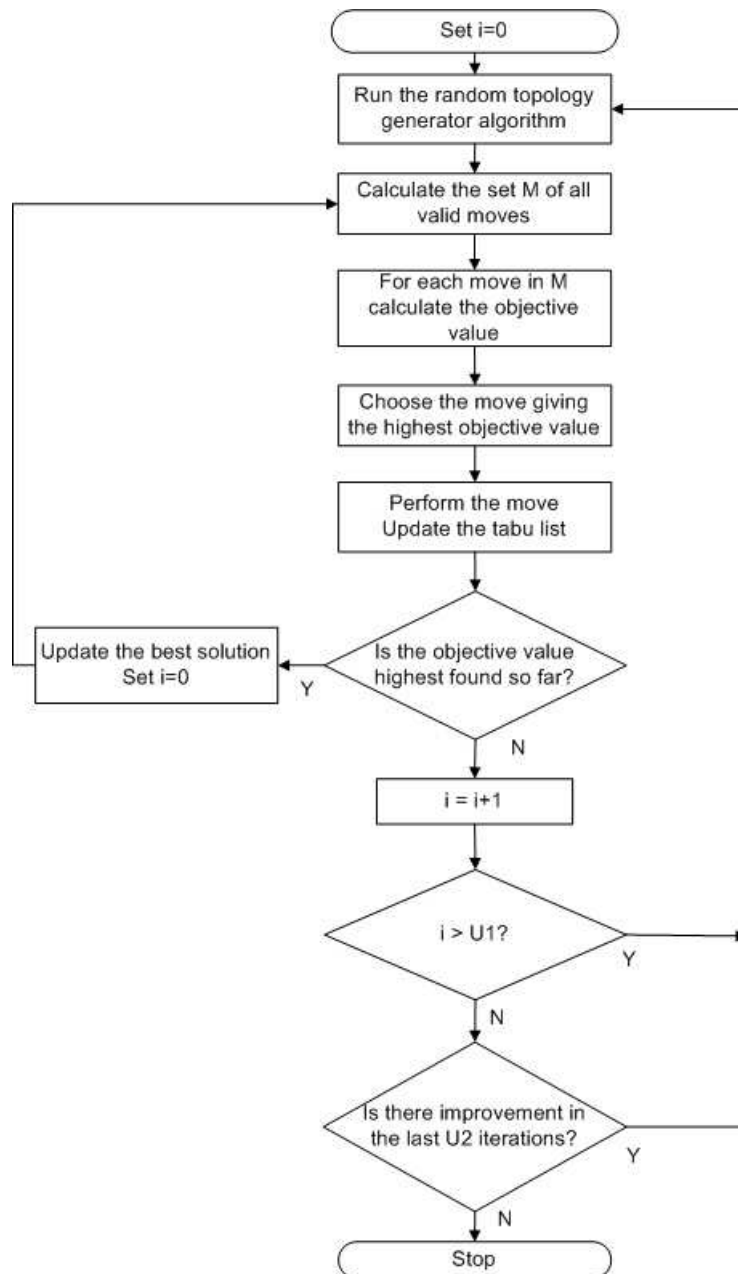
Figure 3.4: Flowchart of the performance oriented tabu search based algorithm

in the topology with the highest objective value is chosen. If there are multiple topologies resulting in the highest objective function, a tie-breaker parameter is used to determine which topology to choose. The tie breaker parameter is calculated as:

$$\sum_{i,j \in N} \sum_{h \in H} S_{ij} \cdot T_{dh}, \ d \text{ is the demand between nodes } i \text{ and } j \qquad (3.14)$$

In (3.14), S_{ij} denotes the number of hops on the shortest path between i and j in the resulting topology.

Among the topologies with the same objective function, the one with the lowest tie breaker parameter is chosen. As it can be seen, the tie-breaker parameter favors setting up the lightpaths between the nodes with higher traffic between. Before the chosen move is done, it is added to the tabu list with the current topology. Each entry in the tabu list has four elements; the set up lightpath, the torn down lightpath, current topology and the tenure value. While searching if a possible move is tabu or not, if there is an entry in the tabu list with the first three elements being the same with the current move, the algorithm decides that the move is tabu and excludes it from the set of valid moves. The tenure value is chosen uniformly randomly between an upper and a lower limit. After a move is made, the tenure of each entry in the list is decremented by one. The entries with zero tenure value are removed from the list.

In order to search different regions of the solution space effectively, we introduced a diversification step to the algorithm. If there is no iteration in the objective function for a certain number of times ($U1$) , the algorithm jumps to another element of the solution space randomly. This is achieved by running the random topology generator algorithm. The stopping criterion of the algorithm is the case of no improvements in the best solution for a specific number ($U2$) of times. If a solution with a higher objective value or an equal objective value and a lower tie breaker value than the best solution found so far cannot be found for a given number of iterations, the algorithm records the best solution and stops.

Table 3.3: The percentages of the routed traffic by the tabu search algorithm and the ILP upper bound

# of lightpaths	13	14	15	16	17
Tabu Search	86.897	93.885	98.816	99.971	100
Upper Bound	93.403	97.886	100	100	100
Optimality Gap (%)	6.966	4.087	1.184	0.029	0

To evaluate the performance of the proposed algorithm, an upper bound on the percentage of routed traffic for a given number of lightpaths, that can be achieved by any algorithm is obtained by solving the MILP formulation introduced in Section 3.2.2. The percentages of traffic carried by each algorithm are given in Table 3.3 for different number of lightpaths. These results are obtained using a lightpath capacity $C = 3tgen^2$. According to the lower bounds, at least 15 lightpaths are needed to route all the traffic demands. Proposed TS-MVTD algorithm achieves this using 17 lightpaths, however it can route close to 100% of the traffic demands for also 15 and 16 lightpaths.

3.3 MPLS Layer Online Traffic Engineering

As stated in Section 3.1, a flow model is used to represent the traffic in our work. In this section, a single LSP is constructed between each source-destination pair and the changes in the traffic amount between these nodes is represented by changing the bandwidth requirement of the constructed LSP. The changes in the bandwidth requirements of the LSPs are modelled by bandwidth update requests with a Poisson arrival model having a fixed rate of $\lambda = 30$ arrivals/hour. At an arrival of a bandwidth update request at time t, the new bandwidth requirement of the LSP is calculated from $T_{\text{actual}}(i, j, t)$.

The online TE mechanism proposed in this work is based on rerouting the LSPs to optimize the network performance. For each LSP to be constructed

between a source-destination pair, a number of shortest paths are calculated be-forehand using a K-shortest path algorithm. When a bandwidth update request arrives for an LSP, among the paths belonging to that LSP, the best one is cho-sen according to the employed routing scheme and the LSP is (re)routed on that path. If there is not sufficient residual capacity along the path to accommodate the LSP, all of the available capacity is dedicated to the LSP and the amount of traffic that cannot be routed is assumed to be blocked.

3.3.1   Dynamic Rerouting Algorithm (DREAM)

DREAM is an alternate routing scheme which chooses the best path according to the number of hop lengths and instantaneous residual capacities of the candidate paths. Each of the candidate paths is assigned a dynamic cost that is calculated by a cost function that utilizes the instantaneous residual capacity information. Then, the path with the minimum cost is chosen for rerouting the LSP. The cost function is designed in a way to choose the shorter paths when the network is lightly loaded and the paths with higher residual capacity when the network is heavily loaded. When there is a large amount of residual capacity along the path, the cost component due to the path length should be the dominant one and the residual capacity cost should be ignorable. As the residual capacity along the path decreases, the residual capacity cost should become more dominant. Therefore, the component due to residual capacity is chosen to be exponential. The resulting cost function for path p, is given by:

$$F_{cost}(p) = L_p + A^{u - \frac{C_{Res}^p}{C}} \qquad (3.15)$$

In this formula, L_p is the number of hops on path p and C_{Res}^P is the residual capacity of the path, i.e. the minimum residual capacity of the links (lightpaths)
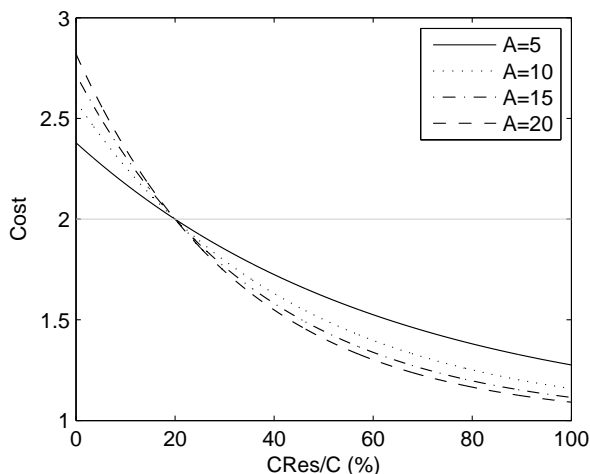
Figure 3.5: The cost function of DREAM vs. residual capacity ratio (C_{Res}/C) for different values of A for $u = 0.2$

along the path, after the LSP is routed along that path and C is the lightpath capacity.

Choosing the Cost Function Parameters

The cost function consists of two components that are summed, the first coming from the path length, the second coming from the residual capacity ratio. Changing the parameter u, we can adjust for which residual capacity ratio the second component increases the total cost by 1 (which gives an increase equal to increasing the length of the path by 1). Moreover, with the parameter A, we can adjust how much the cost increases with decreasing residual capacity. The cost function is plotted for different values of A and u in Figures 3.5 and 3.6 for $L_p = 1$.

The performance of DREAM is tested for various values of the parameters A between 1 and 100 and u between 0 and 1, and the best results were obtained for the values of $A = 10$, $u = 0.5$.
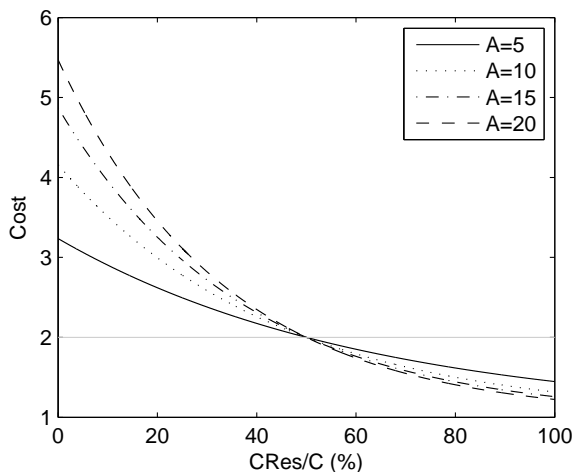
Figure 3.6: The cost function of DREAM vs. residual capacity ratio (C_{Res}/C) for different values of A for $u = 0.5$

3.3.2 Performance Evaluation

We have compared the performance of DREAM with various other schemes in the literature: Shortest Path routing (SP), Available Shortest Path routing (ASP) and Widest Shortest Path routing (WSP) [58, 5]. In SP, no traffic engineering is applied and the LSPs are routed along the fixed shortest paths. ASP only consider the paths with sufficient residual capacity to accommodate the LSP. The shortest among these paths is chosen. If there are multiple such paths, one is chosen randomly. In WSP, similar to ASP, the shortest one is chosen among the paths with sufficient residual capacity. If there are multiple such paths, the one with the highest residual capacity is chosen. In both ASP and WSP, if there is a path with sufficient residual capacity to accommodate the LSP, it is rerouted along the path with the highest residual capacity and the amount of traffic that cannot be routed is assumed to be blocked.

Simulations are run for two different networks each having 10 nodes. The logical topologies are designed using the performance oriented tabu search algorithm presented in Section 3.2.2. Lightpath capacities are $C = 4tgen^2$ for 14 lightpath topology and $C = 2tgen^2$ for 23 lightpath topology respectively. These lightpath
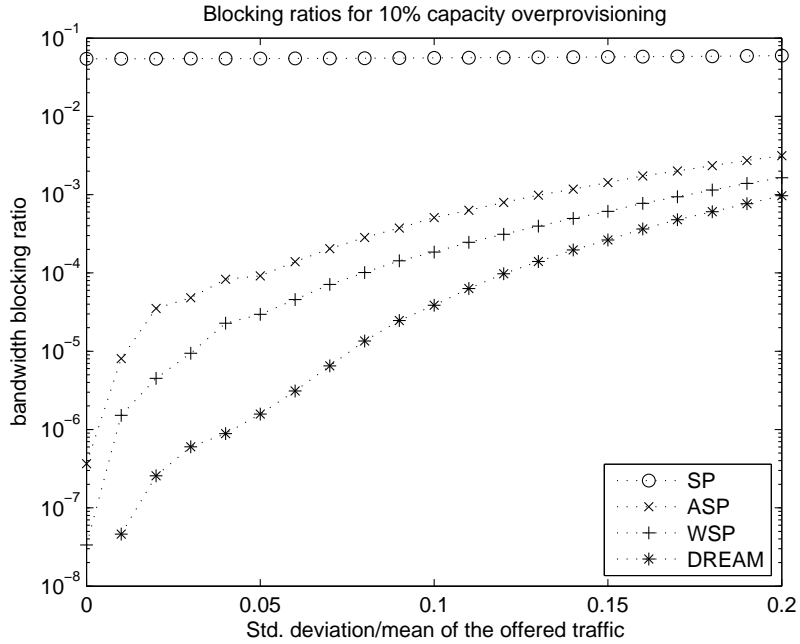
Figure 3.7: Bandwidth blocking ratios for the heuristics on the 14-link network, for $OP = 10\%$

numbers are the minimum values needed by the tabu search algorithm to fulfill all the connection requests with the given capacity. These logical topologies are presented in Section A.1 of Appendix. We define a link capacity overprovisioning ratio, OP, to express the link capacities that are not used in the virtual topology design phase due to the constraint on maximum utilization, as explained in Section 3.2. The overprovisioning ratio can be written in terms of maximum utilization as $OP = (1 - U_{max})/U_{max}$.

The performances of the routing schemes are compared in terms of blocking ratio which is the ratio of the amount of blocked traffic to the total amount of offered traffic. The comparisons are made for $OP = 10\%$ and $OP = 25\%$. The results are presented in Figures 3.7 and 3.8 for the network with 14 nodes and Figures 3.9 and 3.10 for the network with 23 lightpaths, respectively.

In the figures, the x axis is the value of the 'traffic unpredictability parameter' k, which is the ratio of the standard deviation of the offered traffic to its expected value as explained in Section 3.1. The simulations are run for different values of
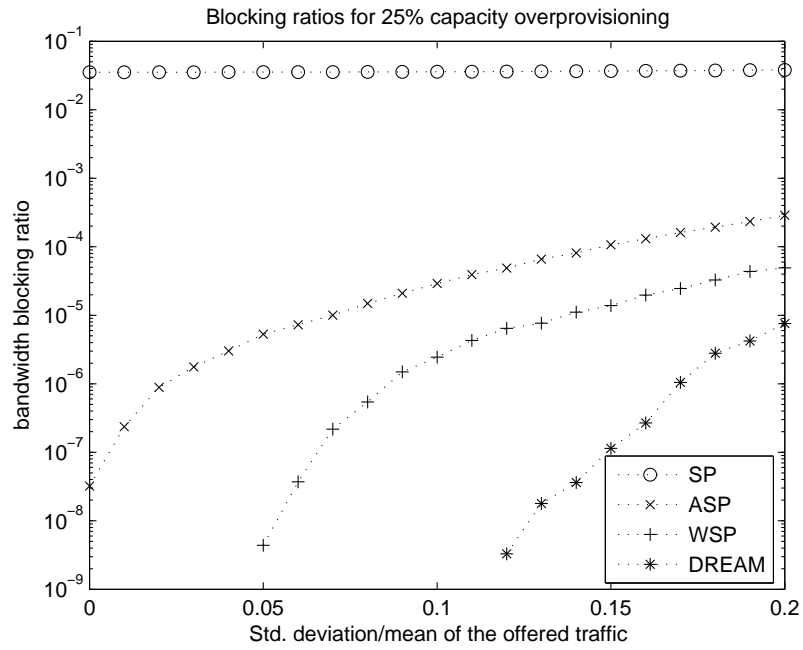
Figure 3.8: Bandwidth blocking ratios for the heuristics on the 14-link network, for $OP = 25\%$
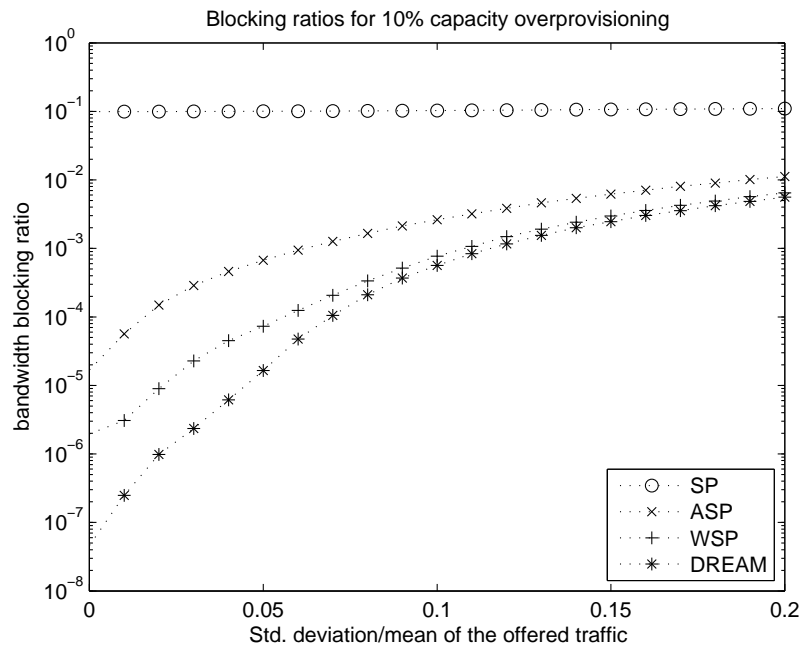
Figure 3.9: Bandwidth blocking ratios for the heuristics on the 23-link network, for $OP = 10\%$
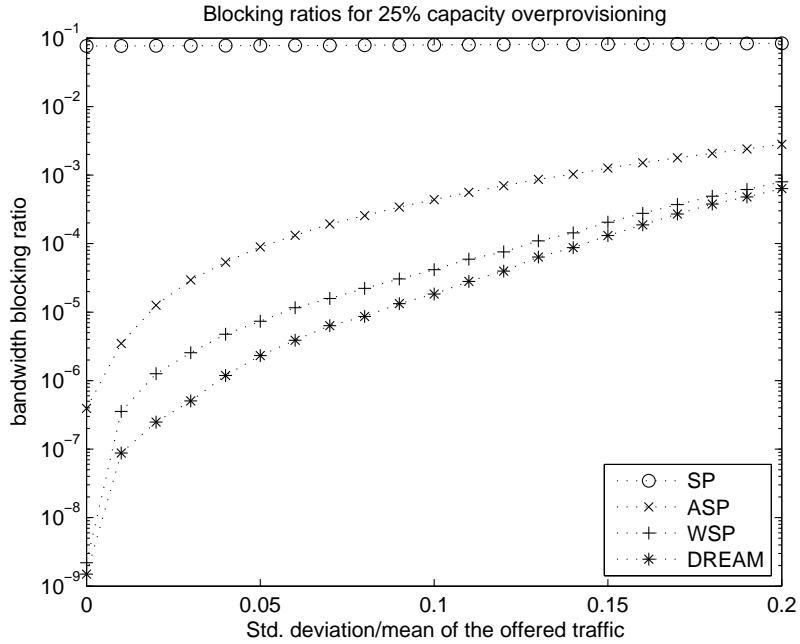
Figure 3.10: Bandwidth blocking ratios for the heuristics on the 23-link network, for $OP = 25\%$

k. The significant difference in blocking ratios of the dynamic rerouting schemes and shortest path routing emphasizes the benefits of traffic engineering. Among the dynamic rerouting schemes, ASP uses only the availability information of the paths (having or not having the sufficient residual capacity), while WSP and DREAM uses the full capacity information of the lightpaths. As a result, these two schemes outperform ASP. Among all the rerouting schemes, DREAM performs best.

3.3.3 LSP Rerouting With Time Limit

Although DREAM achieves the best blocking performance, it may result in a high frequency of LSP reroutings. Each time a bandwidth update request arrives, the best route is calculated and the LSP is rerouted if the calculated route is different than the current one. To prevent excessive number of LSP reroutings which can cause significant signalling overhead, we introduce a lower limit on the minimum amount of time between two consecutive reroutings of the same LSP. Upon the
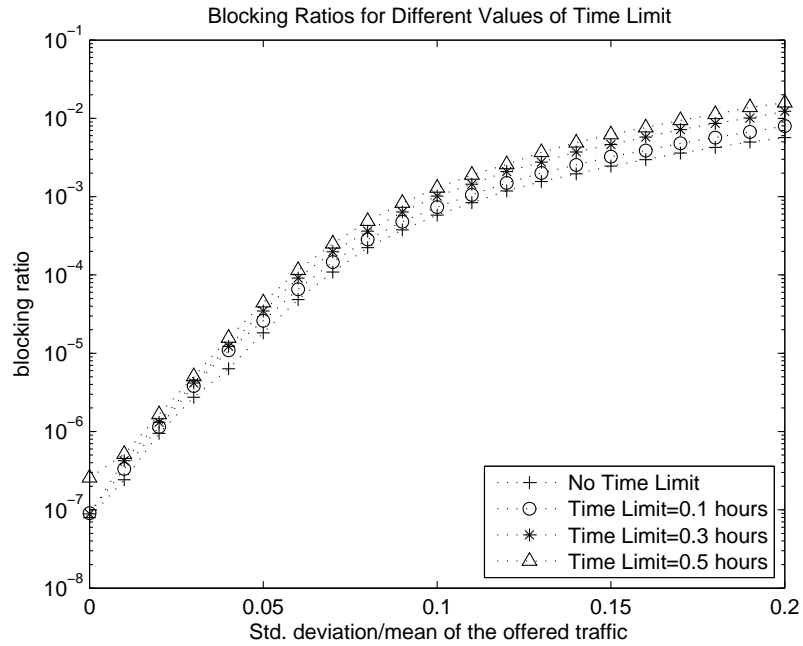
Figure 3.11: Bandwidth blocking ratios for various values of time limit

arrival of a bandwidth update request for an LSP, if sufficient time has not passed after the last rerouting of that LSP, only the bandwidth dedicated to that LSP is updated, however the route is not changed. We investigate the performance of DREAM with different time limits from 0.1 to 0.5 hour using the 23 lightpath network with $OP = 10\%$. The blocking ratios and the maximum number of reroutings per hour per LSP are depicted in Figures 3.11 and 3.12.

As it can be seen from the results, DREAM can generate a little more than 16 reroutings per hour for an LSP in the worst case. Decreasing the number of reroutings by implementing a time limit causes an increase in the blocking ratio. However, it is possible to optimize the blocking ratio and the frequency of reroutings by choosing a time limit that keeps the frequency of reroutings in an acceptable range while not decreasing the throughput below a desired level.
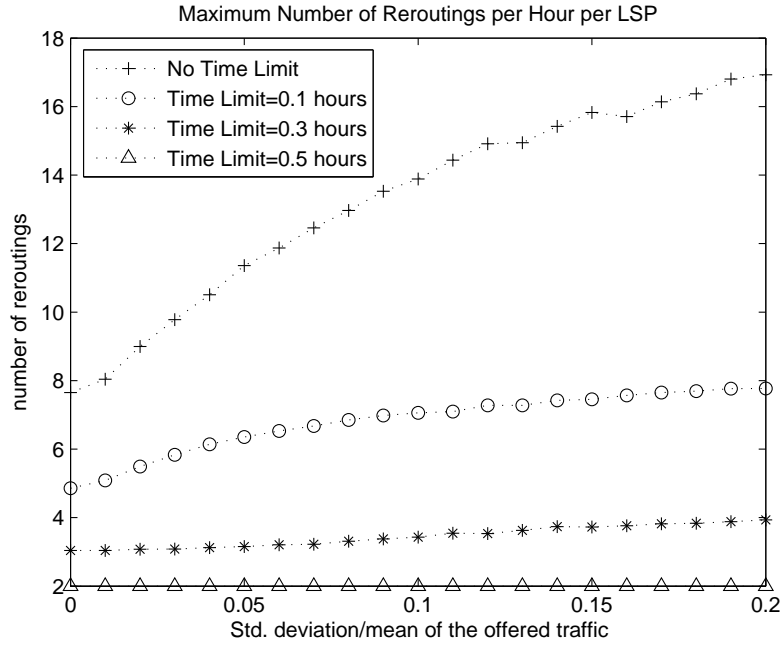
Figure 3.12: Maximum number of reroutings per hour, per LSP, for various values of time limit

3.3.4 DREAM with Multiple Parallel LSPs

If the total traffic between two nodes can be treated as the sum of multiple uninterruptible traffic flows, multiple parallel LSPs can be set up between the source and the sink nodes, and the total traffic can be distributed among these LSPs without splitting the individual flows over multiple LSPs. To model the traffic for the case of P LSPs per node pair, the instantaneous traffic rate of each LSP is calculated independently by using the traffic generation function described in Section 3.1, with an expected value of $1/P$ times the total expected value and a standard deviation of $1/\sqrt{P}$ times the total standard deviation. Hence, the mean and the standard deviation of the total traffic for each node pair is same as the single LSP case. The arrivals of the bandwidth update requests for the LSPs are modeled as independent Poisson processes with a rate of λ/P, where λ is the arrival rate that is used in the case of single LSP per source-destination pair. The blocking ratios of the DREAM are presented for different values of P in Figure 3.13, for a network with 10 nodes and 17 lightpaths and OP=10%. This virtual
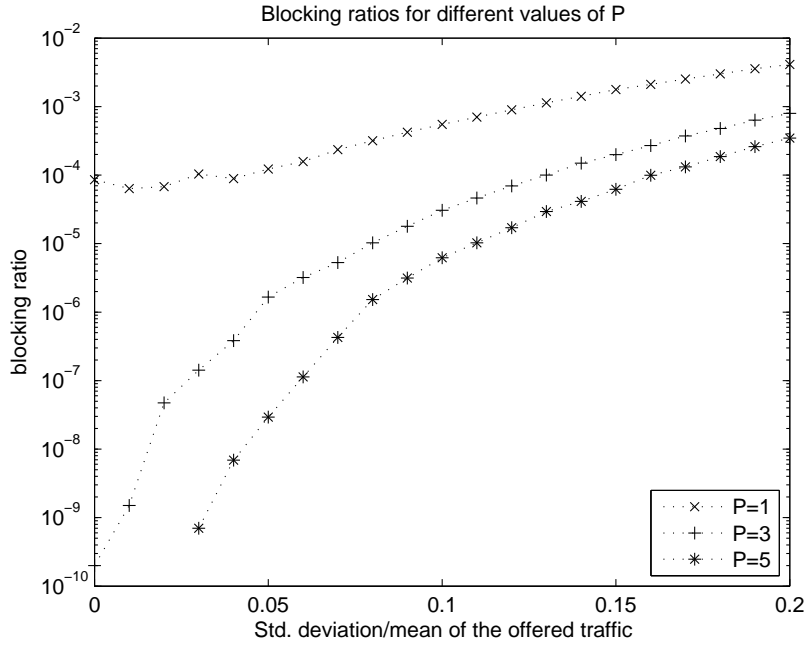
Figure 3.13: Bandwidth blocking ratios for various numbers of parallel LSPs

topology is generated by the tabu search based topology design algorithm and is presented in Section A.1 of Appendix.

The results show that increasing the number of the parallel LSPs brings a significant improvement on the network performance. When the number of LSPs is increased, flow granularity decreases and DREAM can make better use of the residual capacities on the lightpaths at the expense of the additional control plane complexity. As stated in the previous section, splitting the traffic flow between two nodes may cause packet reordering; and achieving a balanced distribution of the incoming packets to the LSPs is another problem that should be considered.

3.3.5 Selecting the Overprovisioning Ratio

In this part, we investigate how much overprovisioning is needed to guarantee a target blocking ratio for different number of parallel LSPs per node pair. Figure 3.14 gives the required overprovisioning, OP, value as a function of the desired blocking probability for various values of number of parallel lightpaths, P. These
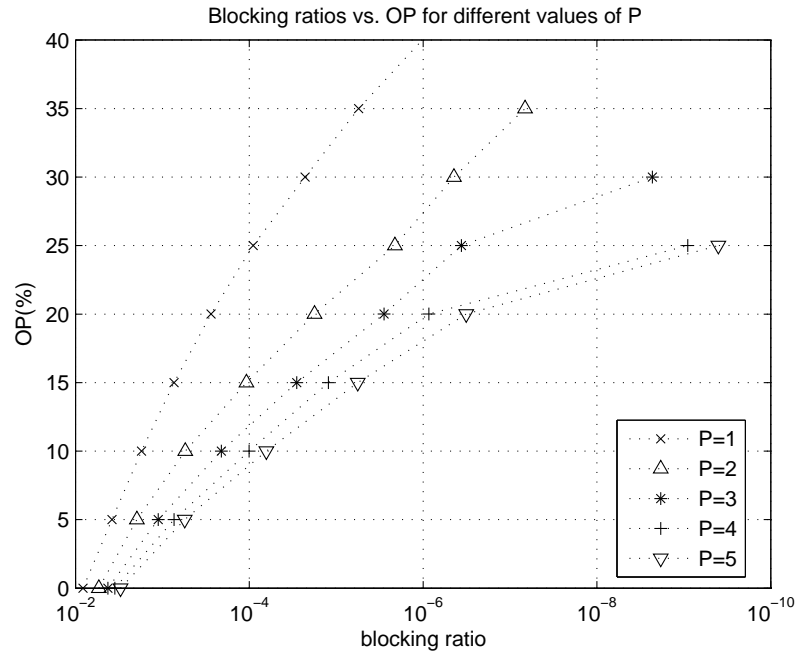
Figure 3.14: Overprovisioning and Blocking ratios for different values of P

results are for a network having 10 nodes and 17 lightpaths. The lightpath capacities without overprovisioning are $3tgen^2$ and the traffic parameter k is 0.15. It is seen from the results that to keep the blocking ratio below 10^{-6}, $OP > 40$ is required if a single LSP is set up between every node pair. If 5 parallel LSPs are set up, the required OP decreases below 20%. Using this figure, the network provider can choose the overprovisioning ratio according to the target blocking ratio and the number of parallel LSPs.

In the following chapter, traffic engineering strategies with static and reconfigurable WDM layers are comparatively studied.

Chapter 4

Comparative Studies of Traffic Engineering Strategies Under Static and Reconfigurable WDM Layers

In this chapter, traffic engineering strategies with static and reconfigurable lightpaths are comparatively investigated. As in Chapter 3, a daily traffic pattern is considered, but as distinguished from the rest of the thesis, it is assumed that WDM layer can be reconfigured by dynamically establishing or tearing down lightpaths. The aim is to evaluate and compare traffic engineering with static and reconfigurable WDM layers.

This chapter is composed of two sections. The first section is based on a common study conducted by Bilkent and Ghent Universities [85]. In this study, traffic engineering strategies with fixed and periodically configurable WDM layers are investigated. The WDM layer constraints are not considered. Section

4.2 is dedicated to a common study of Bilkent University and Budapest University of Technology and Economics (BUTE) [86]. This study compares traffic engineering strategies using fixed and fully dynamic WDM layers. The WDM layer constraints are considered in this study by using the Wavelength Graph Tool developed by BUTE work group and that is responsible for establishing the lightpaths requested by the MPLS layer.

4.1 Comparison of TE with Static and Periodically Reconfigurable WDM Layers

In this section, two TE strategies based on approaches proposed by Bilkent and Ghent Universities [73, 87] are investigated. The former strategy is performed on a fixed WDM layer logical (virtual) topology, while logical topology reconfigurations are involved in the latter. Combining these two TE approaches, a new TE approach is also developed. The performances of the implemented TE strategies are evaluated on a common simulation platform under the same traffic demands. Two different scenarios are investigated: in the first scenario, expected traffic information is available beforehand and the TE strategies make use of this information. In the second scenario, no prior information is available on the traffic and the TE decisions are done according to instantaneous traffic. The benefits of both approaches are discussed based on the results.

The first TE strategy is based on the TE method explained in Chapter 3. It is based on the optimization of the LSP routes by the MPLS layer control plane, on a fixed WDM layer logical topology. In the second strategy, the WDM layer logical topology is reconfigured periodically to adapt to the changing traffic pattern [85]. The third strategy combines the advantages of both approaches, the logical topology is reconfigured periodically and between the topology updates, LSP routes are updated to better accommodate the traffic flows. .

WDM layer is not considered in this Section. It is assumed that there's infinite capacity and perfect physical layer conditions in the WDM layer, and the WDM layer control plane is capable of providing any requested lightpath connection.

4.1.1   TE on Fixed Logical Topology

This TE strategy, denoted as Traffic Engineering Strategy-1 (TES-1), makes use of the available information on expected traffic. An optimized WDM layer virtual topology is constructed by using the performance oriented Tabu Search Topology Design algorithm introduced in Section 3.2.2. Online TE is performed by LSP rerouting, using DREAM TE scheme, which was introduced in Section 3.3.1.

4.1.2   TE with Periodic Logical Topology Updates

This TE strategy (TES-2)is based on a previous study conducted by Ghent University [73]. In this strategy, both routing and topology generation are combined into a single step by relying on a load-based cost function for routing the MPLS flows. In order to groom flows onto IP/MPLS links, the load-based link cost function has a high cost 'bump' (Figure 4.1, taken from [73]) for IP/MPLS links (whether they are setup or not) with a load below a certain threshold load (the Low-Load Threshold, LLT). The cost bump also prevents routing flows with low bandwidth over unutilized links, in other words, it prevents the setup of links for very small amounts of traffic. The resulting 'trench' in the cost function will concentrate link-loads in this optimal region (medium-load cost MC). The cost-function, with some settable parameters such as LLT, and the MC/LC ratio (LC: Low-load Cost) provides for IP/MPLS routing and also logical topology generation through the mechanism described.
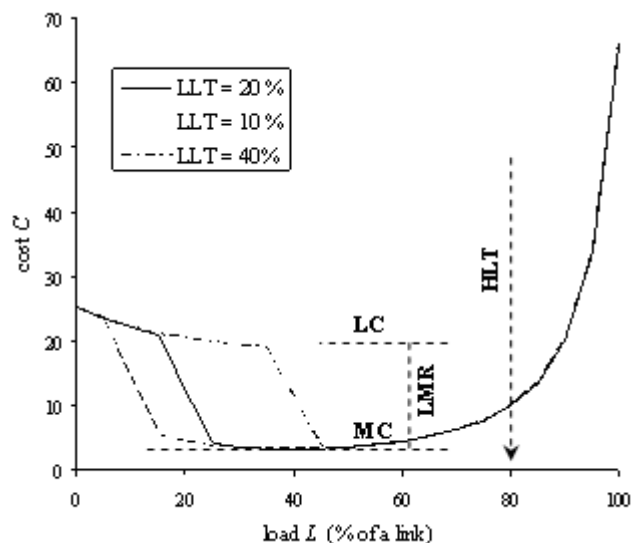
Figure 4.1: Link cost function for TES-2

4.1.3 TE with Periodic Logical Topology Updates and Dynamic LSP Rerouting

In strategy TES-3, the WDM layer logical topology is reconfigured periodically using the same mechanisms as in TES-2 strategy. Between the topology update instances, the routes of the LSP flows are updated dynamically using the DREAM LSP rerouting scheme as used in TES-1, with the modification that the set of the shortest paths are recalculated after each logical topology reconfiguration. This approach combines the strong sides of the single layer and the multi-layer TE actions. While the WDM layer topology is reconfigured to cope with the large fluctuations in the traffic demands that occurs in a longer period, adaptation to the smaller changes are done with the rerouting actions in the upper layer.

4.1.4   Simulation Framework

A common simulation platform is developed to evaluate the performances of the TE strategies. The same 24 hour traffic pattern that is introduced in Section 3.1 is used and it is assumed that the expected values of the traffic flows are previously available in the form of a traffic matrix. A single LSP is established for each source destination pair and the changes in the traffic flow are modelled by updating the bandwidth requirement of the LSP. The bandwidth updates arrive according to a Poisson process and the update times belonging to each LSP are independent. While producing the actual traffic for simulations, to calculate the instantaneous bandwidth of an LSP, a zero mean Gaussian noise is added to the expected bandwidth value of that traffic flow at the bandwidth update instance. The standard deviation of the added noise is proportional to the expected bandwidth value. The ratio of the standard deviation to the expected value is denoted by the parameter k, which is used to represent the amount of uncertainty in the available traffic information and is referred as 'traffic unpredictability parameter' through the rest of this section.

Two different scenarios are investigated in simulations. In Scenario 1, for each traffic flow, the maximum value of the bandwidth expectation belonging to each hour is known. TES-1 strategy designs the fixed logical topology using this information, to maximize the amount of routed traffic during over 24 hours. To make a fair comparison, TES-2 and TES-3 design a separate topology for each hour according to the bandwidth expectation in that hour. In Scenario 2, the algorithms do not use any statistical information on the traffic, and the topology reconfigurations are performed using the instantaneous bandwidth requirements of the traffic flows at the start of each hour.
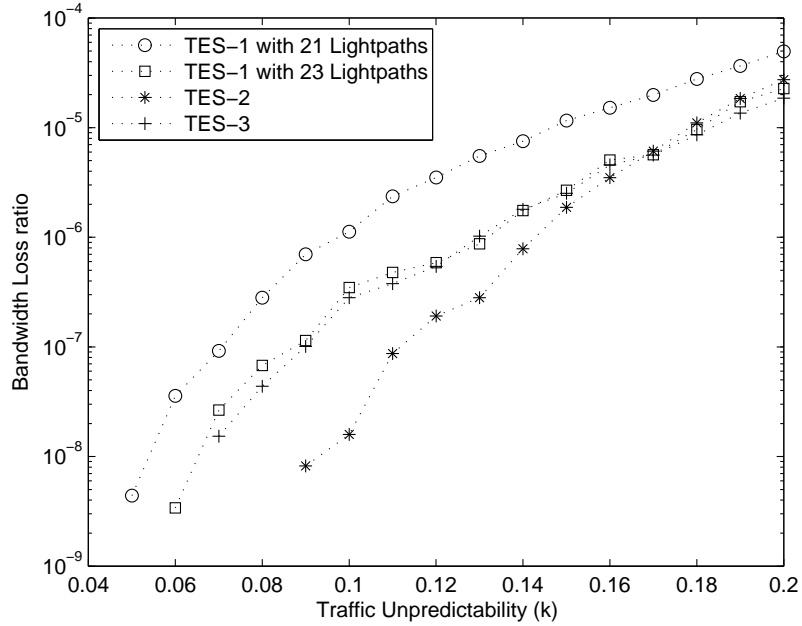
Figure 4.2: Bandwidth blocking ratios for Case 1

4.1.5 Results

Simulations are run for different values of the traffic uncertainty parameter k. For Scenario 1, the bandwidth blocking ratios for the three TE strategies are depicted in Figure 4.2. The number of lightpaths set up by each strategy is used as the metric representing usage of network resources. TES-2 and TES-3 established 20.5 lightpaths per hour on the average. To evaluate the performance of TES-1, two logical topologies are designed with 21 and 23 lightpaths.

Scenario 1: Previously Available Traffic Expectations

As it is seen from the results, the strategies with topology updates, TES-2 and TES-3, outperform TES-1 which uses the fixed topology for the same number of utilized lightpaths. This is an expected result, since these strategies design separate topologies for each hour according to the traffic expectations in that hour. In this study, it is assumed that the transitions between logical topologies can be done instantly, without disrupting the traffic flows. However, in a realistic

scenario transition from one logical topology to another rises another important problem. Establishment of some lightpaths may not be possible before tearing down others and the traffic flows routed on the lightpaths that are torn down will be disrupted. As a result, if large number of lightpath reconfigurations occur, the network will not be fully operational at the reconfiguration instance.

We can also see from Figure 4.2 that, using more network resources, i.e., setting up more lightpaths, it is possible to achieve a similar performance to the dynamic topology TE strategies on a fixed logical topology. In the simulations TES-1 achieves this on a 23 lightpath network which corresponds to approximately 12% more resources.

An interesting observation is that, when the traffic unpredictability is low, TES-2 shows a better performance than TES-3 which performs LSP route updates between the topology reconfigurations. This is because if the traffic information used when designing the logical topologies is more precise, the routes calculated along with the topologies are better suited for the traffic patterns. When the unpredictability increases, rerouting the LSPs becomes effective in preventing blockings.

Scenario 2: No Previously Available Traffic Information

The blocking performances of TES-2 and TES-3 are shown in Figure 4.3 for Scenario 2. TES-1 needs the statistical traffic information in order to design a fixed logical topology, and it is not included in this scenario because it would not be meaningful to compare a strategy designing a fixed topology randomly with no traffic information, with strategies reconfiguring the topology according to the traffic.

The results show that, when there is no available traffic information, TES-3 has a better blocking performance than TES-2. This is expected since the
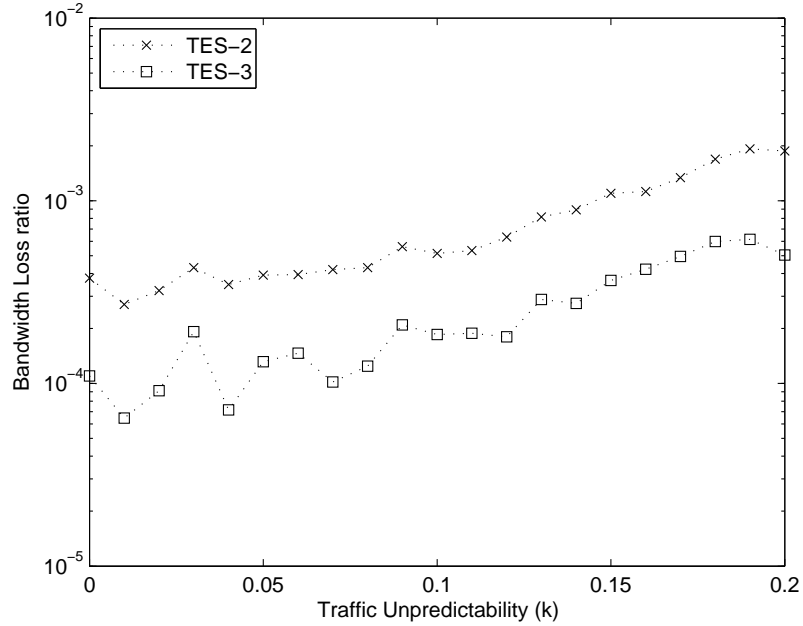
Figure 4.3: Bandwidth blocking ratios for Case 1

previous results also showed that LSP rerouting improves the performance when the utilized traffic information is not accurate. Another important remark is the performance difference of the TE strategies for the two investigated scenarios. When the strategies make use of the information on the traffic expectation in Case 1, their performances improve several orders of magnitude. Even TES-1, which uses a fixed logical topology, outperforms the other two strategies when they use only the instantaneous traffic information.

4.2 Comparison of TE with Static and Dynamic WDM Layers

This section represents a comparative evaluation of two traffic engineering strategies developed by Budapest University of Technology and Economics (BUTE) and Bilkent University, respectively. The first strategy assumes a static WDM layer and relies on a well planned design of WDM layer topology and dynamic

LSP rerouting in the MPLS layer for traffic engineering. The second strategy assumes a fully dynamic WDM layer and performs lightpath reconfigurations to adapt the topology to the changing traffic requirements.

4.2.1 Traffic Engineering With Dynamic Logical Topology

This strategy is based on a previous study of BUTE [88]. The aim is to create a reasonable, feasible and inexpensive lightpath set: as few network resources (wavelength channels and opto-electronic converters) have to be reserved as possible to accommodate the offered traffic. If a new demand arrives at the network, the following actions can happen: Its traffic can be groomed together with the traffic of already existing lightpaths, in this case, lightpaths will carry more traffic; new lightpaths can be created; or existing lightpaths can be fragmented to multiplex/demultiplex the traffic of the new demand at a certain node.

To apply this strategy, a network model is needed, which represents not only different wavelengths but inner structure of network nodes as well, to be able to keep the introduced constraints. To this aim, the so called Wavelength Graph model was introduced [88]. Wavelength graph can be derived from the real physical network. In a wavelength graph, network nodes are modelled by subgraphs. Topologies of these subgraphs are based on the function of the modeled network node. Network links are modeled by as many graph edges as the number of wavelengths that can be utilized in the fiber. The costs of the edges in a wavelength graph are based on their functionality. We will refer to the simulator applying the introduced wavelength graph model as Wavelength Graph Tool (WGT).

In this strategy, dynamic WDM layer means that no constant lightpath set is determined neither in advance, nor periodically. Lightpaths are added/dropped dynamically based on traffic demands appearing/expiring in the upper layer.

Therefore, demands are not routed strictly on the already existing lightpath set. Instead, the common Control Plane investigates how the lightpath set should be modified in order to serve the recently arrived demand the most economical and efficient way. The advantage of this method is that lightpath set is exploited as far as possible. Additionally, a demand is not refused until there are no available resources in the network. However, the disadvantage of the method is that frequent changing of the lightpath set causes delay of the traffic or even traffic loss. To avoid frequent updates of WDM layer, weights of wavelength graph have to be set; so that traffic grooming is preferred against lightpath fragmentation.

4.2.2   Traffic Engineering on Fixed WDM Topology

The traffic engineering strategy applied in this part is based on the Logical Topology Design algorithm and the DREAM TE scheme explained in Sections 3.2.2 and 3.3.1, respectively. Limited physical layer resources are assumed, therefore the feasibility of the designed virtual topology in the designed topology should be verified in the WDM layer. To this aim, the Wavelength Graph Tool (WGT) is used to simulate the WDM layer. Topology design algorithm communicates with the WGT and requests the establishment of the lightpaths in the designed virtual topology. WGT acts as the control plane for the WDM layer and sets up the lightpaths requested by the MPLS layer. If a lightpath connection request cannot be satisfied, WGT informs the MPLS layer control plane and the topology design algorithm searches for the next best lightpath and requests its establishment. The number of lightpaths to be established is determined according to the amount of traffic in the traffic matrix. After a number of unsuccessful tries, topology design algorithm decreases the number of lightpaths and tries to generate a new topology.

4.2.3 Simulation Framework

The performances of the two TE strategies under the same traffic are investigated by simulations. The underlying physical network has 10 nodes and 12 links with two fibers at each link in the opposite directions. The physical topology is given in Section A.2 of Appendix.The traffic is modeled as LSP flows, as in Section 3.1. The traffic unpredictability parameter k is chosen as 0.1. The nodes in the network hava a uniform traffic generation rate, $tgen$. A single LSP is established for each source destination pair using resource reservation and the changes in the traffic flows are modeled by updating the bandwidth requirements of the LSPs. The bandwidth updates arrive according to a Poisson process with rate $\lambda = 30$ arrivals per hour.

In the fixed topology TE method, when a bandwidth update request arrives for an LSP flow, the best path is chosen among the previously calculated paths between the source and destination nodes. Then, the LSP is rerouted along the chosen path with the new bandwidth. In the Dynamic Topology TE strategy, the arrival of a bandwidth update request is treated as departure of the current LSP and arrival of a new one at the same instance with the new bandwidth requirement. In both of the strategies, if the requested bandwidth cannot be satisfied, LSP's bandwidth is not changed and the amount of bandwidth that cannot be satisfied is lost.

The ratio $tgen^2$ to the capacity of a single lightpath is referred as the '**traffic magnitude**'. The loss and resource usage performances of the TE strategies are investigated versus the traffic magnitude for various numbers of wavelengths per fiber. The blocking performance and resource usage of both TE strategies are evaluated both individually and comparatively by simulations carried out with the same traffic demands for each strategy.

4.2.4 Comparative Results

The traffic loss ratio of the two TE strategies are given for 4, 8 and 12 wavelengths in Figure 4.4. The traffic loss ratio of the Dynamic Topology strategy is generally half a magnitude lower than the loss ratio of the Fixed Topology strategy, as expected. When the physical layer resources are not sufficient to construct a fixed virtual topology to accommodate the traffic demands, rerouting LSPs is not sufficient to prevent blockings. But, the Dynamic Topology strategy utilizes every possible resource available in the physical layer to route the traffic demands. This improvement in the blocking ratio is at the expense of WDM topology reconfigurations with a frequency changing between 1.8 and 33 per hour, depending on the number of wavelengths and traffic magnitude (Figure 4.5). In this study, we did not numerically calculate the effects of topology reconfigurations, but in a real life scenario these reconfigurations cause delay and extra traffic loss by interrupting the traffic flows passing through the reconfigured lightpaths.

The wavelength resource usages of the two strategies are given in Figure 4.6 for the same set of wavelength numbers. As it can be seen from the results, Dynamic Topology strategy uses as much resources as possible to route the traffic demands. It uses nearly all the resources in the 12 link physical layer topology for $W = 4$. The Fixed Topology strategy does not have any information on the physical layer. Therefore, in the case of blockings, even if there are sufficient resources in the physical layer to route more traffic, it may not be able to utilize these resources. As a result, wavelength resource usage of the Fixed Topology strategy is considerably lower. As Figure 4.7 shows, the average number of lightpaths established by the Fixed Topology strategy is also significantly lower than the Dynamic Topology strategy. Consequently, the Fixed Topology strategy has lower cost to both in the WDM and in the MPLS layers.
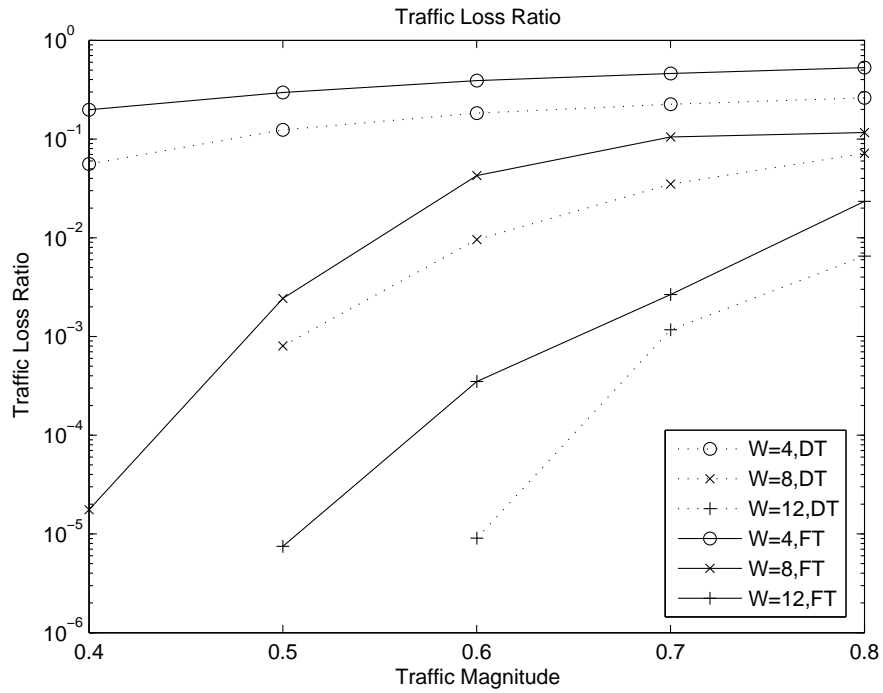
Figure 4.4: Traffic loss ratios for the Fixed Topology(FT) and Dynamic Topology(DT) strategies
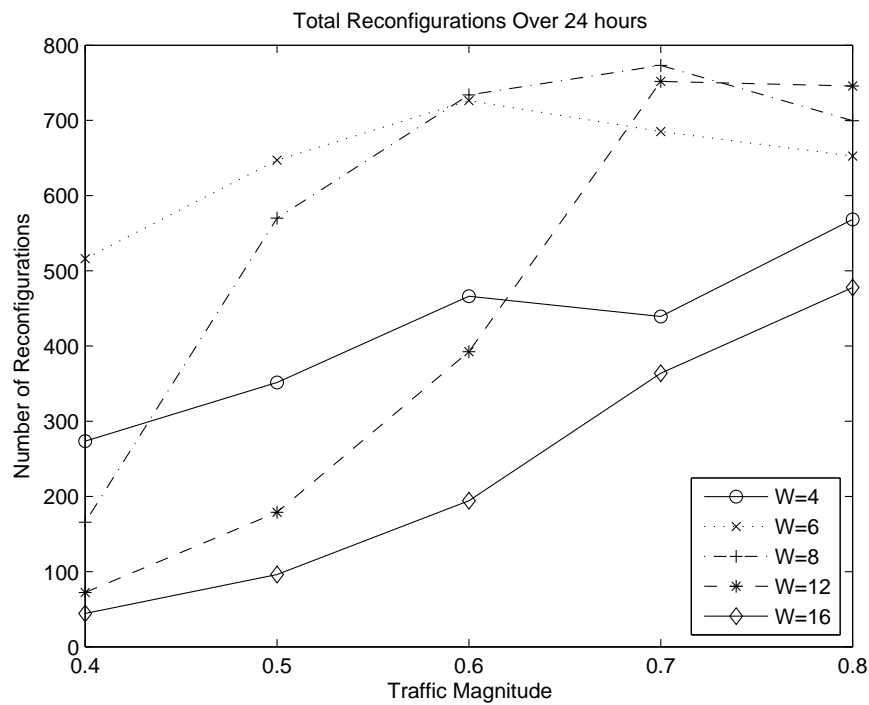
Figure 4.5: Average number of topology configurations per hour for the Dynamic Topology strategy
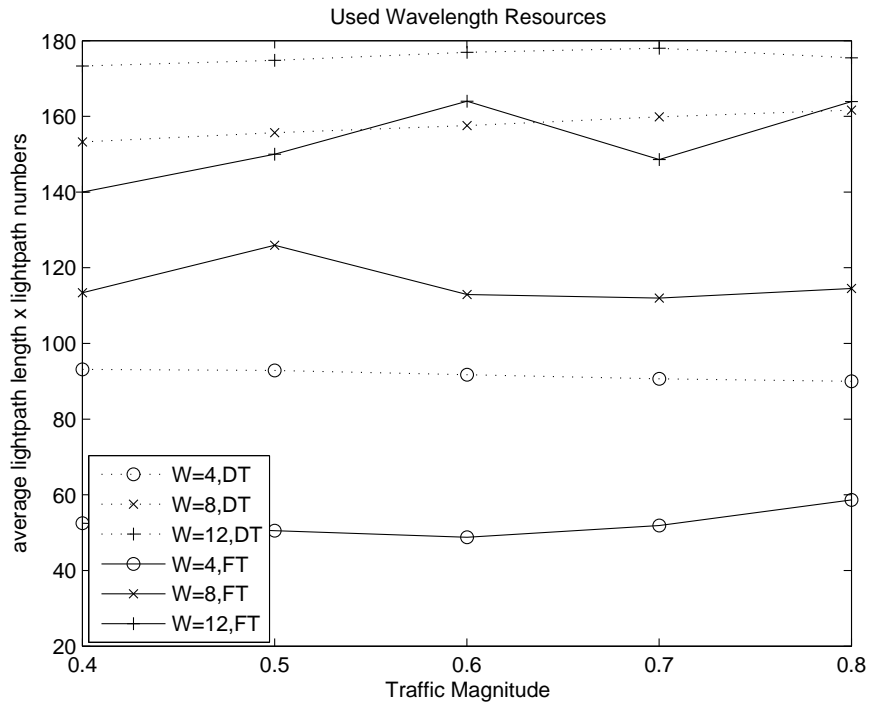
Figure 4.6: Utilized wavelength resources for the Fixed Topology(FT) and Dynamic Topology(DT) strategies
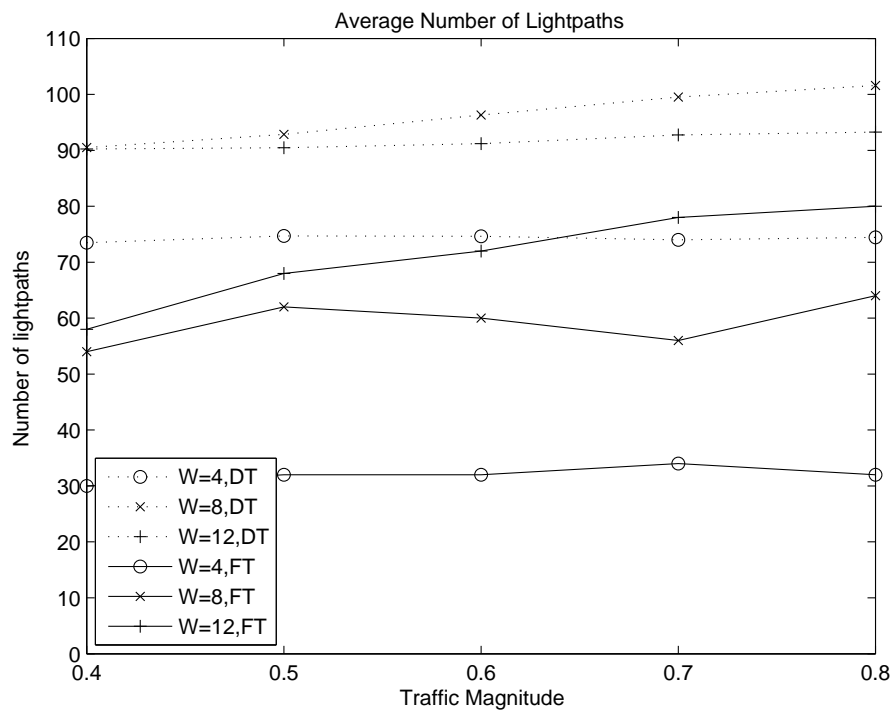
Figure 4.7: Average number of lightpaths established by the Fixed Topology(FT) and Dynamic Topology(DT) strategies
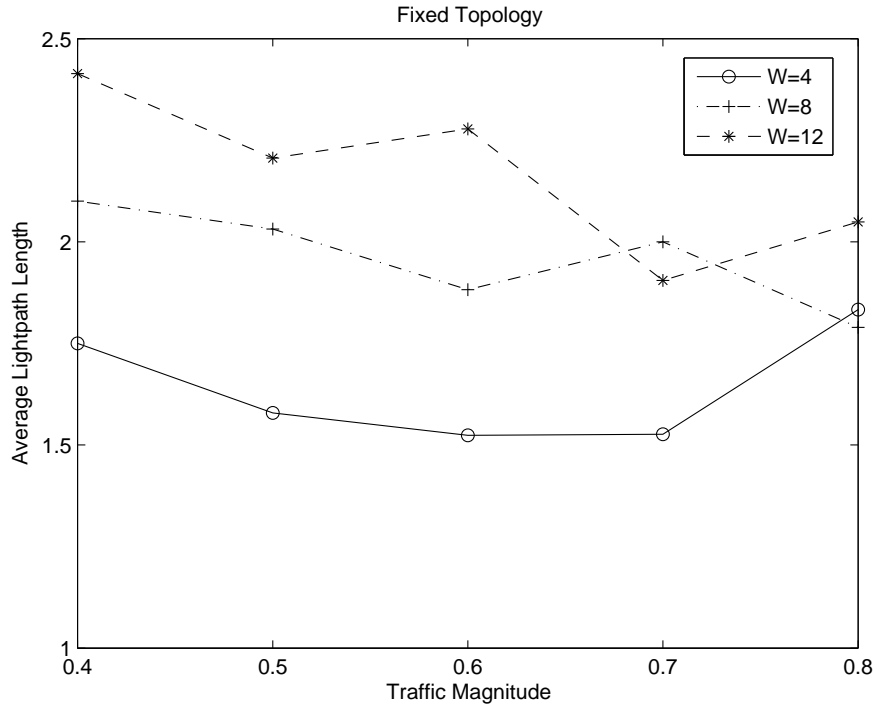
Figure 4.8: Average length of the lightpaths established by the Fixed Topology strategy

The average hop lengths of the established lightpaths, i.e., average number of hops along the lightpaths, for the Fixed Topology and Dynamic Topology strategies are presented in Figures 4.8 and 4.9, respectively. Since the Dynamic Topology strategy prefers direct lightpaths and avoids defragmentation of existing lightpaths, the lightpaths established in this strategy are shorter. In the Fixed Topology strategy, the MPLS layer has no information on the physical layer, therefore it cannot request shorter lightpaths from the WDM layer. The only considered WDM layer resource in this approach is the number of lightpaths. This results in topologies with less but longer lightpaths. Nevertheless, despite the higher average lightpath length, the amount of wavelength resources used by the Fixed Topology strategy is smaller than the wavelength resources used by the Dynamic Topology strategy.

In the following chapter, TE in the WDM layer is investigated. First, an overview of the physical layer impairments and the considered physical layer
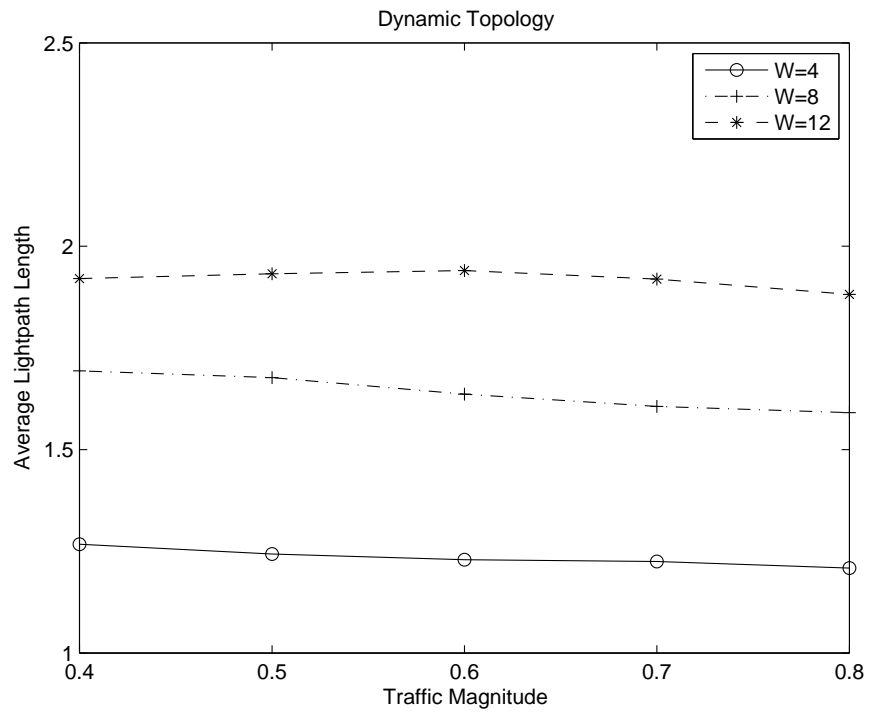
Figure 4.9: Average length of the lightpaths established by the Dynamic Topology strategy

model are given. Then, the TE problem corresponding to the WDM layer, the lightpath establishment problem, and our proposed solution to this problem are introduced.

Chapter 5

Traffic Engineering in WDM Layer

In the multi-layer traffic engineering scheme we developed in this thesis, the corresponding problem in the WDM layer is the establishment of the requested lightpaths by the MPLS layer, which is known as the lightpath establishment problem. Since the set of requested lightpaths is known beforehand, this problem is also referred as the static lightpath establishment problem. In this problem, the objective is to establish as many of the lightpaths from this set as possible, using limited physical layer resources. It is assumed that wavelength conversion is not available in the optical layer, and the wavelength continuity constraint should be satisfied along the established lightpaths. The physical layer impairments are also taken into consideration, so that Bit Error Rates (BERs) along all established lightpaths should remain below the upper threshold.

We propose a polynomial time heuristic solution for the static lightpath establishment problem: ReOrdered Lightpath Establishment (ROLE). We evaluated the performance of ROLE by running it to solve lightpath establishment problems on various topologies with different parameters. We used the ratio of

established lightpaths to the number of offered lightpath demands as the main performance criterion. The fairness in the produced solutions, i.e., providing close acceptance ratio to lightpath demands with different shortest path lengths, is also investigated. ROLE can be incorporated with different RWA algorithms. We implemented a total of eleven combinations of routing and wavelength assignment algorithms, and evaluated performance of ROLE with each of them.

We also developed an ILP formulation for the problem. Since lightpath establishment problem is NP complete, we used this ILP formulation as a performance benchmark for ROLE on smaller size networks, and to provide upper bounds even when the ILP model cannot be solved to optimality, for larger problems. We compared the solutions produced by ROLE and by solving the ILP formulation for a number of lightpath establishment problems. We have observed that the number of lightpaths that can be established by ROLE is close to the optimum solutions for all the problem sets, for which the optimum solution can be obtained. In the solutions generated by solving the ILP formulation, longer lightpath demands have considerably higher blocking probabilities than shorter lightpaths. ROLE can produce solutions with a more fair blocking distribution according to lightpath demand lengths, in which longer lightpaths have a higher probability of being established, compared with the ILP formulation solutions.

Then, we compared the performance of ROLE with a recently proposed heuristic algorithm Pre-Ordering Least Impact Offline-RWA (POLIO-RWA) [34], in terms of number of lightpaths that can be established from the offered demand set. Our numerical studies show that ROLE can establish up to 14% more lightpaths than POLIO-RWA algorithm.

The effect of switch crosstalk, the most dominant physical layer impairment in the utilized model, on the produced solutions is also investigated. According to the results, for values smaller than -35 dB, the switch crosstalk ratio has a negligible effect on the number of established lightpaths and for -25 dB and

higher values, it has the maximum effect. For changing values of switch crosstalk ratio, we investigated the ratio of lightpath demands blocked due to insufficient capacity and due to high BER.

The rest of this chapter starts with an introduction to the most important physical layer impairments that cause optical signal quality degradation. Then, the optical switch architecture used in this study and the model used for calculating BERs are explained. After that, the ILP formulation proposed for the investigated lightpath establishment problem is presented. Then, the proposed heuristic solution, ROLE algorithm, is introduced. The chapter is concluded with numerical results and comparative performance evaluation of ROLE.

5.1 Physical Layer Impairments

5.1.1 Attenuation

In optical fibers, the transmitted optical power decays exponentially along the fiber as stated in the formula $P_{out} = P_{in}.e^{-\lambda L}$, where L is the length and λ is the loss coefficient (m^{-1} or km^{-1}). In linear transmission lines, using the logarithmic unit is more convenient, so the attenuation in decibels is given by the formula :

$$A_{dB} = 10log\frac{P_{in}}{P_{out}} = \lambda.L \qquad (5.1)$$

There are three types of loss mechanisms causing attenuations [89]:

Material Absorption

Material absorption can be of three types: intrinsic material absorption, extrinsic absorption and absorption due to dopants. Intrinsic material absorption is

caused by the fused silica, the main material of the optical fiber. There are three wavelength windows in the IR region, that is used for transmission in fibers: 850, 1300 and 1550 nm. Contemporary systems use the 1550 nm window which has the minimum attenuation [90]. Absorption of silica is significant in the UV region and in the IR region beyond 2 μm. Extrinsic absorption is due to the OH impurities caused by absorption of water molecules during production. OH absorption makes a peak around 1.4 μm region. Today, OH free fibers without this absorption peak at 1.4 μm are available. Dopants such as Ge, Al, P, B, Ti and F also cause absorption but their influence is neglicible near the IR region [89].

Rayleigh Scattering

There exist microscopic density fluctuations of silica in the fiber, which are caused by the fabrication process. This results in fluctuations of the refractive index on a scale smaller than the optical wavelength. The scattering of the light in such a medium is referred as Rayleigh scattering [89]. It is the main contributor of the losses around 1550 nm.

Waveguide imperfections

The bendings in the fiber can be an important source of scattering loss. Macroscopic bends may cause the ray escape out of the fiber. Since macrobending losses are negligible for a radius greater then 5mm and most macroscopic bends have radii greater then this value, macrobendings are negligible in practice. Another type of bending loss is microbending losses, which is related to the random axial distortions occurs during cabling if precautions are not taken to minimize them [89].

5.1.2 Crosstalk

While the optical signal propagates through the fiber or transmitted through optical equipments such as OXCs, it interferes with signals at different channels and the power is transmitted from one channel to the other. This event which degrades the performance of the system is known as the crosstalk. Imperfect natures of the WDM components such as optical filters, de/multiplexers and switches are the main sources of crosstalk. Linear crosstalk can be classified as out of band (hetero-wavelength) crosstalk, which involves signals at different wavelengths; or in band (homo-wavelength) crosstalk, which occurs between signals at the same wavelength while they pass through optical equipments such as optical routers and switches [91]. Nonlinear effects such as FWM, SPM, XPM and Raman scattering can also generate crosstalk. These effects are explained in Section 5.1.5.

5.1.3 Amplified Spontaneous Emission (ASE) Noise

For fiber systems designed for operation over long distances, the losses that accumulate along optical paths need the be compensated. Until 1990s, this was achieved by the use of optoelectronic regenerators (i.e., repeaters) converting the signal to electric domain and then reproducing it in the optical domain. This technique is quite expensive and cumbersome for WDM channels since a separate repeater is needed for each channel. Optical amplifiers, developed during 1980s, can amplify multiple WDM channels simultaneously and they are deployed in almost all WDM optical systems today. These amplifiers can be grouped into two categories as lumped and distributed amplifiers. Erbium-doped fiber amplifiers are of the former category and can compensate losses accumulated over long distances such as 60-80 kms in relatively shorter (about 10 m) lengths [92]. Distributed amplifiers perform the amplification along the fiber itself in

much longer distances (about 12 km for the same amount of amplification [93]). Raman amplifiers are of this category.

Optical amplifiers degrade the Signal to Noise ratio (SNR) of the amplified signal by adding Amplified Spontaneous Emission (ASE) noise, which accumulates along the path of the optical signal. This noise is much smaller for Raman amplifiers due to their distributed nature and more dominant for EDFAs. ED-FAs include a large population of Er^{+3} ions in an Erbium-doped strand of silica fiber. These ions are excited by a laser pump. Amplification is achieved by the excited ions returning to their base state. Some of the excited ions emit photons with random phases by spontaneous emission and this process is the source of the ASE noise [94].

5.1.4 Dispersion

The waveguide equations and boundary conditions governing the propagation of light in the optical fiber has multiple solutions. Each of these solutions is referred as an optical mode [89]. The fibers are classified as single-mode or multimode according to the number of modes they support.

Dispersion of the optical signal causes broadening of the transmitted optical pulses, create Inter-Symbol Interference (ISI) and reduces the bandwidth of the optical fiber. Dispersion can be classified according to its origin as Intramodal (Chromatic) Dispersion or Intermodal Dispersion. Intramodal dispersion occurs in all types of fibers and is caused by the changing of the group velocity depending on the wavelength. It has two main contributors: Material dispersion, caused by the change of the refractive index of the medium with the wavelength; and waveguide dispersion, which depends on fiber parameters such as radius and the index difference between the core and the cladding. Material dispersion is vanishes at about 1280 nm. Waveguide dispersion can be negative and by adjusting

it, it is possible to design fibers with zero dispersion at 1550 nm. This type of fibers are known as dispersion shifted fibers. By the same principle, it is possible to produce dispersion compensating fibers that compensates the dispersion by adding negative dispersion [89]. Intermodal dispersion is the pulse broadening due to the delay differences between the propagation modes in multimode fibers and does not occur in single-mode fibers.

Another source of dispersion is the fiber birefringence. Small departures from the cylindrical symmetry leads to birefringence since the field components along the two principal axes propagates with different propagation constants. This phenomenon is called Polarization Mode Dispersion (PMD). The random changes in the birefringence may induce pulse distortion and cause bit errors at the detector, which is an important factor limiting the performance of optical systems [89].

5.1.5   Nonlinear Effects

Silica is not a highly nonlinear material, however the waveguide of the optical signals with small cross sections and much longer lengths creates nonlinear effects. These effects are quite important in the design of optical systems. There are two sources for the main nonlinear effects in optical fibers: Kerr effect and the Stimulated Light scattering. Due to Kerr effect, the refractive index of silica changes with the intensity of the electromagnetic field propagating through it. Kerr effect is the source of three relevant nonlinear effects in optical systems: Self Phase Modulation, Cross Phase Modulation and Four Wave Mixing.

Self Phase Modulation (SPM)

If an intensity modulated signal propagates through the fiber, the modulation of the intensity modulates the refractive index of silica and this generates a phase

modulation to the signal. As a result the transmitted pulse will be distorted and its spectrum will be broadened [89].

Cross Phase Modulation (XPM)

In the case of multi-channel propagation at different wavelengths, the signals will also modulate each other through index modulation. This phenomenon is referred as XPM [89].

Four Wave Mixing (FWM)

If three optical fields with frequencies w_1, w_2 and w_3 copropagate inside the fiber, a fourth field will be generated with frequency w_4, such that $w_4=w_1+w_2-w_3$ if a phase matching condition is satisfied. This is effect is called four wave mixing [89].

Raman and Brillouin Scattering

In elastic scattering (as in Rayleigh scattering), the energy of the photons and the frequency of the scattered light do not change. In inelastic scattering events such as Raman scattering and Brillouin scattering, the frequency of the scattered light is shifted downward and the energy difference between the photons appear as a phonon (phonons are quantum modes of vibrations in solids). Raman scattering involves optical phonons, while Brillouin scattering, involves acoustic phonons. The influence of spontaneous Raman and Brillouin scattering at low power levels are neglicible. However when the incident power exceeds a threshold, the intensity of the scattered light grows exponentially. This phenomenon is called stimulated Raman or Brillouin scattering [89]. Raman amplifiers make use of Raman scattering and allows the amplification of the signal within the fiber.
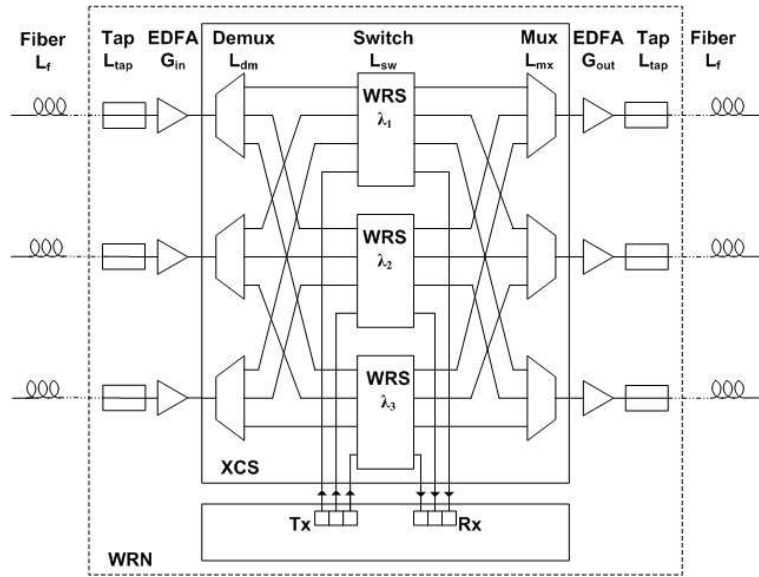
Figure 5.1: Wavelength routing node architecture

5.2 Switch Architecture and BER Calculation

For the wavelength switch architecture, the model proposed in [47] is used. The internal structure of a Wavelength Routing Node (WRN) is presented in Figure 5.1. In this model, the WRN includes a cross connect switch (XCS), a pair of EDFAs and optical power taps for monitoring purposes, on input and output sides at each port. The XCS consists of an array of demultiplexers, optical Wavelength Routing Switches (WRSs), and an array of multiplexers.

For the optical fiber architecture, the model presented in [93] is used. Backward-pumped Distributed Raman Amplifiers (DRAs) are used as in-line amplifiers along the fiber. In each amplification span, a standard single fiber mode (SSMF) is followed by a dispersion compensating fiber (DCF). DRA compensates the attenuation along DCF and SSMF; and DCF compensates the chromatic mode dispersion along SSMF. Attenuation occurring between the last DRA and the WRN; and the internal losses of the WRN resulting from the taps, multiplexers, demultiplexers and the switching fabric of the XCS are compensated by the EDFA amplifiers at the input and output ports of the XCS. While signals are passing through the XCSs, signals at the same wavelength generate crosstalk.

The BER estimation is carried out by using the Q factor approach given the following formulae [95]:

$$\text{BER} = \frac{1}{2}\text{erfc}\left(\frac{Q}{\sqrt{2}}\right) \approx \frac{e^{-Q^2/2}}{Q\sqrt{2\pi}} \tag{5.2}$$

$$Q = \frac{I_1 - I_0}{\sigma_1 + \sigma_0} \tag{5.3}$$

The degradation of the Q factor due to physical impairments can be decomposed into two factors as the eye impairment (the deterioration in the eye diagram of the signal) and the noise impairment (increased noise power in the optical signal) as proposed in [96]. Then, the Q factor at the destination node of the lightpath can be written as:

$$Q_{end} = Q_{start} \times (\text{Eye Impairment}) \times (\text{Noise Impairment}) \tag{5.4}$$

$$= \frac{I_{1,start} - I_{0,start}}{\sigma_{1,start} + \sigma_{0,start}} \times \frac{I_{1,end} - I_{0,end}}{I_{1,start} - I_{0,start}} \times \frac{\sigma_{1,start} + \sigma_{0,start}}{\sigma_{1,end} + \sigma_{0,end}} \tag{5.5}$$

The indices *start* and *end* are used to denote the parameter values at the start and end of the line. I_0 and I_1 are the current levels, and σ_0 and σ_1 denote the noise standard deviations corresponding to bits 0 and 1, respectively. Q_{start} is the initially assumed Q factor at the start of the line. The eye impairment is due to PMD only, since CMD is compensated by the CDFs along the fiber as mentioned before; and it can be calculated as [96]:

$$Q_{PMD} = 10.2B^2D_p^2L \tag{5.6}$$

where, B is the bit rate, D_p is the PMD coefficient and L is the length of the lightpath. Noise impairment is caused by ASE noise at the EDFAs and intra-channel node crosstalk. Other impairments such as FWM and inter-channel crosstalk are disregarded in this model. As proposed in [47], the noise variance at the receiver can be written as the sum of four components:

$$\sigma_m^2 = \sigma_{sxm}^2 + \sigma_{sspm}^2 + \sigma_{shm}^2 + \sigma_{th}^2 \tag{5.7}$$

where m stands for the transmitted bit (0 or 1); σ_{sxm}^2, σ_{sspm}^2, σ_{shm}^2 and σ_{th}^2 are the variances of the signal crosstalk beat noise, ASE beat noise, shot noise and

the thermal noise at the photodetector, respectively. These values depend on the signal, ASE noise and crosstalk power levels at the destination node and can be calculated with the equations given in [47] as follows:

$$\sigma^2_{sxm} = 2\xi_{pol}R^2_\lambda b_m p_{sig}(N, \lambda_w)p_{xt}(N, \lambda_w) \tag{5.8}$$

$$\sigma^2_{sspm} = R^2_\lambda b_m p_{sig}(N, \lambda_w)p_{ase}(N, \lambda_w)B_e/B_o \tag{5.9}$$

$$\sigma^2_{shm} = 2qR_\lambda \left(b_m p_{sig}(N, \lambda_w) + p_{xt}(N, \lambda_w) + p_{ase}(N, \lambda_w)\right)B_e \tag{5.10}$$

$$\sigma^2_{th} = n_{th}B_e \tag{5.11}$$

In these formulae, p_{sig}, p_{xt} and p_{ase} stand for the signal, crosstalk and ASE noise powers at node N, respectively; and λ_w is the wavelength, the signal is carried on. These power levels can be calculated by the recursive equations in [47], starting from the source node.

Let Q_{lim} denote the Q factor corresponding to the maximum acceptable BER. Using (5.5), the noise standard deviation corresponding to Q_{lim} can be written as:

$$\sigma_{\lim} = \frac{Q_{start} \times (\sigma_{1,start} + \sigma_{0,start})}{Q_{lim}} \times Q_{PMD} \tag{5.12}$$

$\sigma_{0,start}$ and $\sigma_{1,start}$ can be obtained from Q_{start} and the channel power at the transmitters [48]. Then, for a lightpath to be established, an upper bound on the noise standard deviation of the lightpath can be defined as follows:

$$\sigma_{1,end} + \sigma_{0,end} \leq \sigma_{lim} \tag{5.13}$$

Eq. (5.13) is the BER criteria for the establishment of al ightpath. A lightpath satisfying this equation is guaranteed to have a BER lower than or equal to maximum the acceptable BER.

5.3   Lightpath Establishment Problem

Let D denote the given set of lightpath demands. The objective is to route as many demands from this set as possible, using the available network resources.

Three conditions should be satisfied in the solution. The lightpath should occupy the same wavelength on all the links along the fiber (wavelength continuity constraints). Each wavelength on a single fiber should be used by only a single lightpath at most (capacity constraints). And the BER along the established lightpaths should be lower than a certain threshold (BER constraints).

5.3.1 ILP Formulation

This problem is shown to be NP complete even in the absence of the BER constraints. We formulated this problem using integer linear programming. The developed ILP formulation is a path based one. The aggregated effect of all physical impairments in the utilized model is considered and each of the established lightpaths in the solution is guaranteed to have a BER that does not exceed the acceptable threshold.

The network topology is represented by a directed graph $G = (N, L)$. N is the set of nodes and L is the set of optical fiber links. A set of shortest paths, P_d, on the physical topology are calculated between the source and destination nodes of each lightpath demand d. The set of wavelengths is denoted by W. The rest of the formulation is as follows:

Constants:

C_l: Number of fibers on link l

T: Light-path incidence matrix. Its elements are defined as

$$
T_{ldp} = \begin{cases} 1, & \text{if link } l \text{ is on } p^{\text{th}} \text{ path for demand } d \\ 0, & \text{otherwise} \end{cases}
$$

$$(5.14)$$

Decision variable:

$$
x_{wdp} = \begin{cases} 1, & \text{if demand } d \text{ is routed on path } p \text{ at } w \\ \\ 0, & \text{otherwise} \end{cases} \tag{5.15}
$$

Objective Function:

$$
\max \sum_{d \in D} \sum_{p \in P_d} x_{wdp} \tag{5.16}
$$

Subject to:

$$
\sum_{w \in W} \sum_{p \in P_d} x_{wdp} \leq 1, \forall d \in D \tag{5.17}
$$

$$
\sum_{d \in D} \sum_{p \in P_d} x_{wdp} \times T_{ldp} \leq C_l, \forall l \in L, \forall w \in W \tag{5.18}
$$

Eq. (5.17) implies that a demand can be routed on a single path and a single wavelength, and (5.18) represents the link capacity constraints.

To generate the constraints on the BER, using the recursive equations provided in [47], we generated linear expressions for the signal power (p_{sig}), crosstalk power (p_{xt}) and ASE noise power (p_{ase}), which are denoted by $P_S(w, d, p)$, $P_A(w, d, p)$ and $P_X(w, d, p)$. In these expressions, d is the index of the lightpath demand, p denotes the path on which the lightpath is routed and w is the index for the wavelength on which the lightpath is carried. Fixed numerical values are calculated for $P_S(w, d, p)$ and $P_A(w, d, p)$ offline for each (w, d, p) triple. However, since the crosstalk power depends on the routes of other lightpaths, the closed form expression of $P_X(w, d, p)$ contains the decision variables of other demands whose paths share at least one common node with the current lightpath candidate. Finally, we obtain the following linear expression for the noise variances at the receiver:

$$
\sigma_0^2 + \sigma_1^2 = \sum_{m \in \{0,1\}} \left(2\xi_{pol} R_\lambda^2 b_m P_S(w, d, p) P_X(w, d, p) \right.
$$

$$
+ 2qR_\lambda B_e \left(b_m P_S(w, d, p) + P_X(w, d, p) + P_A(w, d, p) \right)
$$

$$
\left. + 4R_\lambda^2 b_m P_S(w, d, p) P_A(w, d, p) B_e / B_o + n_{th} B_e \right) \tag{5.19}
$$

Table 5.1: Values of the physical model parameters

D_p	Fiber PMD Coefficient	$0.2ps/\sqrt{km}$
B	Channel data rate	10 Gbps
G_{in}	Input EDFA Gain	22 dB
G_{out}	Output EDFA Gain	16 dB
X_{sw}	Switch Crosstalk Ratio	-30 dB
ξ_{pol}	Polarization mismatch factor	0.5
R_λ	Photodetector responsivity	1
B_e	Receiver electrical bandwidth	$B \times 0.7$ GHz
B_o	Receiver optical bandwidth	50 GHz
q	Charge of an electron	$1.16^{-19}C$
$\sqrt{n_{th}}$	RMS thermal current	$5.3^{-12}\mathrm{Amp}/\sqrt{\mathrm{Hz}}$

The variable b_m in (5.19) is the ratio of the received optical signal power for the corresponding bit $m \in \{0,1\}$ to the average value of the received optical signal power. $b_m = 0$ for $m = 0$, and $b_m = 2$ for $m = 1$. The remaining parameters are listed in Table 5.1. The rest of the physical layer parameters are the same as given in [47].

Eq. (5.19) is a linear expression of the sum of noise variances, in terms of the decision variables x_{wdp}. However, the BER acceptance criteria (5.13) developed in Section 5.2 is in terms of the sum of noise standard deviations for bits 0 and 1. Therefore, to generate a linear constraint on the BER, we need to find a linear expression for the sum of standard deviations. One possible solution to this problem is to neglect the noise variances due to bit 0 and choose a slightly larger Q factor than that corresponding to the target BER [42]. In this study, we use a different approach to guarantee that the resulting BER is lower than the threshold value. We search for a coefficient K, such that the following inequality is always satisfied.

$$K(\sigma_0^2 + \sigma_1^2) \geq (\sigma_1 + \sigma_0)^2 \tag{5.20}$$

Then, the constraint on the BER can be introduced as

$$M \times (1 - x_{wdp}) + \sigma_{lim}^2 \geq K(\sigma_0^2 + \sigma_1^2), \forall w \in W, d \in D, p \in P \tag{5.21}$$

In (5.21), the large constant M is used for implementing the classical big-M linearization [97]. The use of M guarantees that the inequality is satisfied when $x_{wdp} = 0$, and the inequality becomes redundant when $x_{wdp} = 1$. To find the smallest value of M that is guaranteed to satisfy the inequality, all the decision variables in the expression for $P_X(w, d, p)$ are taken as 1 and the numerical value of the right hand side expression is calculated. The minimum value for the coefficient K satisfying (5.20) can be found from the following equation:

$$K = \max \frac{(\sigma_0 + \sigma_1)^2}{\sigma_0^2 + \sigma_1^2} \tag{5.22}$$

If we call the ratio σ_0/σ_1, σ_R, (5.22) becomes

$$K = \max \left(1 + \frac{2\sigma_R}{1 + \sigma_R^2} \right) \tag{5.23}$$

The solution of (5.23) can be found by taking the derivative and also searching the upper and lower limits of σ_R according to the network topology and physical layer parameters, which can be calculated using Eq. (5.7)-(5.11). According to our calculations, the σ_R value satisfying Eq. (5.23) is found to be 0.07, corresponding to a K with the value 1.0139.

5.3.2 ReOrdered Lightpath Establishement (ROLE) Algorithm

The solution time of the ILP formulation introduced in the previous Section increases exponentially with the problem size. Therefore, it becomes infeasible for medium and large size networks with large numbers of wavelengths and demands. To obtain solutions for problems of larger sizes, we propose a heuristic algorithm: ReOrdered Lightpath Establishment (ROLE). ROLE basically consists of three phases: Routing and Wavelength Assignment (RWA), Rerouting and Reordering.

1.Routing and Wavelength Assignment

Various RWA algorithms can be incorporated with ROLE. We implemented three routing and three wavelength assignment algorithms and used their combinations. Together with these routing and wavelength assignment algorithms, two exhaustive RWA algorithms are also implemented. The exhaustive algorithms investigate all possible route-wavelength combinations for each lightpath demand.

A set of shortest paths are previously calculated on the physical topology for each source, destination pair. When routing a lightpath, these paths are searched for an available wavelength. An available wavelength should be unoccupied on all the links along the path and should satisfy the BER constraints on the corresponding path. The first path with an available wavelength is chosen to route the lightpath demand. The search order of the shortest paths depends on the utilized routing algorithm. We implemented the Shortest Path First (SPF), Shortest Widest Path First (SWPF) and Widest Shortest Path First (WSPF) algorithms. The width of a path is defined as the number of unoccupied wavelengths along the path. The length of a path is the number of hops along the path.

The implemented wavelength assignment algorithms are First Fit with BER constraint (FFB), Minimum BER (MB), Minimum Maximum BER (MMB). In the FFB algorithm, the smallest numbered available wavelength that satisfies the BER constraints on the chosen path is selected. In MB algorithm, among the available wavelengths for the chosen path, the one giving the minimum BER is selected. The MMB algorithm selects the wavelength which minimizes the maximum BER among the established lightpaths.

Together with these routing and wavelength assignment algorithms that can be run jointly, we also implemented two exhaustive RWA algorithms: Exhaustive Minimum BER (E-MB) and Exhaustive Minimum Maximum BER (E-MMB).

These algorithms do not stop the search when they find an available wavelength on a path; instead, they search all possible combinations to find the best path-wavelength combination for the lightpath demand. E-MB chooses the path and wavelength resulting in the minimum BER for the lightpath to route. E-MMB chooses the path and wavelength combination that has the minimum of the maximum BER for all established lightpaths in the network.

2.Rerouting

This phase aims to improve the output of the RWA phase. During RWA, the lightpath demands can be blocked due to absence of an unoccupied wavelength, or due to high BER. After RWA, the blocked lightpath demands are classified as wavelength blocked and BER blocked demands. In the rerouting phase, the BER blocked demands are considered first. For each BER blocked demand, the lightpaths routed on the same wavelength and share a common node with the blocked demand are listed. The algorithm tries to reroute each of the lightpaths in the list on another path or wavelength. By doing so, it reduces the effect of node crosstalk. This procedure is finished when all the lightpaths in the list are tried or the BER blocked lightpath can be routed. This process is applied to each BER blocked lightpath.

After that, wavelength blocked lightpath demands are considered. For each wavelength blocked lightpath demand, the algorithm calculates the minimum number of reroutings needed to free a wavelength along a path of the lightpath demand; and it records the corresponding path and wavelength. Then, it tries to reroute the lightpaths occupying the chosen wavelength on the chosen path. If it succeeds, it tries to route the wavelength blocked demand on the chosen path and wavelength. If the lightpath demand cannot be routed, the rerouted lightpaths are assigned their previous paths and wavelengths back.

3.Reordering

At the start of the ROLE algorithm, the demands are sorted in an initial order according to the lengths of their shortest paths. They are served in this order in the RWA and rerouting phases. Then, the ordering of the lightpath demands is updated, and RWA and rerouting phases are run from the beginning with the new ordering. In the reordering phase, the first blocked lightpath demand which is not marked is moved to the first place in the demand list, and marked. The marking procedure avoids loops by preventing a marked lightpath demand from being moved to the first place in the list, in another iteration. This process of reordering and performing RWA and rerouting with the new order, is applied until there is no unsatisfied lightpath demand that is not marked, and the best result is recorded.

The flowchart of the ROLE algorithm is given in Figure 5.2.

Computational Complexity

Because of the rerouting and reordering phases, the computational complexity of the ROLE algorithm is higher than the complexity of the RWA phase alone. A number of extra Q factor calculations are done in the rerouting phase. Let H denote the average number of paths sharing at least one common node with a given path, and k represent the number of considered shortest paths for each source destination pair. Then the number of extra Q factor calculations during rerouting is in the order of $O(|D|^2|W|^2k^2H^2)$. After each reordering event, RWA and rerouting are done from the beginning. This process increases the computational complexity by a factor of $|D|$.
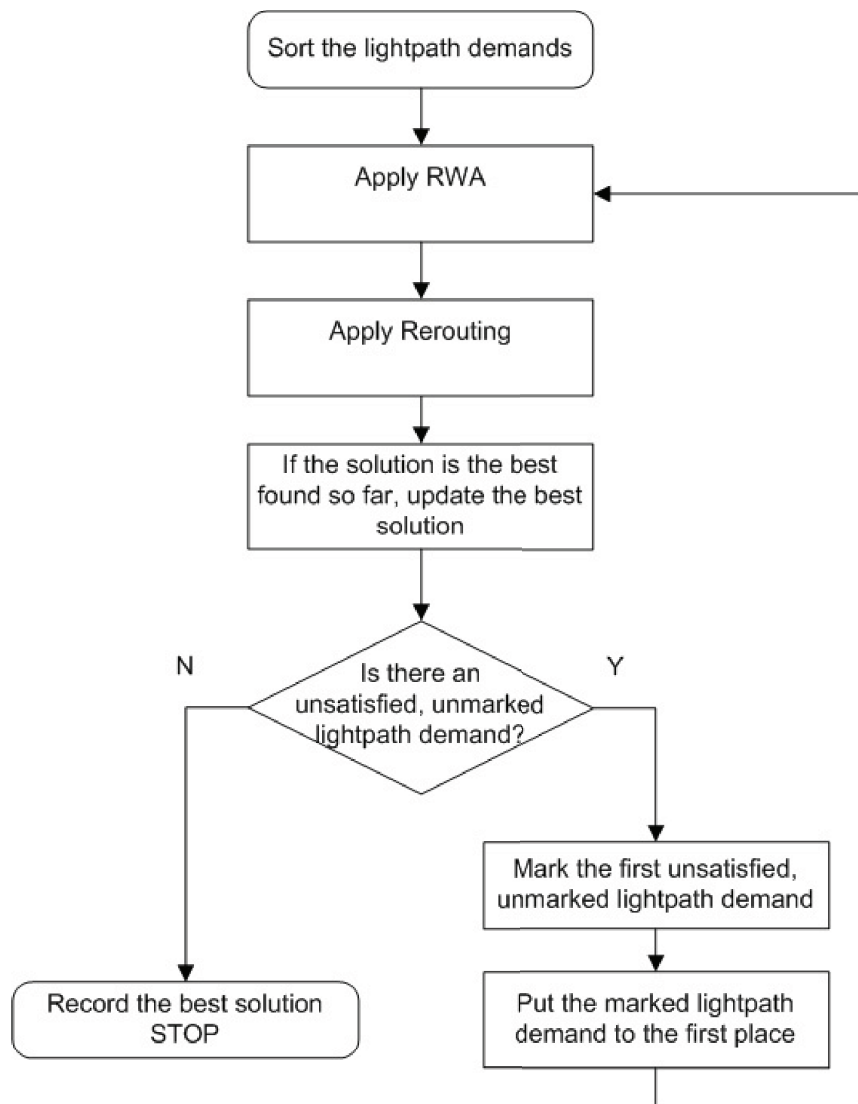
Figure 5.2: Flowchart of the ROLE algorithm

5.3.3   Performance Evaluation

Performance evaluation of the ROLE algorithm is carried out in this section. In the first part, the effect of the initial demand sorting order is investigated. Defining the length of a lightpath demand as the hop length of the shortest path between its source and destination nodes, ROLE is run with two different demand sorting orders: Shortest Demand First (SDF) and Longer Demand First (LDF). The results are evaluated in terms of ratio of routed lightpath demands and distribution of the blocked lightpath demands according to the length.

In the second part, we investigate the performance of ROLE with various RWA algorithms. As mentioned in the previous Section, ROLE can be run with different RWA algorithms. Three routing (SPF, SWPF, WSPF,) and three wavelength assignment algorithms (FFB, MB, MMB) among the most commonly used ones in the literature are implemented. We also implement two exhaustive RWA algorithms (E-MB, E-MMB) and compare their performances. The details on the RWA algorithms were given in Section 5.3.2.

Then, we compare the performance of ROLE with the ILP solutions for small sized networks. The ILP solutions are generated by solving the formulation introduced in Section 5.3.1. In the cases where the optimum solution could not be achieved, upper bounds and the best feasible solutions are reported.

In the next part, we compare the performance of ROLE with a recently proposed heuristic algorithm, POLIO-RWA [34], on a realistic network topology based on the Deutsche Telekom (DTAG) Network [98]. We show that ROLE significantly outperforms POLIO-RWA, in terms of routed lightpath demands. We also demonstrate the effect of rerouting and reordering mechanisms employed in ROLE.

In the last part, we investigate the effect of switch crosstalk, the most dominant physical layer impairment in the utilized model. We calculate the percentage of wavelength blocked and BER blocked lightpath demands to find the main source of blockings, and how they change with switch crosstalk ratio.

Effect of Initial Demand Sorting

In this section, the effect of the initial sorting of the lightpath demands on the solutions produced by ROLE is investigated. When evaluating the solutions to the lightpath establishment problem, the main criterion is the percentage of the routed lightpaths from the demand set. However, a solution may seem to show a better performance by rejecting most of the lightpath demands between the nodes which are further away in the physical topology and only establishing the lightpaths between closer nodes. This is not a desired situation since it violates fairness among the lightpath demands and it may also restrict the type of virtual topologies that can be established on top of the physical topology. This problem can be overcome by using proper approaches for the initial sorting of the demands. Defining the length of a lightpath demand as the shortest hop distance between the source and destination nodes of the demand on the physical topology, we implemeted two different initial demand sorting orders: SDF and LDF. We compared the solutions produced with both demand sorting orders in terms of routed lightpath demands and distribution of the blocked lightpath demands according to their lengths.

In this section, ROLE is run on four randomly generated physical topologies, each with 20 nodes and having 25, 30, 35 and 40 bi-directional links (Topologies 1-4), respectively. These topologies are presented in Section A.3.1 of Appendix. Simulations are run for three different number of wavelengths: $|W| = 4$, 8 and 16. The lightpath demands, i.e., the logical topology, are generated randomly. Number of lightpath demands, $|D|$, in the demand set depends on $|W|$ and

(a) on Topology1

(b) on Topology2
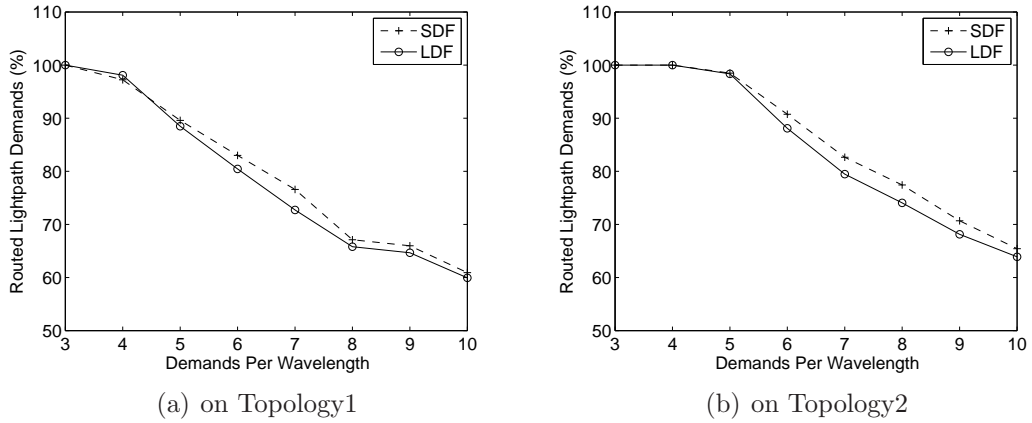
Figure 5.3: Percentage of the routed demands by ROLE

three sets of demands are generated for each value of $|D|$. For $|W| = 4$, $|D| = 12, 16, 20, 24, 28, 32, 36, 40$, for $|W| = 8$, $|D| = 24, 32, 40, 48, 56, 64, 72, 80$ and for $|W| = 16$, $|D| = 48, 64, 80, 96, 112, 128, 144, 160$ are used. 10 shortest paths are calculated for each source destination pair. The chosen threshold for the minimum value of Q factor is 6 (15.5dB), which corresponds to a BER about 10^{-9} without application of Forward Error Correction (FEC), for a channel data rate of 10 Gbps.

We first compare the demand sorting approaches in terms of the ratio of the lightpath demands that can be satisfied from the offered demand set, for different values of *demands per wavelength* ($|D|/|W|$). The RWA algorithm employed by ROLE is SPF-FFB. The results are given in Figures 5.3(a), 5.3(b), 5.4(a) and 5.4(b) for the 25, 30, 35 and 40-link topologies referred as Topology1, Topology2, Topology3 and Topology4, respectively.

According to the results, with SDF initial sorting ROLE can satisfy a higher ratio of the offered lightpath demands and the maximum difference is approximately 5% of the offered lightpath demands. However, it is has a tendency of denying the longer lightpath demands, and thus causes unfairness among the offered demands. This may also bring an important restriction on the type of virtual topologies that can be established. To examine this effect, we calculated

(a) on Topology3 (b) on Topology4
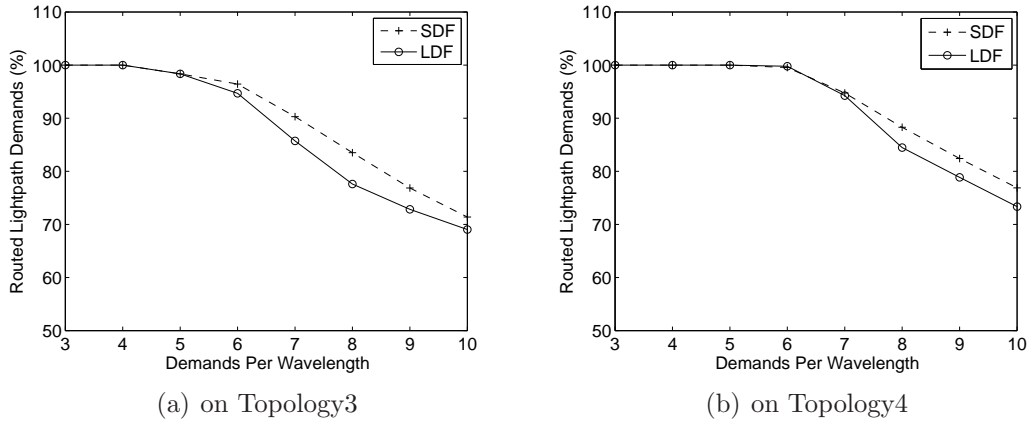
Figure 5.4: Percentage of the routed demands by ROLE

(a) on Topology1 (b) on Topology2
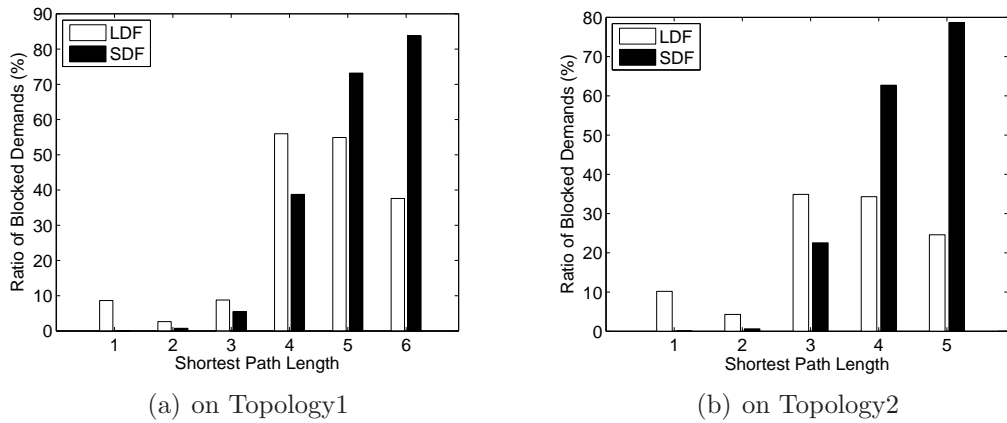
Figure 5.5: Distribution of the blocked lightpath demands according to their lengths

the percentage of the blocked lightpath demands for each length. The results are presented in Figures 5.5(a)-5.6(b). The mean value and coefficient of variation (std. deviation/mean) for the lengths of the blocked lightpaths are given in Table 5.2. As it is observed from the results, the LDF initial Sorting achieves a more fair distribution of the blocked lightpath demands in terms of demand lengths. Thus, it allows virtual topologies with longer lightpaths to be established.

To show that ROLE can be scaled to solve larger problems with higher number of wavelengths and demands, and to investigate whether the effect of demand sorting is similar in these cases, we compare the two demand sorting methods for $|W|$=16, 32 and 64 on the reference DTAG network [98] with 14 nodes and 23

(a) on Topology3   (b) on Topology4
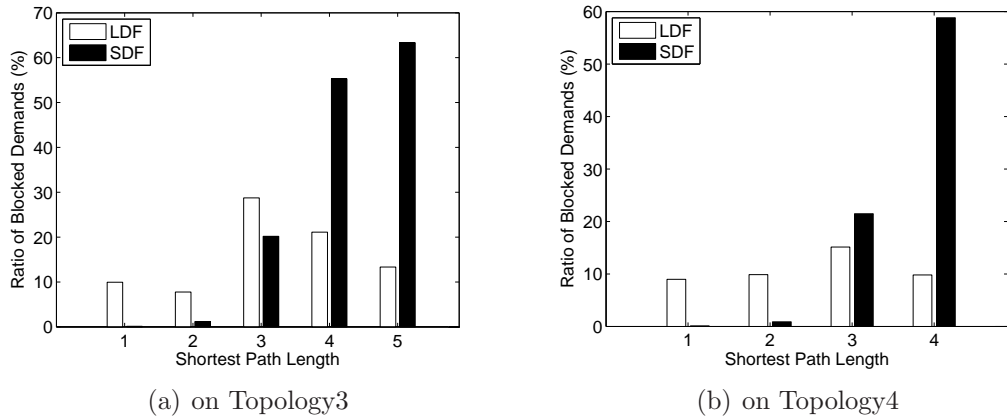
Figure 5.6: Distribution of the blocked lightpath demands according to their lengths

Table 5.2: The statistics on the lengths of the blocked lightpaths for SDF and LDF demand sorting, on Topologies 1-4

Topology	Mean Length		Coe. Var.	
	SDF	LDF	SDF	LDF
1	4.65	4.20	0.16	0.24
2	3.63	3.05	0.17	0.28
3	3.54	2.76	0.19	0.32
4	3.17	2.34	0.15	0.33

bidirectional links. The topology of DTAG network is given in Section A.3.3 of Appendix. The percentage of routed lightpath demands is calculated for changing values of $|D|$. $|D|$ is changed between 25-130 for $|W|$=16, 50-260 for $|W|$=32, and 100-520 for $|W|$=64. The percentages of the routed lightpath demands are presented in Figures 5.7-5.8. The percentages of the blocked lightpath demands according to their lengths are given in Figures 5.9-5.10, and the mean value and coefficient of variation for the blocked lightpath lengths are presented in Table 5.3. The results are similar to the previous results for smaller $|W|$. With SDF demand sorting, ROLE can satisfy a slightly higher ratio of the offered lightpath demands, but produces more fair solutions in terms of lengths of the blocked lightpath demands.
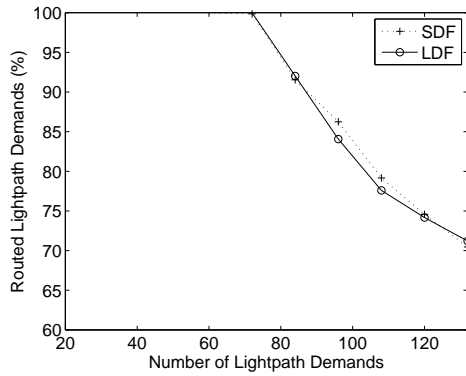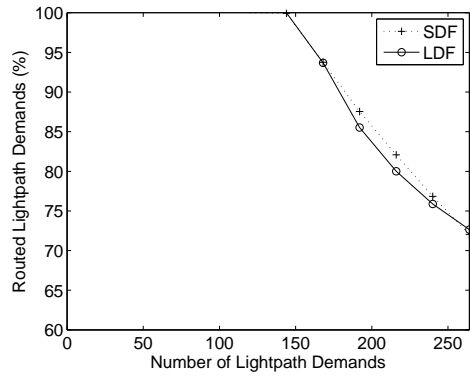
(a) for $|W|{=}16$ (b) for $|W|{=}32$

Figure 5.7: Percentage of the routed demands by ROLE on DTAG topology
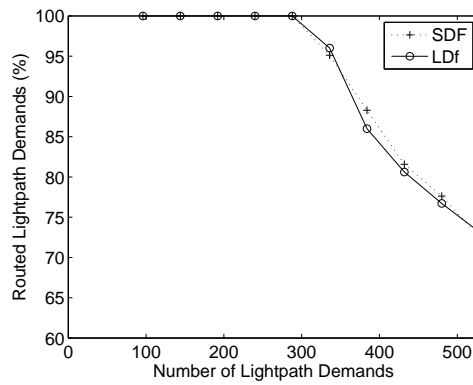
Figure 5.8: Percentage of the routed demands by ROLE on DTAG topology for $|W|{=}64$
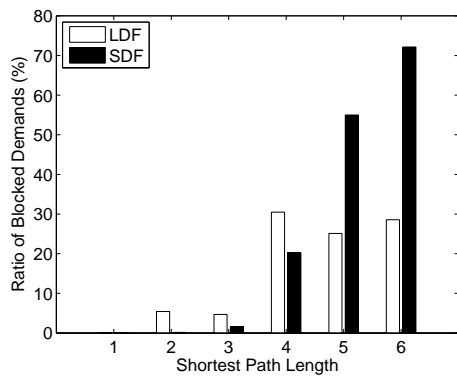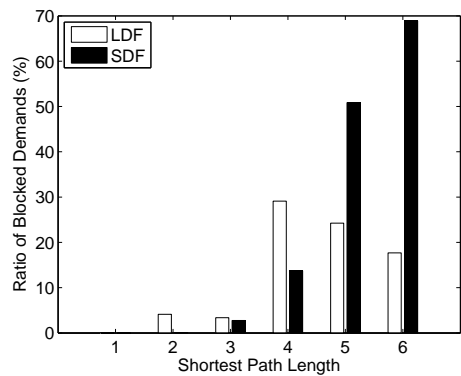
(a) for $|W|{=}16$ (b) for $|W|{=}32$

Figure 5.9: Distribution of the blocked lightpath demands according to their lengths on DTAG topology
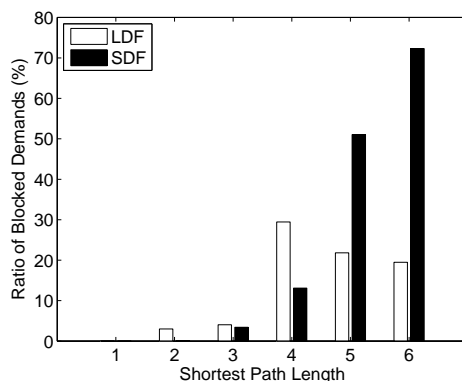
Figure 5.10: Distribution of the blocked lightpath demands according to their lengths on DTAG topology for $|W|$=64

Table 5.3: The statistics on the lengths of the blocked lightpaths for SDF and LDF demand sorting, on the DTAG topology

$|W|$	Mean Length		Coe. Var.	
	SDF	**LDF**	**SDF**	**LDF**
16	3.64	3.00	0.20	0.30
32	3.69	3.06	0.21	0.28
64	3.62	3.05	0.22	0.26

Performance With Different RWA Algorithms

In this section, ROLE's performance with the implemented RWA algorithms is investigated. The combinations of the three implemented routing algorithms (SPF, WSPF, SWPF) with the wavelength assignment algorithms (FFB, MB, MMB); and the two exhaustive routing algorithms (E-MB and E-MMB) are compared in terms of ratio of the routed lightpath demands. The results are shown in Figures 5.11(a)-5.12(b) for Topologies 1-4. In each figure, each routing algorithm is paired with the wavelength assignment algorithm, with which it has performed best; and among the two exhaustive algorithms, the one performing better is shown. The initial demand sorting is LDF. The averaged results over all values of demands per wavelength and all topologies are presented in Table 5.4.

The results show that, SWPF performs the best among the routing algorithms, when incorporated in ROLE. The performance of SPF is also close, and

106

(a) Topology1   (b) Topology2
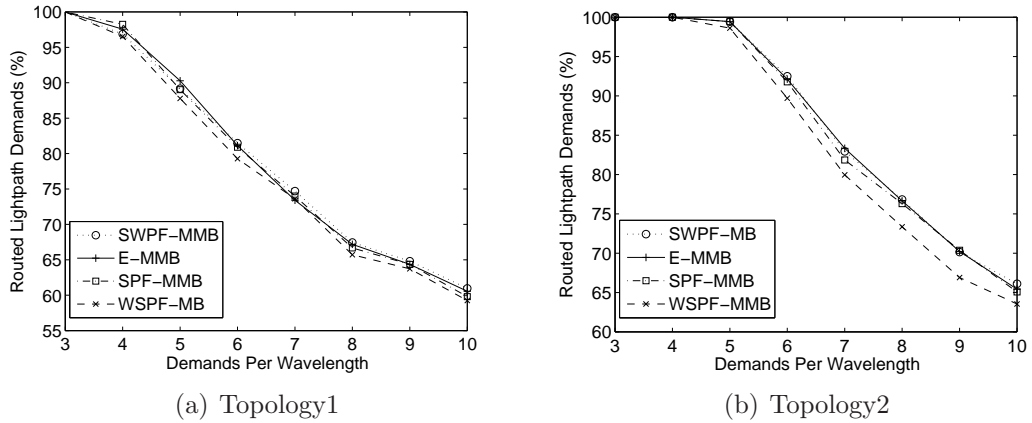
Figure 5.11: Percentage of the routed demands by ROLE with different RWA algorithms

both algorithms perform considerably better than WSPF. Among the wavelength assignment algorithms, MB and MMB have a similar performance which is better than that of FFB algorithm. The performances of exhaustive RWA algorithms are also among the highest ones together with the combinations of SPF and SWPF routing algorithms with MB and MMB wavelength assignment algorithms. The best performance is achieved by the SWPF-MB combination. The exhaustive algorithms cannot outperform SWPF-MB and SWPF-MMB combinations, because they use the BER criterion when choosing the route and wavelength combination. SWPF algorithm prefers the shorter lightpaths when there is an available wavelength, and thus it may utilize the network resources more efficiently when the primary blocking reason is capacity rather than high BER.

According to the results, the MB and MMB wavelength assignment algorithms' performances are very close. We investigated the reason for this similar performance. A BER blocked lightpath may be blocked because of two reasons. The first is that, the BER of that lightpath exceeds the BER threshold. The second reason is that, BER of that lightpath remains below the acceptable threshold, but it causes the BER of an already established lightpath to increase and exceed the threshold. In both cases, the lightpath demand to be established is blocked. We computed the average percentage of blocked lightpath requests

(a) Topology3 (b) Topology4
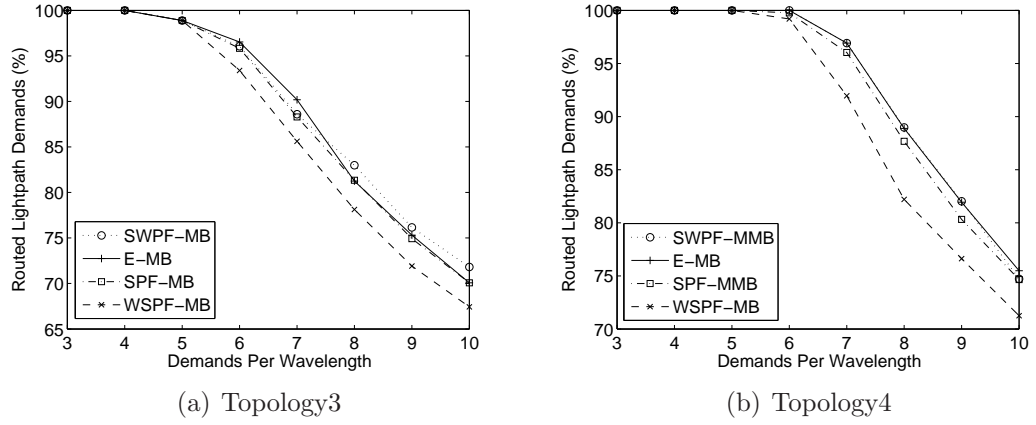
Figure 5.12: Percentage of the routed demands by ROLE with different RWA algorithms

Table 5.4: The percentage of the established lightpath demands by ROLE with different RWA algorithms averaged on Topologies 1-4

RWA Algorithm		Routed %
SPF	**FFB**	85.34
	MB	86.31
	MMB	86.37
SWPF	**FFB**	85.95
	MB	86.81
	MMB	86.79
WSPF	**FFB**	83.16
	MB	84.82
	MMB	84.78
Exhaustive	**MB**	86.69
	MMB	86.63

Table 5.5: Average values of the Maximum BERs among the lightpaths in the established virtual topologies, on Topologies 1-4

| Topology | RWA Algorithm | |
	SPF-MB	SPF-MMB
1	3.9×10^{-10}	3.94×10^{-10}
2	2.96×10^{-10}	2.72×10^{-10}
3	2.71×10^{-10}	2.57×10^{-10}
4	2.26×10^{-10}	2.18×10^{-10}

which are blocked because of the first reason, over all simulation events using Topologies 1-4. The result is about 68% for both SPF-MB and SPF-MMB algorithms. This means, in 68% of the blockings due to high BER, the BER of the current lightpath demand to establish exceeds the BER threshold. In these cases, applying the MinMax approach of the MMB algorithm would not prevent the blocking, since the blocking is not resulted from the BER of the other lightpaths already established in the network.

MB and MMB algorithms have similar performances in terms of routed lightpath demands. However, because of the nature of the MMB algorithm, it can be expected to cause a lower maximum BER in the network, in the generated solutions. To investigate the validity of this case, we calculated the maximum BER in the established virtual topologies for both algorithms. The employed routing algorithm is SPF. The results that are averaged over all demand sets and wavelengths are presented in Table 5.5. As the results show, except for the simulations run on Topology 1, the value of the maximum BER in the solutions where MMB algorithm is used, is lower. Since Topology 1 has the smallest number of physical links, physical layer resources are excessively insufficient and MinMax approach cannot reduce the maximum BER in the network. In the remaining topologies, even though SPF-MMB slightly outperforms SPF-MB in terms of maximum BER, the number of lightpaths that do not satisfy the maximum BER threshold is very close for the two algorithms. Therefore, their performances are similar in terms of the amount of established lightpaths.

Comparison with ILP Solutions

This Section presents comparisons of the results produced by the ROLE algorithm and by solving the ILP formulation presented in Section 5.3.1. Three randomly generated physical topologies, each with 10 nodes, are used for this purpose: Topology5, Topology6 and Topology7 each with 12, 16 and 20 links, respectively. These topologies are presented in Section A.3.2 of Appendix. Simulations are run for $|W| = 4, 8, 12$. For $|W| = 4$, $|D| = 10, 15, 20, 25$, for $|W| = 8$, $|D| = 20, 30, 40, 50$ and for $|W| = 12$, $|D| = 30, 45, 60, 75$ are used. Since the solution of the ILP formulation requires excessive amounts of memory requirements and CPU time, the problem sizes are chosen to be smaller than the ones in previous sections.

ROLE is run employing E-MMB RWA algorithm with the SDF and LDF demand sorting orders. The ILP formulation is solved using ILOG CPLEX 8.1 optimization problem solver, applying the branch and cut method. The solver is run with an upper limit on the spent CPU time of 10000 seconds. (On the other hand, for a comparison of solution times, the longest run time for ROLE was recorded and it is around 8 seconds). For the cases in which the problem could not be solved to optimality within the runtime limit, the best solution produced by branch and cut is recorded as the ILP solution. The branch and cut algorithm also produces upper bounds for these cases, by taking the best non-integer solution in the unexplored region.

The number of the routed lightpath demands are given in Tables 5.6, 5.7 and 5.8 for Topologies 5, 6 and 7, respectively. As the results show, for smaller values of $|W|$ and $|D|$, the ILP formulation could be solved to optimality. However, as the problem size grows, the optimum solution cannot be reached within the applied CPU time constraint.

Table 5.6: Number of routed demands with the ILP and heuristic solutions and upper bounds for Topology5

$|W|$	$|D|$	U.B.	ILP	ROLE SDF	ROLE LDF
4	10	10	*10	*10	*10
	15	14	*14	*14	*14
	20	17	*17	16	16
	25	17	*17	*17	16
8	20	20	*20	*20	*20
	30	29	28	28	28
	40	35	31	30	29
	50	37	34	33	33
12	30	30	*30	*30	*30
	45	44	*44	42	42
	60	53	50	48	48
	75	52	50	47	44
Total	420	358	345	335	330

* denotes the optimum solution

Table 5.7: Number of routed demands with the ILP and heuristic solutions and upper bounds for Topology6

$|W|$	$|D|$	U.B.	ILP	ROLE SDF	ROLE LDF
4	10	10	*10	*10	*10
	15	13	*13	*13	*13
	20	18	17	16	15
	25	22	18	17	16
8	20	20	*20	*20	*20
	30	30	*30	*30	*30
	40	39	33	33	33
	50	43	37	36	35
12	30	30	*30	*30	*30
	45	45	*45	*45	*45
	60	59	51	51	50
	75	66	54	54	54
Total	420	395	358	355	351

* denotes the optimum solution

Table 5.8: Number of routed demands with the ILP and heuristic solutions and upper bounds for Topology7

$|W|$	$|D|$	U.B.	ILP	ROLE SDF	ROLE LDF
	10	10	*10	*10	*10
	15	13	*13	*13	*13
4	**20**	20	19	18	19
	25	24	21	21	18
	20	20	*20	*20	*20
	30	30	*30	*30	*30
8	**40**	40	39	38	38
	50	47	40	41	39
	30	30	*30	*30	*30
	45	45	*45	*45	*45
12	**60**	60	57	*60	*60
	75	75	61	62	61
Total	**420**	414	385	388	383

* denotes the optimum solution

For the problems on Topologies 5 and 6, the ILP solutions are slightly better than the solutions produced by the heuristic ROLE with SDF initial demand sorting. As the number of links in the physical topology increases, the number of paths between node pairs also increase, and this increases the problem size. As the problem size grows, ROLE with SDF starts to outperform the ILP solution obtained within run time limits, as can be seen from the solutions produced on Topology7.

The distribution of the blocked lightpath demands according to the lengths is presented in Figures 5.13(a), 5.13(b) and 5.14 for topologies 5, 6 and 7, respectively. The mean lengths and coefficients of variation (std. deviation/meanlength) for the blocked lightpaths are given in Table 5.9. The results show that, longer lightpath demands have a higher probability of rejection also in the ILP solutions. When ROLE uses LDF initial demand sorting, it can produce more fair solutions according to lightpath demand lengths, and thus reduce the probability of rejection for longer lightpath demands, in exchange for a small reduction in the number of routed demands.

(a) on Topology5   (b) on Topology6
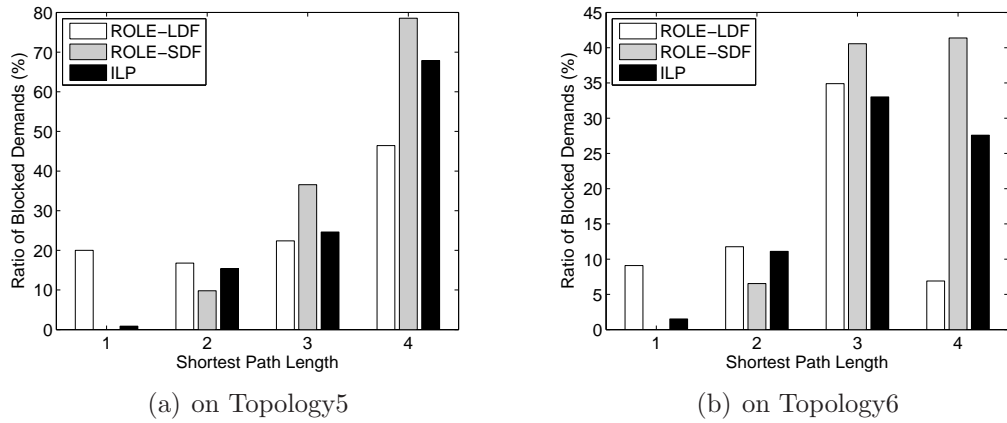
Figure 5.13: Distribution of the blocked lightpath demands according to their lengths
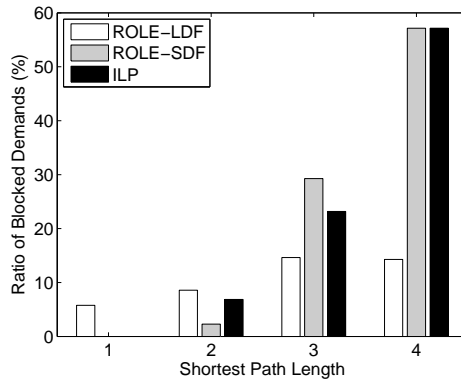
Figure 5.14: Distribution of the blocked lightpath demands according to their lengths on Topology7

Table 5.9: The statistics on the lengths of the blocked lightpaths for the ILP solution and ROLE with SDF and LDF demand sorting, on Topologies 5-7

Topology	Mean Length			Coe. Var.		
	ILP	ROLE SDF	ROLE LDF	ILP	ROLE SDF	ROLE LDF
5	2.93	3.09	2.37	0.26	0.21	0.43
6	2.79	3.03	2.42	0.25	0.19	0.33
7	2.77	3.00	2.14	0.23	0.17	0.38

Comparison With Other Heuristics

In this section, we compared the performance of ROLE with another recently proposed heuristic algorithm, POLIO-RWA [34]. In POLIO-RWA, the lightpath demands are sorted according to their lengths (lengths of the shortest paths between the source and destination nodes) in an increasing manner, as in the SDF sorting, and served in this preprocessed order. For each lightpath demand, 10 shortest and 2 distinct paths are calculated dynamically on a layered wavelength graph constructed by considering only the unoccupied wavelengths. In RWA, the path and wavelength is chosen to minimize the maximum BER among all established lightpaths. If a route and free wavelength combination that satisfies the BER constraints cannot be found, the lightpath demand is blocked.

To demonstrate the performance improvement brought by the rerouting and reordering processes applied in ROLE, we implemented two other heuristic algorithms: Lightpath Establishment without ReRouting (LERR) and Lightpath Establishment without ReOrdering (LERO). These algorithms perform RWA once, and do not apply reordering. LERR stops after the RWA process while LERO also performs rerouting as in the ROLE algorithm. For a fair comparison, both of these heuristics and ROLE are run with 10 shortest paths for each source destination pair.

The simulations are carried out on the reference DTAG network [98] for $|W| = 16$. The percentage of routed lightpath demands is calculated for different values of $|D|$ between 24 and 132, and 10 demand sets are generated for each value.

The results are given in Figure 5.15 for all four algorithms. Performances of POLIO-RWA and LERR are similar as can be expected, since they use similar approaches. The difference between the performance of LERR and LERO demonstrate the improvement brought by rerouting, since the only difference of LERO from LERR is the rerouting phase. According to the results, the rerouting
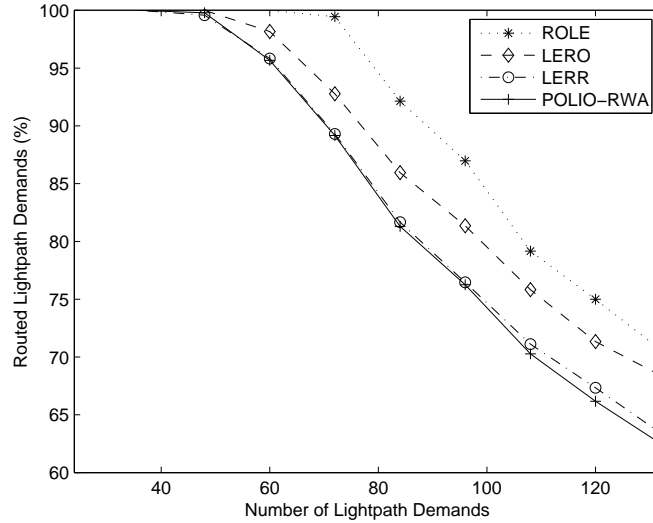
Figure 5.15: Percentage of the routed demands by the heuristic algorithms on the DTAG topology

process increases the performance of LERR by up to 7.9%. When we compare the performances of all algorithms, ROLE clearly outperforms the other three in terms of number of routed lightpath demands. It has a performance up to 14% higher than POLIO-RWA and LERR, and up to 7.2% higher than LERO, which shows the improvement brought by applying reordering. In conclusion, the results verify that the rerouting and reordering mechanisms utilized in ROLE provide significant performance improvement in terms of routed lightpath demands, and ROLE is superior to the compared heuristics.

The running times for LERR, LERO and ROLE algorithms are given in Table 5.10 for varying number of lightpath demands. Since ROLE changes the sorting order of the lightpath demands at each iteration and applies RWA and rerouting with the new order, it has a longer running time than the algorithms that do not apply reordering. Nevertheless, for very large number of demands, the number of reorderings can be bounded by a specified value in order to reduce the running time in terms of seconds, at the expense of possibly reduced performance.

Table 5.10: Running times for LERR, LERO and ROLE algorithms on the DTAG topology for $|W| = 16$

$|D|$	Algorithm Running Time (s)		
	LERR	LERO	ROLE
24	0.115	0.115	0.115
36	0.203	0.203	0.203
48	0.300	0.300	0.300
60	0.375	0.381	6.028
72	0.469	0.500	17.722
84	0.556	0.610	40.153
96	0.656	0.735	62.828
108	0.762	0.853	172.666
120	0.894	1.053	462.459
132	0.940	1.116	488.613

Influence of Switch Crosstalk Ratio and Number of Wavelengths

With the physical layer parameters used in our study, the most dominant physical layer impairment source turned out to be the node crosstalk occurring in the optical switches. In this section, we investigate the effect of switch crosstalk ratio (X_{sw}) on the amount or routed lightpath demands, by running ROLE with varying values of X_{sw}. We also investigate the ratio of wavelength blocked and BER blocked lightpath demands, to determine the main reason of lightpath demand blockings.

Simulations are carried out on the DTAG network topology for two different values of $|W|$, $|W| = 16$ and $|W| = 128$. The initial demand sorting order is SDF. For $|W| = 16$, ROLE is run with applying SWPF-FFB and E-MMB RWA algorithms. Since their performances turn out to be very close, ROLE is not run with the E-MMB algorithm, which has a higher complexity, for $|W| = 128$. The number of lightpath demands are chosen proportionally with $|W|$, so that the number of lightpath demands per wavelength ($|W|/|D|$) remains the same. The results for various numbers of lightpath demands are shown in Figure 5.16 and 5.17 for $|W| = 16$ and $|W| = 128$, respectively.

The results show that the number of routed demands change similarly with X_{sw} for both $|W| = 16$ and $|W| = 128$. The number of routed lightpaths per wavelength is higher to some extent, for $|W| = 128$, due to more efficient statistical multiplexing as the number of wavelengths increase. For a switch crosstalk value larger than -25 dB, the percentage of routed demands stays constant as the crosstalk increases. After this value, the switch crosstalk ratio has the maximum effect and in the generated solutions no two lightpaths having a common node in their paths are assigned the same wavelength. For crosstalk values of -35 dB and smaller, the effect switch crosstalk ratio on the percentage of blocked lightpath demands is minimal.

We also investigate the ratio of wavelength blocked and BER blocked lightpath demands to find out the major factor of lightpath demand blockings. The results are shown in Figure 5.18 for $|W| = 16$ and $|W| = 128$, for various values of X_{sw}. The number of offered lightpath demands is 132 for $|W| = 16$ and 1056 for $|W| = 128$. As can be seen from the results, for large values of X_{sw}, BER blocking is dominant. For -35 dB and smaller values, most of the blockings are wavelength blockings, i.e., blockings due to insufficient capacity.

Figure 5.19 represents the change of the wavelength blocked and BER blocked lightpath demands with the number of offered demands per wavelength, for a fixed value of $X_{sw} = -30$ dB. With 96 lightpath demands for $|W| = 16$ and 864 lightpath demands for $|W| = 128$, no wavelength blockings occur, which means that the capacity would be sufficient to route all the offered demands, in the absence of physical layer impairments. Beyond these values, the amount of BER blockings stays constant, which implies that the increase in the blocked lightpath demands is due to insufficient capacity. Hence, as the number of offered lightpath demands increases, wavelength blockings also increase and become more dominant.
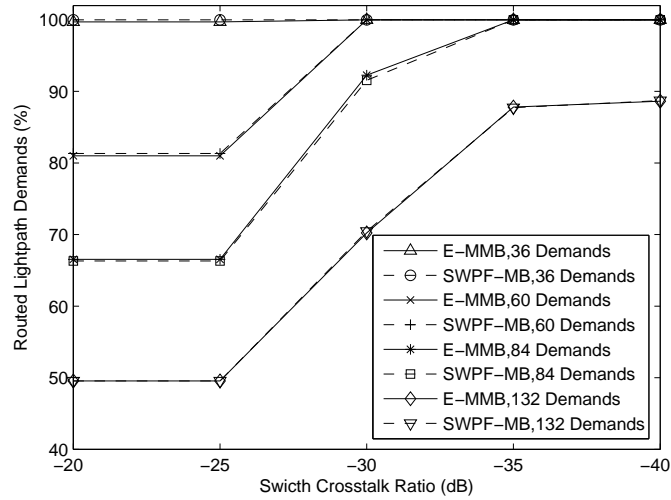
Figure 5.16: Routed demand percentage vs switch crosstalk ratio for various numbers of lightpath demands, for $|W| = 16$

From Figures 5.16-5.19, it can be observed that as the number of wavelengths and the number of offered lightpath demands are increased proportionally, the percentage of routed lightpaths increases (comparing the results for $|W| = 16$ and $|W| = 128$). Figures 5.18 and 5.19 suggest that, the reason for this increase is the reduction in the ratio of wavelength blocked lightpath demands, rather than BER blocked demands. That is an expected result, because for larger numbers of lightpath demands, the demands are distributed more fairly and a smaller number bottlenecks are created in the network.

In the following chapter, our proposed solution for multi-layer traffic engineering is presented, and integration of the TE methods proposed for MPLS and WDM layers is explained.
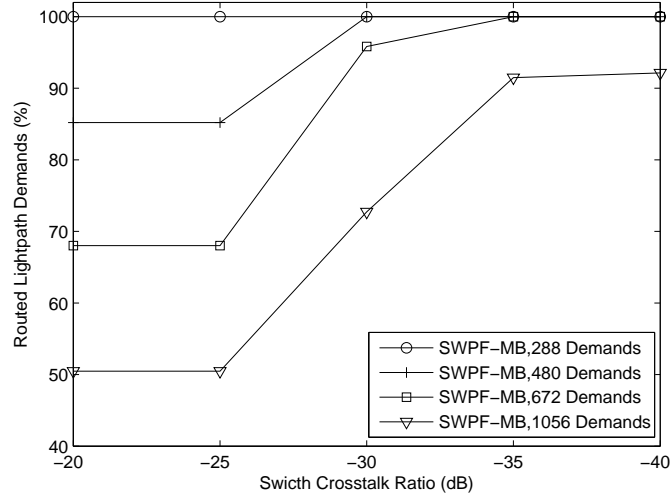
Figure 5.17: Routed demand percentage vs switch crosstalk ratio for various numbers of lightpath demands, for $|W| = 128$
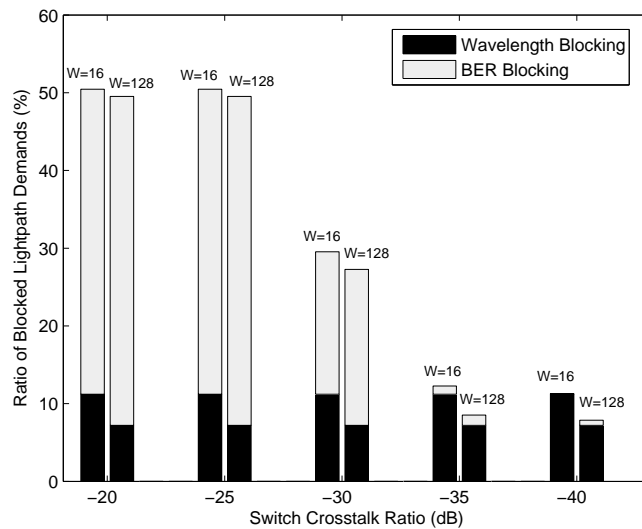
Figure 5.18: Ratio of wavelength blocked and BER blocked lightpath demands vs. switch crosstalk ratio
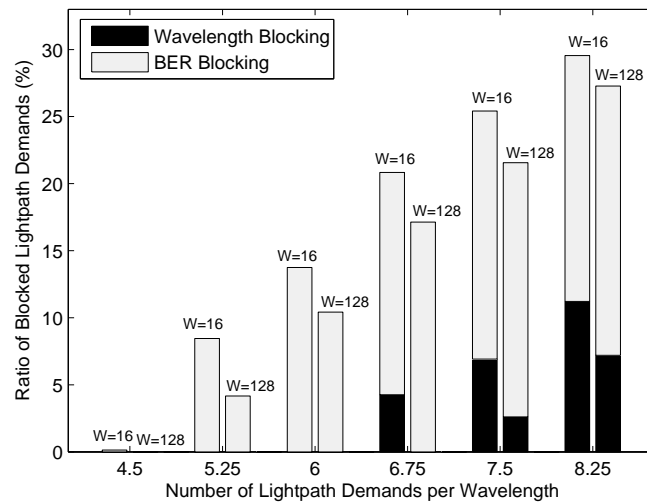
Figure 5.19: Ratio of wavelength blocked and BER blocked lightpath demands vs. number of offered lightpath demands per wavelength

Chapter 6

Multi-layer Traffic Engineering Under Physical Layer Impairments

In this chapter, we introduce the Multi-layer Traffic Engineering scheme we developed, which considers the effect physical impairments in the optical layer. In the proposed scheme, while the MPLS and WDM layer control planes apply TE in their individual layers to optimize the blocking performance and resource usage, they communicate and collaborate in the construction of the WDM layer virtual topology seen by the MPLS layer. Depending on the collaboration scheme between the layers, this scheme can be applicable in all three inter-operation scenarios (overlay, augmented and peer).

We consider a traffic pattern changing dynamically with the time of the day. This pattern is chosen to reflect the characteristic daily behavior of the internet traffic that depends on the provider and consumer activities [16]. As in the MPLS layer TE scheme proposed in Chapter 3, the MPLS layer has the information of the expected traffic values between each node pair, for each hour of the

day. Using this information, the MPLS layer control plane designs a WDM layer virtual topology by communicating with the WDM layer control plane. On the constructed virtual topology, the control plane dynamically reroutes the LSPs using the DREAM algorithm proposed in Section 3.3.1, in order to compensate for the deviations of the traffic demands from the expected values. Longer term variations may also occur in the traffic pattern, however this is beyond the scope of this study. Nevertheless, these variations can be treated as a change in the traffic expectations and our proposed scheme can be used to handle these long term changes by adjusting the input traffic information of the MPLS layer, accordingly.

The WDM layer control plane employs the ROLE algorithm proposed in Section 5.3.2 to establish the lightpaths in the virtual topology requested by the MPLS layer control plane, on top of the physical topology. The resources on the physical layer are limited and the effect of physical layer impairments are considered while establishing the lightpaths. Along each of the established lightpaths, wavelength continuity constraint should be satisfied and the BER should remain within the acceptable range for successful transmission.

Design of the WDM layer virtual topology is carried out according to the Collaborative Lightpath Topology Design (COLD) scheme that will be introduced in the following Section. In the COLD scheme, the WDM and MPLS layer control planes design and construct the virtual topology by working interactively. We investigate various interaction strategies between the WDM and MPLS layers. The amount of collaboration and the information exchanged between the layers vary with each interaction strategy. We compare the performances of these interaction strategies in terms of blocking and resource usage and evaluate the benefits of information sharing between the layers.

6.1 Collaborative Lightpath Topology Design (COLD)

The flowchart in Figure 6.1 represents the COLD scheme. The MPLS layer control plane runs a Virtual Topology Design Tool (VTDT) which designs the WDM layer virtual topology using a heuristic algorithm that is based on the tabu search topology design methods proposed in Section 3.2. The objective function of VTDT is to maximize the amount of routed MPLS layer traffic over the whole time period. To calculate the value of the objective function, for each hour the traffic demands are routed on the virtual topology, using a shortest path algorithm with link weights inversely proportional to the free capacities on the links.

VTDT starts from an initial topology and searches the solution space by a series of topology update moves. The solution space consists of the topologies satisfying optical to electrical interface constraints, i.e., the topologies in which the maximum number of lightpaths emanating from a node is below the specified threshold.

There are two types of topology update moves: setting up a new lightpath (add move) and tearing down an existing lightpath (delete move). At the start of each iteration, all the topology update moves leading to a topology in the solution space are calculated. These moves make up the set of candidate moves in that iteration. Then, the value of the objective function is calculated for each move in the candidate moves set, and the moves are sorted according the resulting value of the objective function, in a decreasing order. To sort the moves resulting with the same objective value among themselves, a tie-breaker function is used.

After the moves in the candidate moves set are sorted, the first move in the list, that results with a topology that is feasible in the WDM layer, is performed.
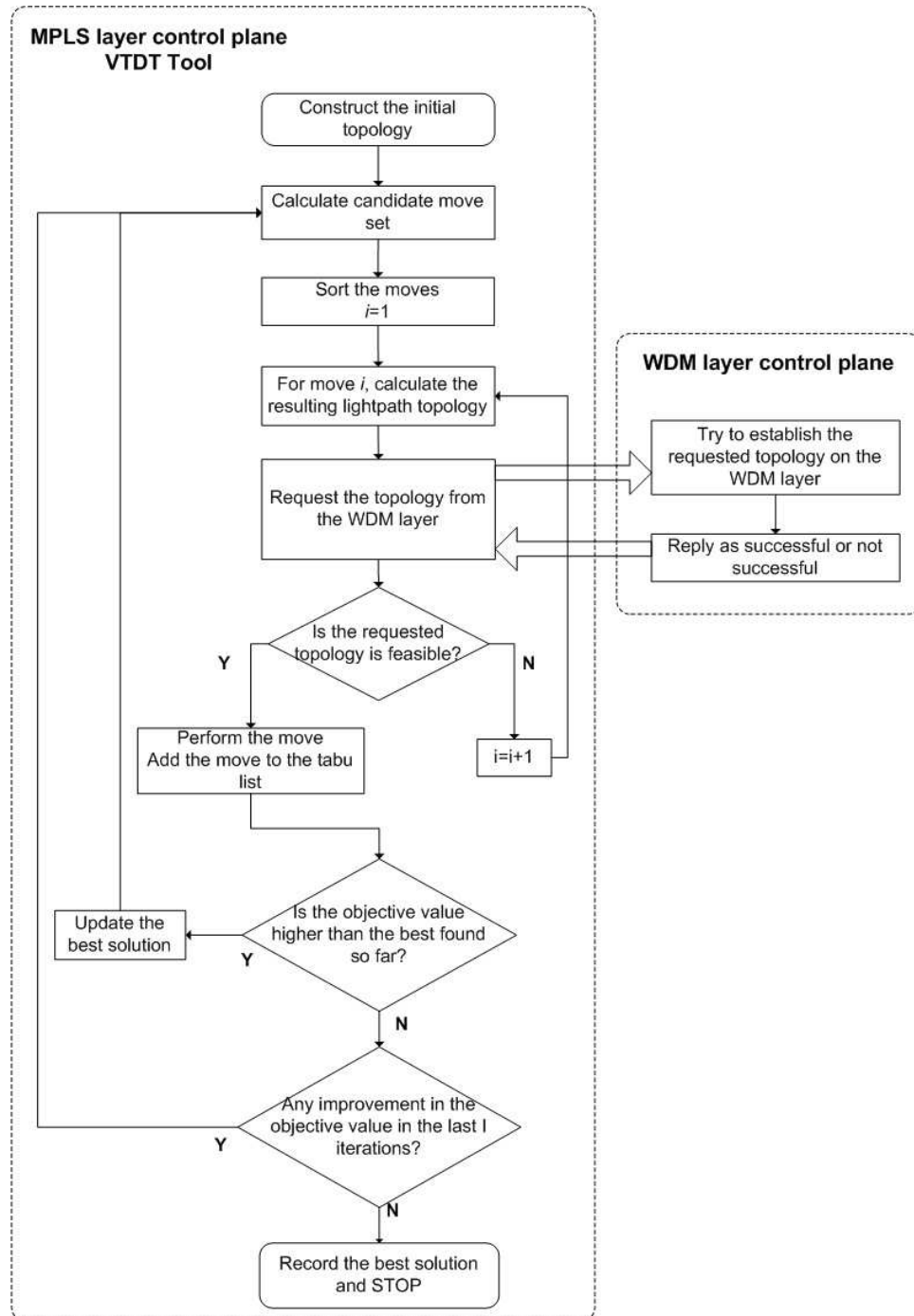
Figure 6.1: Flowchart of the COLD Scheme

To this aim, starting from the first move in the set, establishment of the resulting virtual topology for the current move is requested from the WDM layer. This process continues until an affirmative is received from the WDM layer for one of the resulting topologies, which states that the requested topology is feasible in the WDM layer.

When the VTDT requests the establishment of a virtual topology from the WDM layer control plane, the WDM layer control plane checks the feasibility of the requested topology in the WDM layer. This can be achieved by a tool that simulates the physical layer and employs the ROLE algorithm for the establishment of the lightpaths in the requested topology. If the virtual topology is feasible, a positive answer, otherwise a negative answer is sent to the VTDT. By reception of a positive answer, VTDT performs the corresponding move and the virtual topology is updated. Upon a negative answer, it requests the resulting virtual topology for the next move in the list.

VTDT declares the performed moves 'tabu', these moves are stored in a tabu list and forbidden for a number of iterations in order to prevent entrapment of the algorithm in cycles. When adding an entry to the tabu list, the performed move and the topology configuration before the move, are stored. When constructing the set of candidate moves, if a possible move is in the tabu list along with the current topology, it is not included in the set. Each entry in the tabu list is assigned a 'tenure' which is decremented at each iteration. When the 'tenure' of an entry expires, that entry is removed from the tabu list.

If the objective function has not improved for a number of iterations, the algorithm stops. The solution with the highest value of the objective function (the amount of routed traffic) is recorded as the final solution. If there are multiple topologies giving the same objective function value, then the final solution is chosen according to the value of a tie-breaker function.

Construction of the initial topology and the utilized tie-breaker function varies with the interaction strategy between the MPLS and WDM layer control planes. We implemented two interaction strategies that can be applied under different interoperation models.

6.1.1   Interaction Strategy 1 (IS1)

In Interaction Strategy 1 (IS1), the MPLS layer control plane has no information on the WDM layer. It generates the initial topology by requesting establishment of random lightpaths one by one from the WDM layer until the resulting topology is connected.

The utilized tie-breaker function is the number of lightpaths in the WDM layer virtual topology. For each candidate move, VTDT calculates the number of lightpaths in the resulting virtual topology. During sorting of the candidate moves, among two moves resulting with a topology giving the same objective function value, the one with the smaller number of lightpaths is placed before the other. Also when recording the final solution, if there are multiple solutions with the highest objective value, the one with the smallest number of lightpaths is recorded as the final solution. This interaction model is suitable to apply under the overlay interoperation model since no physical layer information is shared with the MPLS layer.

6.1.2   Interaction Strategy 2 (IS2)

In the second strategy, Interaction Strategy 2 (IS2), at the beginning of the algorithm the VTDT receives the connectivity information of the physical topology, from the WDM layer control plane. Using this information, it calculates the minimum physical hop distances between each node pair. The initial topology is

generated by setting up lightpaths between nodes that are single hop away from each other. The resulting initial topology has the same connectivity with the physical layer topology.

The tie-breaker function used in this strategy is the sum of physical hop distances between the nodes of the lightpaths on the resulting topology. It can be expressed as $\sum_{\{i,j\}\in L} l_{min}(i,j)$, where L is the set of lightpaths in the resulting topology of the move and $l_{min}(i,j)$ denotes the hop distance between nodes i and j in the physical layer topology.

When the candidate set of moves is being sorted, among two moves resulting with topologies giving the same objective function value, the one with the smaller tie-breaker function value is placed before the other. The aim of this strategy is to prefer opening lightpaths between the nodes which are closer in the physical topology, in terms of hop counts. This approach disfavors opening lightpaths that traverse a large number of fiber links and helps to provide a more efficient usage of the physical layer resources.

This interaction strategy can be applied under augmented and peer inter-operation models, because the WDM layer shares the connectivity information with the MPLS layer.

6.2 Simulation Setting

The blocking and resource usage performance of COLD, when used with the developed strategies, is investigated by simulations under various scenarios. The topology design algorithm employed by VTDT utilizes the available capacity in the network in the most efficient way, by assigning different paths to the traffic flows for different time periods, according to the changing traffic conditions. As a result, it is best suited to WANs whose nodes are spread over a large geographical

area and the busiest hour is not the same for all the traffic flows in the network. NSFNET topology [99] with 21 links and 14 nodes spread over four different time zones, satisfies this criterion and is commonly used in the literature. Therefore we run our simulations on the NSFNET topology which is presented in Section A.4 of Appendix. The physical layer parameters for the nodes and links of the topology are chosen as given in Table 5.1 of Section 5.3.1. The link lengths are calculated from the geographical distances between the nodes.

6.3   Traffic Generation

The traffic is generated using the same method introduced in Section 3.1. This method considers the user activity changing with the time of day and the populations of the cities, the nodes in the network are associated with. In Wide Area Networks (WANs) spreading over a large geographical area, the traffic between a node pair depends on the time zones of the nodes. For each node i, a time zone offset τ_i and a traffic generation rate $tgen_i$, representing the population, are defined. To generate the traffic flows, an activity function $act(i,t)$ depending on these values is defined as:

$$act(i,t) = \begin{cases} \sqrt{0.1} & \text{if } t_{local}(i,t) \in [0:00;6:00) \\ 1 - (1 - \sqrt{0.1}) \left(cos \left(\frac{(t_{local}(i,t)-6)\pi}{18} \right) \right)^{10} & \text{if } t_{local}(i,t) \in [6:00;24:00) \end{cases}$$

$$(6.1)$$

In this formula, $t_{local}(i,t)$ is the local time at node i in hours, which depends on the time zone of the node and the universal coordinated time t. The expected instantaneous traffic of a traffic flow between nodes i and j at time t is calculated as

(a) the same time zone (b) 4 hours time zone difference
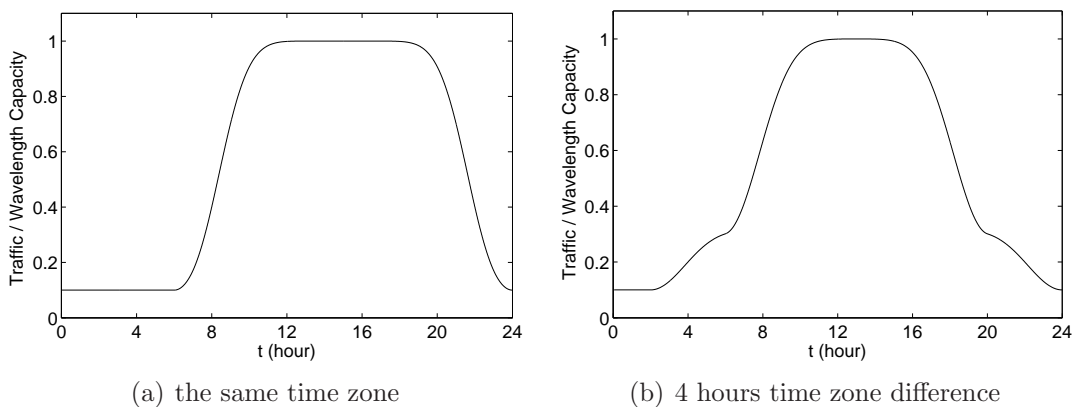
Figure 6.2: Traffic between two nodes

$$T_{\text{expected}}(i, j, t) = tgen_i \times act(i, t) \times tgen_j \times act(j, t). \qquad (6.2)$$

Figure 6.2(a) and 6.2(b) represents two traffic flows for two node pairs with traffic generation rates ($tgen$) equal to square root of the wavelength capacity. The nodes are in the same time zone in Figure 6.2(a). In Figure 6.2(b), they have a time zone difference of 4 hours which corresponds to the largest longitude difference between two nodes in the NSFNET topology.

In a real life scenario, the traffic generated from and destined to a node may depend on other factors such as the industrial and commercial activities and the frequency of internet usage among the population. To represent this effect, in our simulations we define a unit traffic generation rate, $tgen_u$, and the traffic generation rate of each node is chosen by adding a random variable to $tgen_u$ between $\pm 10\%$ of $tgen_u$ for each simulation case. Simulations are run for various values of $tgen_u^2/W_C$ between 0.15 and 0.2, where W_C is the wavelength capacity. 5 simulation instances are run for each value and their average is taken for performance and resource usage statistics.

In the simulations, two different values are used for the number of wavelengths per fiber-optic link, $|W| = 4$ and 8. To keep the ratio of the traffic amount to

the capacity the same, while a single traffic flow is generated between each node pair for $|W| = 4$ and two traffic flows are generated per node pair for $|W| = 8$.

6.3.1 Scenario 1: Uniform Physical Impairment Characteristics

The interaction strategies are first evaluated for a scenario in which all the nodes and links in the network have the same physical layer characteristics. The aim is to evaluate the effect of sharing of physical topology information between the MPLS and WDM layers.

6.3.2 Scenario 2: Non-Uniform Fiber-optic Links

In this scenario, the PMD coefficient (D_{PMD}) of each link is determined randomly. According to real life measurements fibers have D_{PMD} values between 0.01-10 $ps/\sqrt{km}$, for modern fibers it is typically lower than 0.1 $ps/\sqrt{km}$ [89]. In this scenario, D_{PMD} value of each fiber is chosen among the values 0.1, 0.2 and 0.4 $ps/\sqrt{km}$, randomly.

6.3.3 Scenario 3: Non-Uniform Switch Crosstalk Ratios

In the utilized model, switch crosstalk is the most significant contributor for the noise related penalty. Its effect on the lightpath establishment performance of the WDM layer was investigated in Section 5.3.3 and it was shown that the ratio of successfully established lightpaths changes with the switch crosstalk ratio (X_{SW}) for the values between -25 dB and -35 dB. In this scenario, the X_{SW} value of each node is chosen randomly within this range.

6.3.4 Simulation Results

The bandwidth blocking ratios for IS1 and IS2 interaction strategies in scenario 1 are given in Figures 6.3(a) and 6.3(a) for $|W|$=4 and $|W|$=8, respectively. As it can be seen from the results, IS2 has a lower blocking ratio than IS1, and the difference is more significant for $|W|$=8. IS2 achieves this by using the physical topology information and preferring to setup lightpaths between nodes that are closer in the physical topology, in terms of number of hops. Figures 6.4(a) and 6.4(b) represents the average lightpath lengths for IS1 and IS2.

(a) for $|W| = 4$ (b) for $|W| = 8$
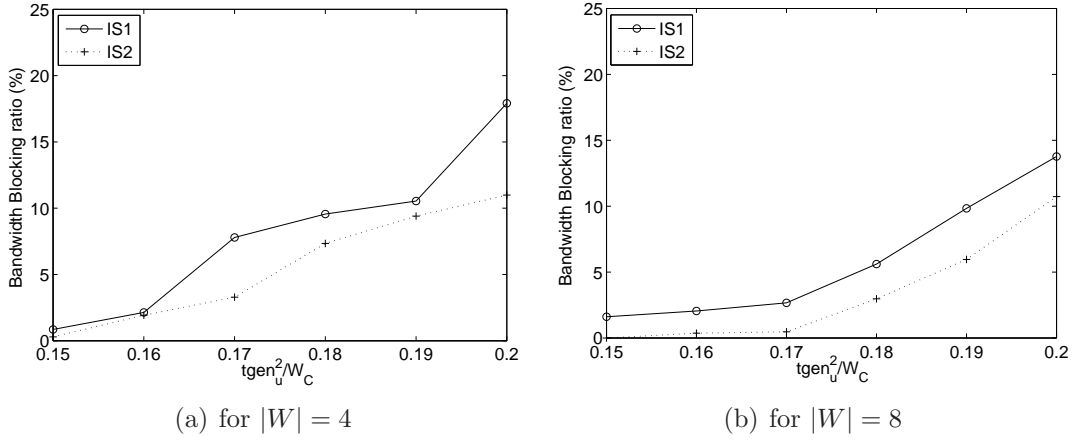
Figure 6.3: Bandwidth blocking ratio of Interaction Strategies IS1 and IS2 in Scenario 1

(a) for $|W| = 4$ (b) for $|W| = 8$
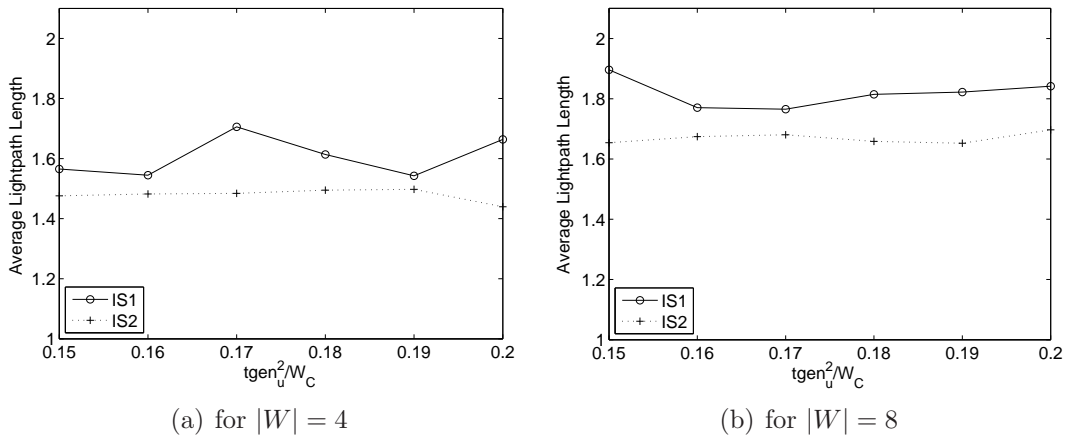
Figure 6.4: Average lightpath length for Interaction Strategies IS1 and IS2 in Scenario 1

The WDM layer cost of the virtual topologies generated by COLD using IS1 and IS2 strategies are also investigated. The considered cost metric is the amount

(a) for $|W| = 4$ (b) for $|W| = 8$
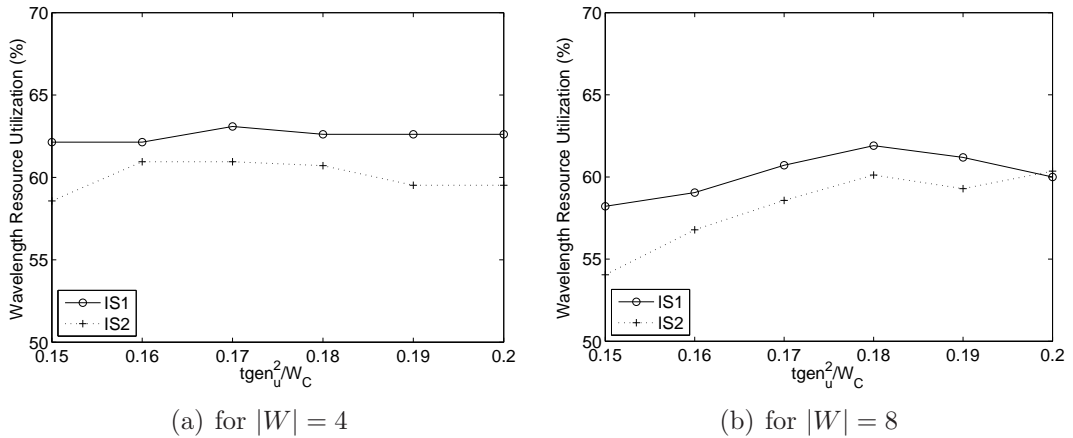
Figure 6.5: Wavelength resource usage of Interaction Strategies IS1 and IS2 in Scenario 1

of utilized wavelength resources. This value is the total number of wavelengths occupied by the established lightpaths, in all the optical fibers in the physical topology. The percentage value for this metric is calculated by taking its ratio to the total available wavelength resources in the physical topology, which is the product of number of wavelengths and number of fiber-optic links in the physical topology. The percentage of utilized wavelength resources by IS1 and IS2 are given in Figures 6.5(a) and 6.5(b) for $|W|=4$ and $|W|=8$, respectively. As it is seen from the results, IS2 uses less wavelength resources and therefore the topologies it generates have smaller cost for the WDM layer. The reason for lower resource usage is the fact that IS2 sets up shorter lightpaths in terms of number of hops.

We also calculated the average number of lightpaths in the topologies produced by ROLE using the two interaction strategies. Since optical ports should be deployed on the MPLS routers at the start and end of each lightpath, the number of lightpaths determines the total cost of optical ports. This value reflects the cost of the established virtual topology, to the MPLS layer operator. The same values are calculated also in scenario 2 and scenario 3, in which non-uniform physical impairments are assumed in the fibers and nodes, respectively. The results are given in Figures 6.7(a)-6.10(b) for scenarios 2 and 3.

(a) for $|W| = 4$ (b) for $|W| = 8$
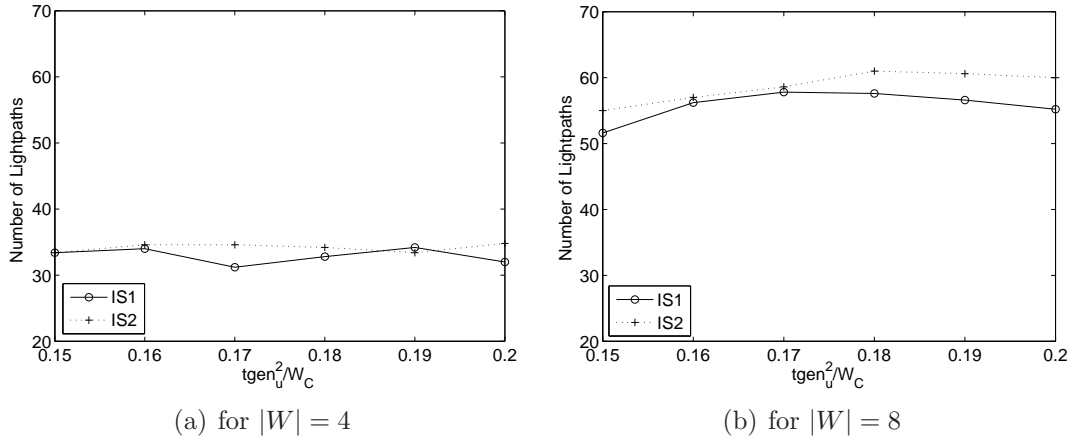
Figure 6.6: Average number of lightpaths established with Interaction Strategies IS1 and IS2 in Scenario 1

(a) for $|W| = 4$ (b) for $|W| = 8$
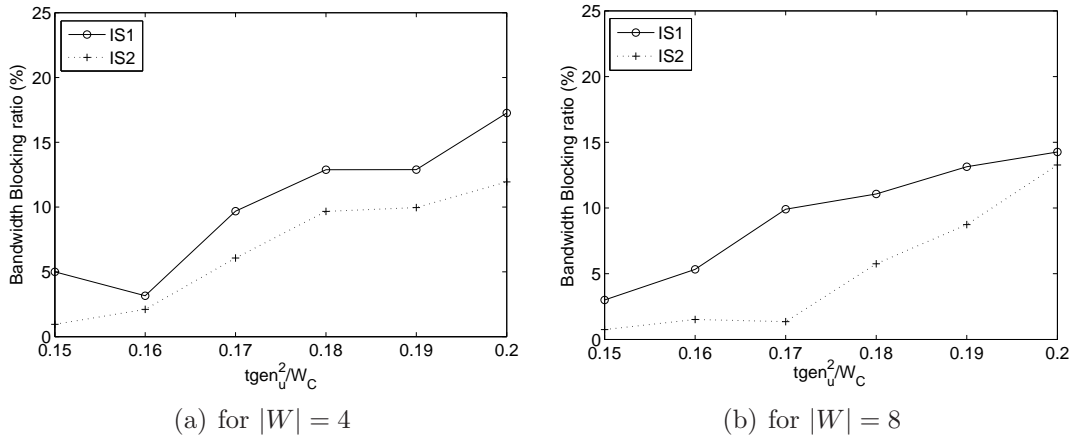
Figure 6.7: Bandwidth blocking ratio of Interaction Strategies IS1 and IS2 in Scenario 2

The results show that the bandwidth blocking ratio is higher for non-uniform physical layer impairments. For non-uniform PMD coefficient, this increase is smaller than in the case of non-uniform X_{sw}. As stated in Chapter 5, switch crosstalk is the most dominant physical layer impairment with the chosen parameters. Due to the non-uniform distribution, some nodes in the network have high X_{sw} value and this decreases the number of lightpaths that can be established, as a result bandwidth blockings increase. This is verified by the results presented in Figures 6.9 and 6.10, which show that the average number of established lightpaths is significantly smaller for non-uniform distribution of X_{sw}. The resource utilization is also smaller as Figures 6.11 and 6.12 show, since less
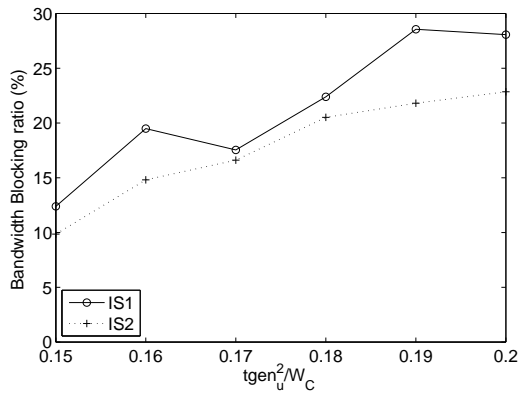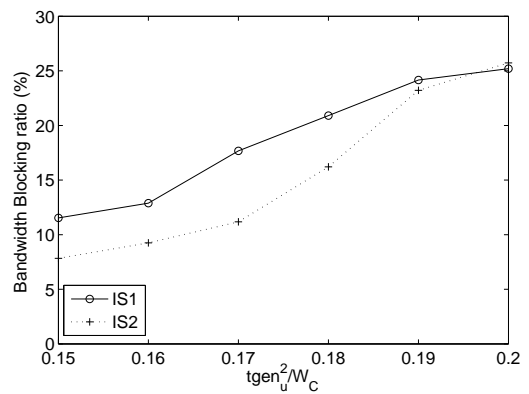
(a) for $|W| = 4$ (b) for $|W| = 8$

Figure 6.8: Bandwidth blocking ratio of Interaction Strategies IS1 and IS2 in Scenario 3
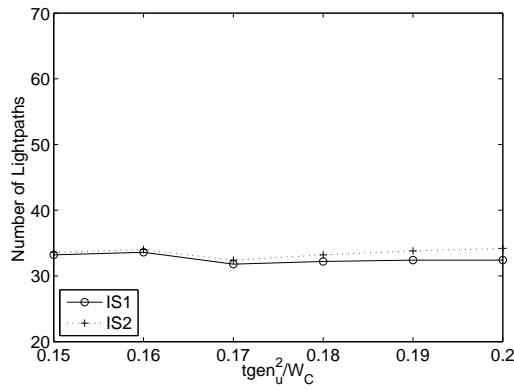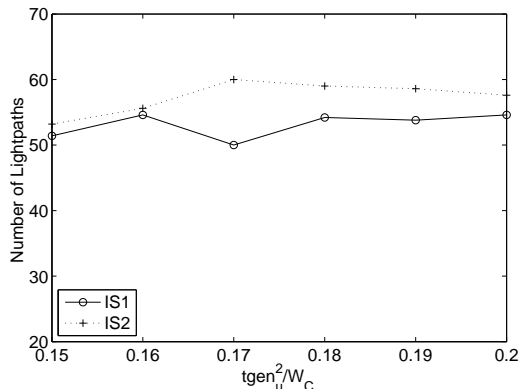
(a) for $|W| = 4$ (b) for $|W| = 8$

Figure 6.9: Average number of lightpaths established with Interaction Strategies IS1 and IS2 in Scenario 2
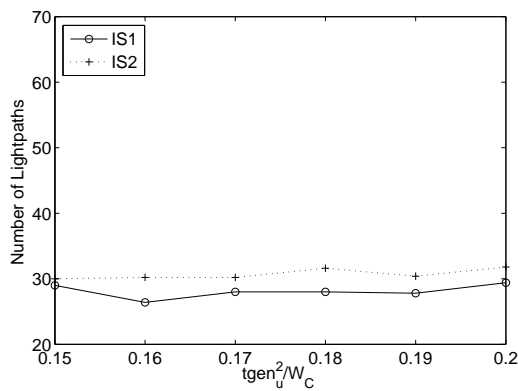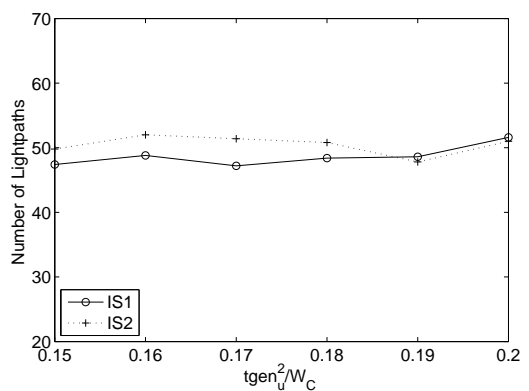
(a) for $|W| = 4$ (b) for $|W| = 8$

Figure 6.10: Average number of lightpaths established with Interaction Strategies IS1 and IS2 in Scenario 3
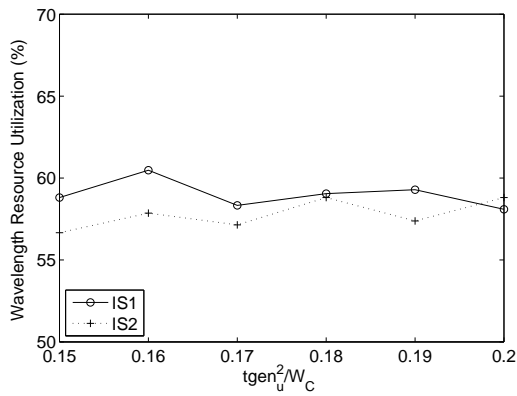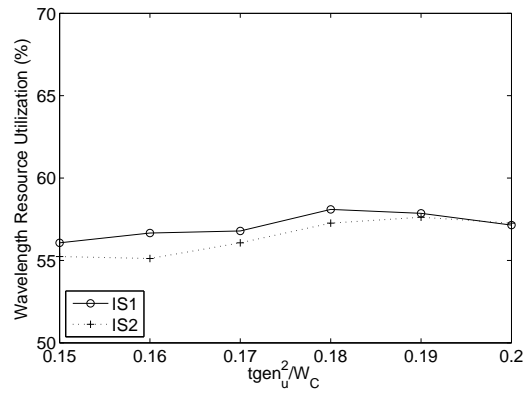
(a) for $|W| = 4$

(b) for $|W| = 8$

Figure 6.11: Wavelength resource usage of Interaction Strategies IS1 and IS2 in Scenario 2
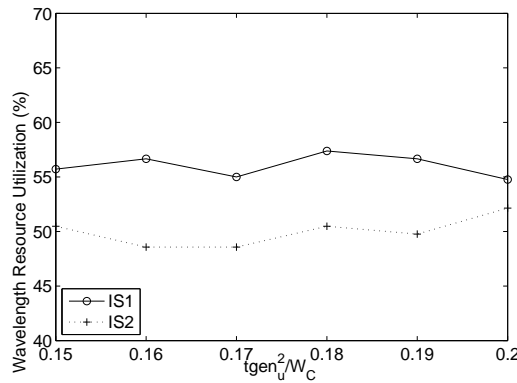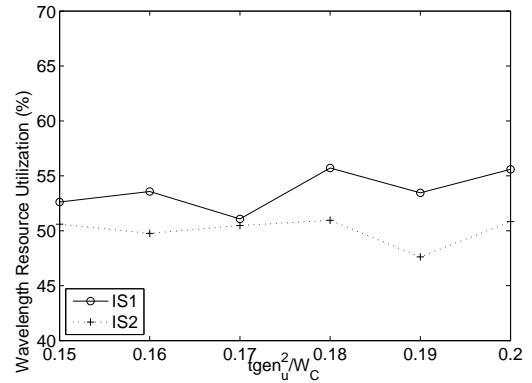
(a) for $|W| = 4$

(b) for $|W| = 8$

Figure 6.12: Wavelength resource usage of Interaction Strategies IS1 and IS2 in Scenario 3
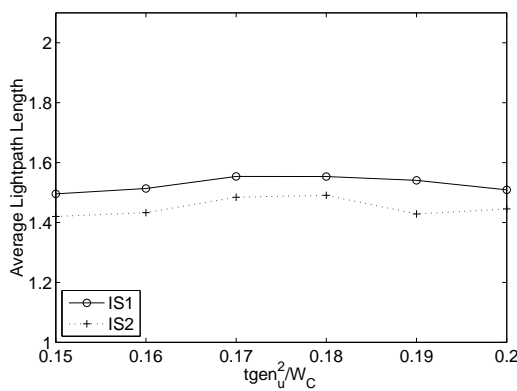
(a) for $|W| = 4$
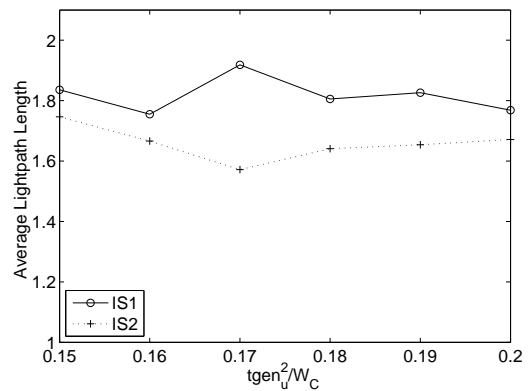
(b) for $|W| = 8$

Figure 6.13: Average lightpath length for Interaction Strategies IS1 and IS2 in Scenario 2

(a) for $|W| = 4$ (b) for $|W| = 8$
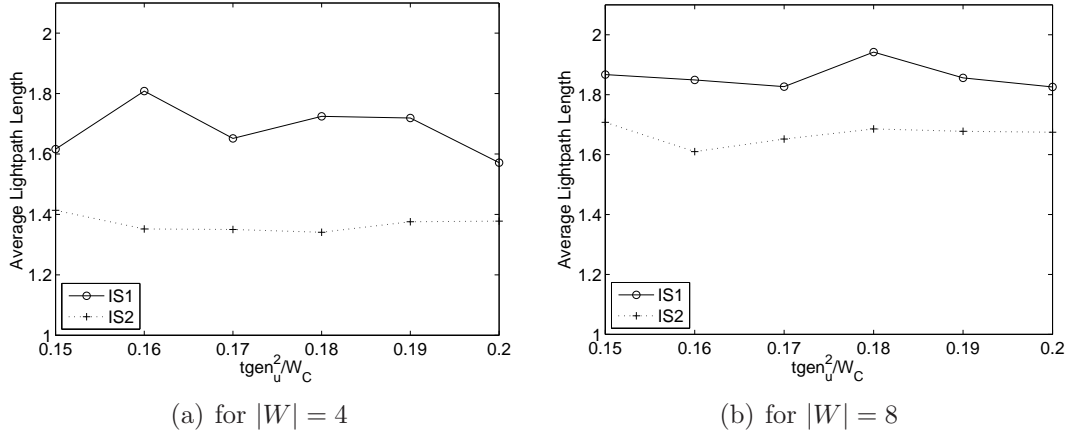
Figure 6.14: Average lightpath length for Interaction Strategies IS1 and IS2 in Scenario 3

lightpaths can be established. The average hop length of the established lightpaths is not effected much, since this value is already between 1 and 2 (Figures 6.13 and 6.15).

Using Impairment Information in MPLS Layer

In this part, we investigate whether the performance of COLD TE scheme can be increased further by making use of the physical layer impairment information in the MPLS layer. To this aim, we implemented two different interaction strategies, IS3 and IS4 for scenarios 2 and 3, respectively. These interaction strategies are similar to strategy IS1, but they use different tie-breaker functions. In Interaction Strategy 3 (IS3), the VTDT receives the connectivity information and the length and PMD coefficient for each fiber optic link in the physical topology, from the WDM layer control plane. Using this information, it calculates a least PMD path for each node pair. To calculate the least PMD path, link weights are chosen as $D_p \cdot l_{phy}$, where D_p is the PMD coefficient and l_{phy} is the physical length of the corresponding fiber-optic link, and Dijkstra's shortest path algorithm is run. To calculate the tie-breaker function value, IS3 takes the summation of the costs of the least PMD paths between the source and destination nodes of the lightpaths in the virtual topology. In Interaction Strategy 4 (IS4), the VTDT uses the

switch crosstalk ratio information in the tie-breaker function. To calculate the tie-breaker function value of a move, IS4 takes the summation of the switch crosstalk values of the source and destination nodes of each lightpath in the resulting virtual topology.

Solutions generated by IS2 and IS3 are compared in scenario 2 and solutions generated by IS2 and IS4 are compared in scenario 3. The blocking performances and resource usage statistics of IS3 and IS4 are very similar to that of IS2. The bandwidth blocking ratios for $|W| = 8$ are given in Figures 6.15(a) and 6.15(b) for scenarios 2 and 3, respectively. In some cases, IS3 and IS4 were able to generate better solutions than IS2, but the reverse is also true and their overall performances are quite similar. The performance similarity can be explained by the fact that both algorithms start from the same initial topology and the objective function is the same for both of them. Moreover, since the physical impairments are cumulative, in most of the cases a shorter lightpath will accumulate less physical impairments than a longer one. Therefore, both approaches converge to similar solutions. Another fact is that, the physical layer impairments are already considered by the WDM layer control plane. Whichever of the interaction strategies is used, if the topology requested by VTDT is not feasible, WDM layer will send a negative reply and the first feasible topology in the constructed set will be established. Therefore using the physical layer impairment information directly in the MPLS layer virtual topology design algorithm does not increase the performance of the COLD TE scheme further.
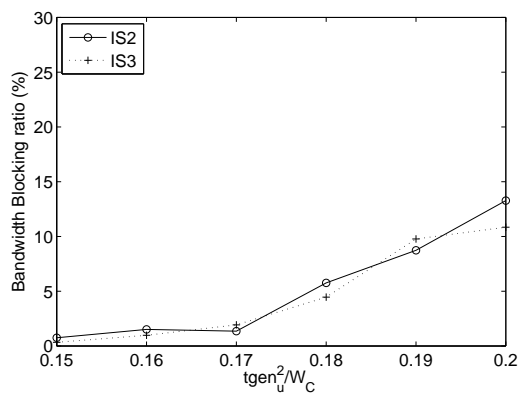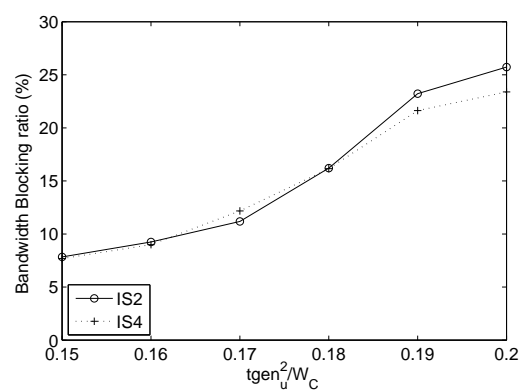
(a) in scenario 2   (b) in scenario 3

Figure 6.15: Bandwidth blocking ratios of the interaction strategies for $|W| = 8$

Chapter 7

Conclusions and Future Work

In this thesis, we have proposed a multi-layer solution for traffic engineering in MPLS/WDM networks. The proposed traffic engineering scheme consists of a dynamic rerouting mechanism that is employed in the MPLS layer and a multi-layer TE scheme that solves the Multi-layer Virtual Topology Design (MVTD) problem.

The dynamic rerouting method proposed for the MPLS layer aims to compensate the instantaneous traffic fluctuations. It can be run in a distributed fashion. Since each LSP is rerouted at random times and independently from the other LSPs, the reroutings can be performed using the 'make before break' functionality of MPLS and thus without disrupting traffic flows. We developed a dynamic rerouting algorithm, DREAM, that uses a specially designed cost function and showed that it outperforms well known widest shortest path first and available shortest path first algorithms commonly used in the literature, in terms of bandwidth blocking ratio.

In our solution to the MTVD problem, we assume a static virtual topology in the WDM layer. We consider a multi-hour traffic pattern and assume that the traffic information is available beforehand, in the form of traffic matrices

representing the expected traffic between each source destination pair, in each hour. The resulting problem is the multi-hour MVTD problem, which involves deciding the lightpaths of the virtual topology, routes of the LSPs on the virtual topology and the routes and wavelengths of the lightpaths in the physical layer. Even the single hour and single layer version of this problem, in which the WDM layer constraints are not considered is NP complete. Therefore, we used a decomposition approach to cope with the huge computational burden of the combined solution for real-life networks.

In our solution method, the complete MVTD problem is decomposed into two sub-problems: Single Layer Virtual Topology Design (SVTD) that corresponds to the MPLS layer and Static Lightpath Establishment (SLE) problem that is solved in the WDM layer. First, we developed independent solution methods for each of these single layer sub-problems. Then, we combined these solution methods in a multi-layer TE scheme to solve the VTD problem in both layers jointly.

SVTD problem is known to be NP-complete and reaching the optimum solutions is not possible except for small problem sizes. We investigated two versions of the SVTD problem, resource oriented and performance oriented. We proposed heuristic solutions utilizing Tabu Search meta-heuristic, for both versions. We also developed ILP formulations allowing splitting of flows, to produce lower bounds for the resource oriented and upper bounds for the performance oriented version. We evaluated the performances of the proposed heuristics by the bounds produced by solving the ILP formulations. The heuristic proposed for the resource oriented version of the problem produced solutions with 10% gap with the lower bounds; and the one proposed for the performance oriented version produced solutions with 7% gap with the upper bounds. Since the bounds are calculated by allowing the traffic flows to be split, the proposed algorithm can be said to produce quite good solutions.

In MVTD, the problem corresponding to the WDM layer is the SLE problem. When solving the SLE problem, along with the capacity and wavelength continuity constraints, we also consider the Bit Error Rate (BER) constraints due to physical layer impairments such as attenuation, polarization mode dispersion and switch crosstalk. The SLE problem is NP-complete even without the BER constraints. We developed a heuristic solution method, ROLE algorithm, and an exact ILP formulation to evaluate the performance of the proposed method for small problem sizes. According to the numerical results, our proposed method produces solutions close to the optimum solutions for the cases in which the ILP formulation could be solved to optimality. We also implemented a heuristic solution, POLIO-RWA, which is recently proposed and shown to outperform other heuristic solutions in the literature. The simulation results show that ROLE can establish up to 14% more lightpaths than the proposed heuristic.

Then, these solution methods for the single layer sub-problems are combined in a multi-layer TE scheme to solve the VTD problem in both layers jointly. The proposed multi-layer TE scheme can be realized by tools that are run by the MPLS and WDM layer management or control planes and communicate with each other. Therefore, it can be employed in all interoperation models by keeping each layer's information hidden from the other layer. However, the simulations show that it can produce more effective and efficient solutions when the physical layer topology information is shared with the MPLS layer, which is suitable to the augmented and peer interoperation models.

We also investigated the effect of non-uniform optical components in terms of impairment characteristics. We implemented two different scenarios for this aim. In the first scenario, the PMD coefficients of the fibers are chosen in a non-uniform manner, in the second scenario the switch crosstalk ratios (X_{sw}) of the switches are non-uniform. In both scenarios, the blocking ratios were higher compared to the case of uniform impairments, but they were even higher in the

second scenario. This is an expected result since the BER calculations in Chapter 6 showed that switch crosstalk is the most dominant physical layer impairment. The results suggest that more traffic can be routed when all the components in the network have moderate impairment characteristics, compared to the case in which some components have better and some have worse impairment characteristics.

When developing the dynamic rerouting method, DREAM, we assumed that the changes in the link capacities are disseminated to all the nodes in the network instantly, as a result the route calculations are done always with correct link state information. However, this is not usually the case in real networks. The link state information in the nodes may not always be accurate. The investigation of the performance of DREAM in such cases may be the subject of a future study. In this study, we did not consider protection and restoration issues when designing the virtual topologies. Extension of the proposed virtual topology design algorithms to cover these issues may also be a possible future study topic. Furthermore, the utilized physical layer model in this study does not include non-linear impairments such as FWM, SPM and XPM. Accuracy of the physical layer model can be increased with the inclusion of these effects, which also can be studied as a future work.

Other assumptions we have made in this study are, the designed WDM layer virtual topology is static and the traffic demand matrices are known beforehand. In scenarios where there is no available information on the traffic demands, a large amount of overprovisioning would be required when designing a static topology, and even with that large amount of overprovisioning, a significant part of the offered traffic could be lost. The proposed multi-layer TE scheme in this study does not cover such scenarios. In such cases, and in scenarios where the traffic information is highly inaccurate, dynamic lightpath provisioning would be a

requirement in order to use the network resources efficiently and improve the performance of the network.

Appendix A

Topologies Used in This Thesis

A.1 Virtual Topologies in Chapter 3

In this section, the virtual topologies used in Chapter 3 and designed by the Tabu Search based heuristics in that chapter are given. The virtual topologies have 10 nodes, the number of links is different for each topology. The links are bi-directional. 14 link topology is used in the simulations in Section 3.3.2 and link capacity is $4tgen^2$. 23 link topology is used in the simulations in Sections 3.3.2 and 3.3.3, link capacity is $2tgen^2$. 17 node topology is used in the simulations in Sections 3.3.4 and 3.3.5, link capacity is $3tgen^2$. The link information is given in Table A.1.

Table A.1: Link information for the virtual topologies (L: Link index, S: source node, D: destination node)

(a) 14 link topology

L	S	D
1	1	3
2	1	5
3	1	9
4	1	10
5	2	8
6	2	9
7	3	7
8	4	7
9	4	9
10	5	7
11	6	7
12	6	9
13	7	8
14	7	9

(b) 17 link topology

L	S	D
1	1	2
2	1	3
3	1	4
4	1	5
5	1	9
6	1	10
7	2	3
8	2	5
9	2	8
10	3	4
11	3	5
12	3	6
13	3	10
14	4	5
15	4	7
16	5	7
17	6	7
18	6	8
19	6	9
20	7	8
21	7	10
22	8	9
23	9	10

(c) 23 link topology

L	S	D
1	1	2
2	1	4
3	1	10
4	2	3
5	2	5
6	2	8
7	3	4
8	3	9
9	4	6
10	4	7
11	5	6
12	5	7
13	6	8
14	6	9
15	7	10
16	8	10
17	9	10

A.2 Physical Topology in Chapter 4

A 10 node topology with 12 links is used in the simulations in Section 4.2. The link information is given in Table A.2.

Table A.2: Link information for physical topology in Section 4.2 (L: Link index, S: source node, D: destination node)

L	S	D
1	1	2
2	2	3
3	2	4
4	4	5
5	4	9
6	5	6
7	6	7
8	6	9
9	7	8
10	7	10
11	8	9
12	9	10

A.3 Physical Topologies in Chapter 5

In this section, the physical topologies used in Chapter 5 are given.

A.3.1 20 Node Topologies

Four randomly generated physical topologies with 20 node with different number of links are used in Sections 5.3.3. Multiple fibers are installed on some of the links. Each link has a length of 500 km. The link information is given in Tables A.3 and A.4.

Table A.3: Link information for physical Topologies 1 and 2 (L: Link index, S: source node, D: destination node)

(a) Topology 1

L	S	D	# of Fibers
1	1	4	1
2	1	7	1
3	1	18	1
4	2	7	1
5	2	16	1
6	3	5	1
7	3	8	1
8	3	15	1
9	3	19	1
10	3	20	1
11	4	9	1
12	4	16	1
13	5	11	1
14	6	19	1
15	7	10	1
16	7	15	1
17	8	14	1
18	9	10	1
19	10	11	1
20	10	15	1
21	12	14	1
22	12	17	1
23	13	17	1
24	14	19	1
25	17	18	1

(b) Topology 2

L	S	D	#of Fibers
1	1	3	1
2	1	5	1
3	1	6	1
4	2	3	1
5	2	14	1
6	2	15	1
7	3	7	1
8	3	15	1
9	4	6	1
10	4	14	1
11	5	14	1
12	5	16	1
13	6	7	1
14	6	9	1
15	6	11	1
16	6	16	1
17	6	18	1
18	8	9	1
19	9	18	1
20	10	15	1
21	10	20	1
22	11	12	1
23	11	19	1
24	11	20	1
25	12	13	1
26	12	15	1
27	12	17	1
28	12	19	1
29	15	18	1
30	18	20	1

Table A.4: Link information for physical Topologies 3 and 4 (L: Link index, S: source node, D: destination node)

(a) Topology 3

L	S	D	# of Fibers
1	1	3	1
2	1	7	1
3	1	14	1
4	1	17	1
5	2	5	1
6	2	6	1
7	2	14	1
8	3	10	1
9	3	11	1
10	3	14	1
11	4	5	1
12	4	7	1
13	4	14	1
14	5	12	1
15	5	20	1
16	6	12	1
17	6	14	1
18	7	8	1
19	7	11	1
20	7	15	1
21	7	17	1
22	8	9	1
23	8	10	1
24	8	12	1
25	8	13	1
26	9	12	1
27	10	12	1
28	10	18	1
29	11	18	2
30	11	19	1
31	12	15	1
32	14	16	1
33	14	17	1
34	16	20	1

(b) Topology 4

L	S	D	#of Fibers
1	1	4	1
2	1	9	1
3	2	3	1
4	2	5	2
5	2	14	1
6	2	17	1
7	3	9	1
8	3	11	1
9	3	12	1
10	3	13	1
11	3	15	1
12	3	17	2
13	4	10	1
14	4	14	1
15	4	18	2
16	5	7	1
17	5	9	1
18	5	14	1
19	6	7	1
20	6	16	1
21	6	18	1
22	7	17	1
23	8	15	1
24	9	20	2
25	9	14	1
26	10	17	1
27	10	16	1
28	11	15	1
29	12	15	1
30	14	15	1
31	15	20	1
32	16	18	1
33	16	19	1
34	17	19	1
35	18	19	1
36	18	20	1

Table A.5: Link information for physical Topologies 5-7 (L: Link index, S: source node, D: destination node)

(a) Topology 5

L	S	D	# of Fib.
1	1	8	2
2	1	10	1
3	2	10	1
4	3	6	2
5	3	9	1
6	4	5	1
7	5	6	1
8	5	8	1
9	5	10	1
10	7	9	1
11	9	10	1

(b) Topology 6

L	S	D	#of Fib.
1	1	3	1
2	1	5	1
3	1	6	1
4	2	3	1
5	3	4	1
6	3	5	1
7	4	5	1
8	4	6	2
9	4	8	1
10	5	9	1
11	5	10	1
12	6	7	1
13	7	8	3

(c) Topology 7

L	S	D	#of Fib.
1	1	3	1
2	1	5	1
3	1	8	1
4	1	10	1
5	2	3	2
6	2	6	1
7	2	7	1
8	2	10	1
9	3	7	1
10	4	5	1
11	4	8	2
12	4	10	1
13	5	7	1
14	6	8	2
15	6	10	2
16	7	9	1

A.3.2 10 Node Topologies

Three randomly generated physical topologies (Topologies 5-7) with 10 node with different number of links are used in Sections 5.3.3. Multiple fibers are installed on some of the links. Each link has a length of 500 km. The link information is given in Table A.5.

A.3.3 Deutsche Telekom (DTAG) Network Topology

The Deutsche Telekom (DTAG) topology [98] used in the simulations in Section 5.3.3 is presented in Figure A.1. The link information is given in Table A.6. A single fiber is installed on each link. The link information is given in Table A.6.
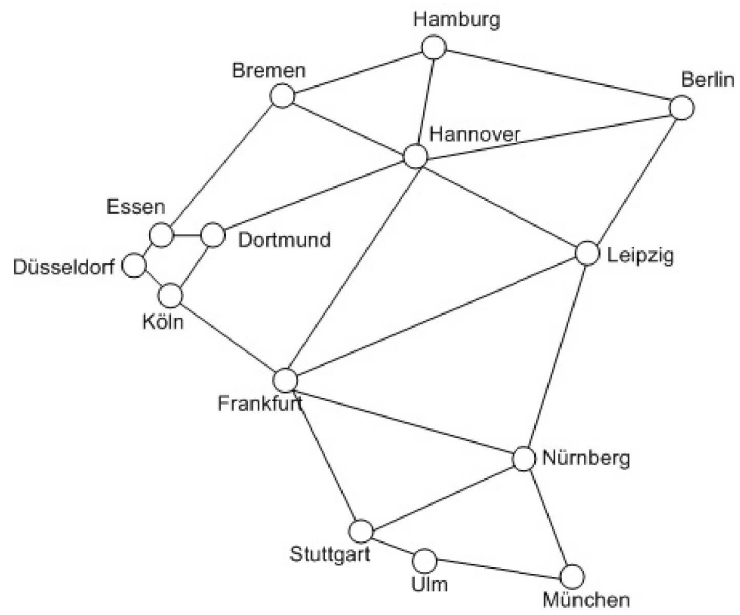
Figure A.1: Deutsche Telekom network topology

A.4 Physical Topology in Chapter 6

The NSFNET topology [99] used in the simulations in Chapter 6 is presented in
Figure A.2. The link information is given in Table A.7. A single fiber is installed
on each link.

Table A.6: Link information for the Deutsche Telekom (DTAG) topology

Link ID	Source	Destination	Length (km)
1	Hamburg	Bremen	299
2	Hamburg	Hannover	230
3	Hamburg	Berlin	95
4	Bremen	Essen	199
5	Bremen	Hannover	190
6	Berlin	Hannover	207
7	Berlin	Leipzig	37
8	Hannover	Leipzig	287
9	Hannover	Dortmund	180
10	Hannover	Frankfurt	149
11	Dortmund	Essen	164
12	Essen	Dusseldorf	126
13	Dortmund	Koln	277
14	Dusseldorf	Koln	320
15	Koln	Frankfurt	330
16	Leipzig	Frankfurt	187
17	Leipzig	Nurnberg	240
18	Frankfurt	Stuttgart	90
19	Frankfurt	Nurnberg	353
20	Nurnberg	Stuttgart	49
21	Stuttgart	Ulm	127
22	Munchen	Ulm	264
23	Munchen	Nurnberg	44
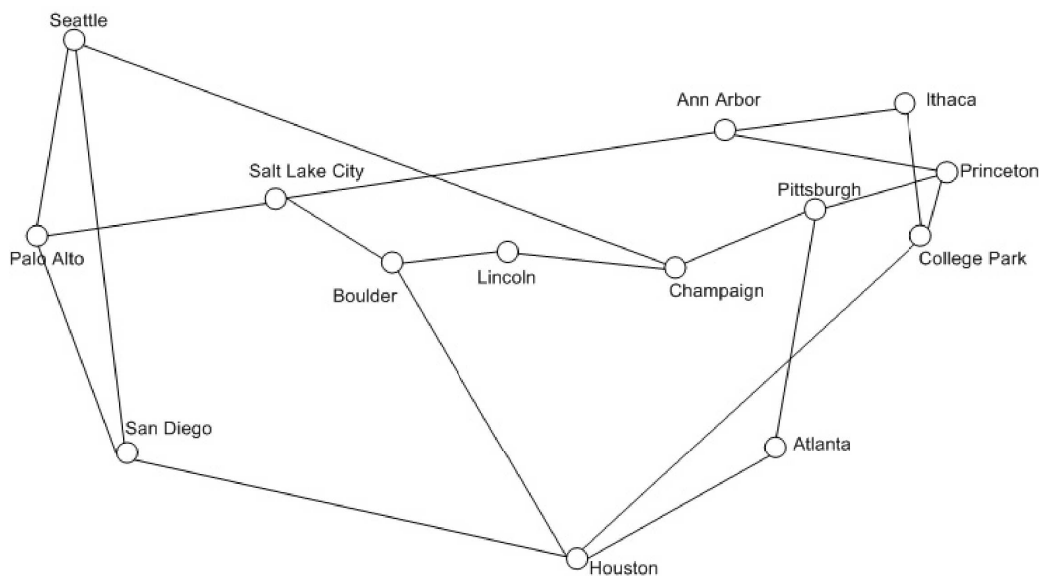
Figure A.2: NSFNET topology

Table A.7: Link information for the NSFNET topology

Link ID	Source	Destination	Length (km)
1	Lincoln	Boulder	733
2	Salt Lake City	Palo Alto	955
3	Salt Lake City	Ann Arbor	2337
4	Salt Lake City	Boulder	565.8
5	Seattle	Palo Alto	1129
6	Seattle	San Diego	1710
7	Seattle	Champaign	2828
8	Palo Alto	San Diego	692
9	San Diego	Houston	2093
10	Houston	Atlanta	1129
11	Houston	College Park	1972
12	Houston	Boulder	1452
13	Atlanta	Pitssburg	838
14	College Park	Ithaca	385
15	College Park	Princeton	246
16	Ithaca	Ann Harbor	595
17	Ithaca	Pitssburg	367
18	Princeton	Ann Arbor	788
19	Princeton	Pitssburg	451
20	Pitssburg	Champaign	700
21	Champaign	Lincoln	716

Bibliography

[1] R. Sabella and P. Iovanna, "Traffic engineering in next generation multi-layer networks based on the GMPLS paradigm," *Proc. HET-NETs 04, West Yorkshire, UK*, 2004.

[2] P. Iovanna, R. Sabella, M. Settembre, *et al.*, "A traffic engineering system for multilayer networks based on the GMPLS paradigm," *IEEE network*, p. 29, 2003.

[3] D. Awduche, A. Chiu, A. Elwalid, I. Widjaja, and X. Xiao, "RFC3272: Overview and principles of Internet traffic engineering," *RFC Editor United States*, 2002.

[4] X. Xiao, A. Hannan, B. Bailey, and L. Ni, "Traffic engineering with MPLS in the Internet," *Network, IEEE*, vol. 14, no. 2, pp. 28–33, 2000.

[5] B. Wang, X. Su, and C. Chen, "A new bandwidth guaranteed routing algorithm for MPLS traffic engineering," *Proceedings of ICC*, vol. 2, pp. 1001–1005, 2002.

[6] E. Rosen, A. Viswanathan, and R. Callon, "RFC3031: Multiprotocol label switching architecture," *Internet RFCs*, 2001.

[7] D. Awduche, J. Malcolm, J. Agogbua, M. O'Dell, and J. McManus, "Requirements for traffic engineering over MPLS," tech. rep., IETF RFC 2702, 1999.

[8] D. Awduche, L. Berger, D. Gan, T. Li, V. Srinivasan, and G. Swallow, "RSVP-TE: Extensions to RSVP for LSP tunnels," tech. rep., IETF RFC 3209, 2001.

[9] B. Rajagopalan, J. Luciani, and D. Awduche, "IP over optical networks: A framework," tech. rep., IETF RFC 3717, March 2004.

[10] J. E. Gabeiras, V. Lopez, J. Aracil, J. Palacious, C. Argos, O. Dios, F. Chico, and J. Hernandez, " Is multilayer networking feasible?," *Optical Switching and Networking*, vol. 6, no. 2, pp. 129–140, 2009.

[11] B. Chen, S. Bose, W. Zhong, and H. Wang, "A new lightpath establishing method for dynamic traffic grooming under the overlay model," *Photonic Network Communications*, vol. 17, no. 1, pp. 11–20, 2009.

[12] F. Ricciato, S. Salsano, A. Belmonte, and M. Listanti, "Off-line configuration of a MPLS over WDM network under time-varying offered traffic," *INFOCOM 2002. Twenty-First Annual Joint Conference of the IEEE Computer and Communications Societies. Proceedings. IEEE*, vol. 1, 2002.

[13] B. Fortz and M. Thorup, "Optimizing OSPF/IS-IS weights in a changing world," *IEEE Journal on Selected Areas in Communications*, vol. 2, no. 4, pp. 756–767, 2002.

[14] A. Feldmann, A. Greenberg, C. Lund, N. Reingold, J. Rexford, and F. True, "Deriving traffic demands for operational IP networks: Methodology and experience," *IEEE/ACM Transactions on Networking (TON)*, vol. 9, no. 3, pp. 265–280, 2001.

[15] A. Feldmann, J. Rexford, and R. Cáceres, "Efficient policies for carrying web traffic over flow-switched networks," *IEEE/ACM Transactions on Networking (TON)*, vol. 6, no. 6, p. 685, 1998.

[16] J. Milbrandt, M. Menth, and S. Kopf, "Adaptive bandwidth allocation: Impact of traffic demand models for wide area networks," in *19th International Teletraffic Congress (ITC19)*, (Beijing, China), 2005.

[17] D. Medhi, "Multi-hour, multi-Traffic class network design for virtual path-based dynamically reconfigurable wide-area ATM networks," *IEEE/ACM Transactions on Networking (TON)*, vol. 3, no. 6, pp. 809–818, 1995.

[18] O. Gerstel and H. Raza, "On the synergy between electrical and photonic switching," *IEEE Communications Magazine*, vol. 41, no. 4, pp. 98–104, 2003.

[19] S. Sengupta, V. Kumar, and D. Saha, "Switched optical backbone for cost-effective scalable core IP networks," *IEEE Communications Magazine*, vol. 41, no. 6, pp. 60–70, 2003.

[20] C. Assi, A. Shami, M. Ali, R. Kurtz, and D. Guo, "Optical networking and real-time provisioning: An integrated vision for the next-generation internet," *IEEE network*, vol. 15, no. 4, pp. 36–45, 2001.

[21] M. OMahony, D. Simeonidou, D. Hunter, and A. Tzanakaki, "The application of optical packet switching in future communication networks," *IEEE Communications Magazine*, p. 128, 2001.

[22] G. Karmous-Edwards, D. Reeves, G. Rouskas, L. Battestilli, P. Vegesna, and A. Vishwanath, "Edge Reconfigurable Optical Network (ERON): Enabling dynamic sharing of static lightpaths," in *5th International Conference on Broadband Communications, Networks and Systems, 2008. BROADNETS 2008*, pp. 332–334, 2008.

[23] A. Zapata and P. Bayvel, "Do we really need dynamic wavelength-routed optical networks?," *High Performance Computing and Communications, Lecture Notes in Computer Science*, vol. 4208, pp. 477–486, 2006.

[24] H. Huang and J. Copeland, "Optical networks with hybrid routing," *IEEE Journal on Selected Areas in Communications*, vol. 21, no. 7, pp. 1063–1070, 2003.

[25] O. Gerstel, G. Sasaki, S. Kutten, and R. Ramaswami, "Worst-case analysis of dynamic wavelength allocation in optical networks," *IEEE/ACM Transactions on Networking (TON)*, vol. 7, no. 6, pp. 833–846, 1999.

[26] A. Zapata, M. Düser, J. Spencer, P. Bayvel, I. Miguel, D. Breuer, N. Hanik, and A. Gladisch, "Next-generation 100-gigabit metro Ethernet (100 GbME) using multiwavelength optical rings," *Journal of Lightwave Technology*, vol. 22, no. 11, p. 2420, 2004.

[27] A. Zapata and P. Bayvel, "Dynamic vs. static lightpath allocation in WDM networks," in *31st European Conference on Optical Communication, 2005. ECOC 2005*, pp. 273–274, 2005.

[28] SURFnet, "Measuring the use of lightpath services," tech. rep., 0:13, 2007.

[29] P. Pavon-Marino, R. Aparicio-Pardo, B. Garcia-Manrubia, and N. Skorin-Kapov, "Virtual topology design and flow routing in optical networks under multihour traffic demand," *Photonic network communications*, vol. 19, no. 1, pp. 42–54, 2010.

[30] L. Gouveia, P. Patrício, A. de Sousa, and R. Valadas, "MPLS over WDM network design with packet level QoS constraints based on ILP models," in *IEEE INFOCOM 2003. Twenty-Second Annual Joint Conference of the IEEE Computer and Communications Societies*, vol. 1.

[31] K. Lee and M. Shayman, "Optical network design with optical constraints in IP/WDM networks," *IEICE Transactions on Communications*, vol. 88, no. 5, pp. 1898–1905, 2005.

[32] B. Megyer, S. Zsigmond, Á. Szödényi, and T. Cinkler, "Design of traffic grooming optical vpns obeying physical limitations," *IEEE IFIP WOCN*, 2005.

[33] K. Sivarajan and R. Ramaswami, "Design of logical topologies for wavelength-routed optical networks," *IEEE Journal on Selected Areas in Communications*, vol. 14, no. 5, 1996.

[34] S. Azodolmolky, Y. Pointurier, M. Klinkowski, E. Marin, D. Careglio, J. Solé-Pareta, M. Angelou, and I. Tomkos, "On the offline physical layer impairment aware RWA algorithms in transparent optical networks: State of the art and beyond," in *Proceedings of the 13th international conference on Optical Network Design and Modeling*, pp. 13–18, 2009.

[35] M. K. Girish, B. Zhou, and J. Q. Hu, "Formulation of the traffic engineering problems in MPLS based IP networks," in *The 5th IEEE Symposium on Computers and Communications Antibes, France*, July 2007.

[36] B. Józsa and G. Magyar, "Reroute sequence planning for label switched paths in multiprotocol label switching networks," in *IEEE Symposium on Computers and Communications, ISCC*, pp. 319–325, 2001.

[37] O. Klopfenstein, "Rerouting tunnels for MPLS network resource optimization," *European Journal of Operational Research*, vol. 188, no. 1, pp. 293–312, 2008.

[38] R. Ramaswami and K. Sivarajan, "Routing and wavelength assignment in all-optical networks," *IEEE/ACM Transactions on Networking (TON)*, vol. 3, no. 5, pp. 489–500, 1995.

[39] H. Zang, J. Jue, and B. Mukherjee, "A review of routing and wavelength assignment approaches for wavelength-routed optical WDM networks," *Optical Networks Magazine*, vol. 1, no. 1, pp. 47–60, 2000.

[40] K. Manousakis, K. Christodoulopoulos, and E. Varvarigos, "Impairment-aware offline RWA for transparent optical networks," in *Proc. IEEE Conference on Computer Communications (INFOCOM)*, pp. 1557–1565, 2009.

[41] I. Tomkos, D. Vogiatzis, C. Mas, I. Zacharopoulos, A. Tzanakaki, and E. Varvarigos, "Performance engineering of metropolitan area optical networks through impairment constraint routing," *IEEE Communications Magazine*, vol. 42, no. 8, pp. S40–S47, 2004.

[42] K. Christodoulopoulos, K. Manousakis, and E. Varvarigos, "Considering physical layer impairments in offline RWA," *IEEE Network*, vol. 23, no. 3, pp. 26–33, 2009.

[43] X. Yang, L. Shen, and B. Ramamurthy, "Survivable lightpath provisioning in WDM mesh networks under shared path protection and signal quality constraints," *Journal of Lightwave Technology*, vol. 23, no. 4, p. 1556, 2005.

[44] M. Lima, A. Cesar, and A. Araujo, "Optical network optimization with transmission impairments based on genetic algorithm," in *Proceedings of the 2003 SBMO/IEEE MTT-S International Microwave and Optoelectronics Conference*, vol. 1, 2003.

[45] D. Monoyios, K. Vlachos, M. Aggelou, and I. Tomkos, "On the use of multi-objective optimization algorithms for solving the impairment aware-rwa problem," in *IEEE International Conference on Communications*, 2009.

[46] M. Ezzahdi, S. Al Zahr, M. Koubàa, N. Puech, and M. Gagnaire, "LERP: a quality of transmission dependent heuristic for routing and wavelength assignment in hybrid WDM networks," in *Proceedings of ICCCN*, pp. 125–136, Citeseer, 2006.

[47] B. Ramamurthy, D. Datta, H. Feng, J. Heritage, and B. Mukherjee, "Impact of transmission impairments on the teletraffic performance of wavelength-routed optical networks," *Journal of Lightwave Technology*, vol. 17, no. 10, pp. 1713–1723, 1999.

[48] S. Zsigmond, B. Megyer, T. Cinkler, A. Tzanakaki, and I. Tomkos, "A new method for considering physical impairments in multilayer routing," in *Design of Next Generation Optical Networks. COST291/GBOU ONNA Workshop on*, 2006.

[49] Y. Huang, J. Heritage, and B. Mukherjee, "Connection provisioning with transmission impairment consideration in optical WDM networks with high-speed channels," *Journal of Lightwave Technology*, vol. 23, no. 3, p. 982, 2005.

[50] S. Azodolmolky, M. Klinkowski, E. Marin, D. Careglio, J. Pareta, and I. Tomkos, "A survey on physical layer impairments aware routing and wave-length assignment algorithms in optical networks," *Computer Networks*, vol. 53, no. 7, pp. 926–944, 2009.

[51] R. Dutta and G. Rouskas, "A survey of virtual topology design algorithms for wavelength routed optical networks," *Optical Networks Magazine*, vol. 1, no. 1, pp. 73–89, 2000.

[52] R. Dutta and G. Rouskas, "Traffic grooming in WDM networks: Past and future," *IEEE network*, vol. 16, no. 6, pp. 46–56, 2002.

[53] K. Zhu and B. Mukherjee, "A review of traffic grooming in WDM optical networks: Architectures and challenges," *Optical Networks Magazine*, vol. 4, no. 2, pp. 55–64, 2003.

[54] D. Banerjee and B. Mukherjee, "Wavelength-routed optical networks: Lin-ear formulation, resource budgeting tradeoffs, and a reconfiguration study," *IEEE/ACM Transactions on Networking (TON)*, vol. 8, no. 5, p. 607, 2000.

[55] T. Cinkler, D. Marx, C. Larsen, and D. Fogaras, "Heuristic algorithms for joint configuration of the optical and electrical layer in multi-hop wavelength routing networks," in *IEEE INFOCOM 2000. Nineteenth Annual Joint Conference of the IEEE Computer and Communications Societies. Proceedings*, vol. 2, 2000.

[56] R. Krishnaswamy and K. Sivarajan, "Design of logical topologies: A linear formulation for wavelength-routed optical networks with no wavelength changers," *IEEE/ACM Transactions on Networking (TON)*, vol. 9, no. 2, pp. 186–198, 2001.

[57] M. Kodialam and T. Lakshaman, "Minimum interface routing with applications to MPLS traffic engineering," *INFOCOM 2000. Nineteenth Annual Joint Conference of the IEEE Computer and Communications Societies. Proceedings. IEEE*, 2000.

[58] S. Suri, M. Waldvogel, and P. Warkhede, "Profile-based routing: A new framework for MPLS traffic engineering," *Quality of Future Internet Services, Lecture Notes in Computer Science*, vol. 2156, 2001.

[59] G. Retvari, J. J. Biro, T. Ciinkler, and T. Henk, "A precomputation scheme for minimum interference routing: the least-critical-path-first algorithm," in *IEEE INFOCOM 2005. 24th Annual Joint Conference of the IEEE Computer and Communications Societies. Proceedings*, vol. 1, 2005.

[60] J. He, M. Brandt-Pearce, Y. Pointurier, and S. Subramaniam, "QoT-aware routing in impairment-constrained optical networks," in *Proceedings of IEEE GLOBECOM*, pp. 2269–2274, 2007.

[61] J. He, M. Brandt-Pearce, Y. Pointurier, C. Brown, and S. Subramaniam, "Adaptive wavelength assignment using wavelength spectrum separation for distributed optical networks," in *IEEE International Conference on Communications, 2007. ICC'07*, pp. 2406–2411, 2007.

[62] J. He, M. Brandt-Pearce, and S. Subramaniam, "QoS-aware wavelength assignment with BER and latency guarantees for crosstalk limited networks," in *IEEE International Conference on Communications, 2007. ICC'07*, pp. 2336–2341, 2007.

[63] R. Cardillo, V. Curri, and M. Mellia, "Considering transmission impairments in configuring wavelength routed optical networks," in *OFC/NFOEC 2006, Anaheim, CA, USA*, 2006.

[64] Y. Zhai, Y. Pointurier, S. Subramaniam, and M. Brandt-Pearce, "QoS-aware RWA algorithms for path-protected DWDM networks," in *Proceedings of OFC/NFOEC*, 2007.

[65] B. Mukherjee, Y. Huang, and J. Heritage, "Impairment-aware routing in wavelength-routed optical networks," in *The 17th Annual Meeting of the IEEE Lasers and Electro-Optics Society, 2004. LEOS 2004*, pp. 428–429, 2004.

[66] X. Niu, W. Zhong, G. Shen, and T. Cheng, "Connection establishment of label switched paths in IP/MPLS over optical networks," *Photonic Network Communications*, vol. 6, no. 1, pp. 33–41, 2003.

[67] C. Assi, A. Shami, M. Ali, Y. Ye, and S. Dixit, "Integrated routing algorithms for provisioning "sub-wavelength" connections in IP-over-WDM Networks," *Photonic Network Communications*, vol. 4, no. 3, pp. 377–390, 2002.

[68] E. Oki, K. Shiomoto, D. Shimazaki, N. Yamanaka, W. Imajuku, and Y. Takigawa, "Dynamic multilayer routing schemes in GMPLS-based IP+ optical networks," *IEEE Communications Magazine*, vol. 43, no. 1, pp. 108–114, 2005.

[69] E. Oki, D. Shimazaki, and K. Shiomoto, "GTEP: generalized traffic engineering protocol for multi-layer GMPLS networks," in *Global Telecommunications Conference Workshops, 2004. GlobeCom Workshops 2004. IEEE*, pp. 357–362, Nov.-3 Dec. 2004.

[70] B. Chen, W. Zhong, and S. BOSE, "A path inflation control strategy for dynamic traffic grooming in IP/MPLS over WDM network," *IEEE Communications letters*, vol. 8, no. 11, pp. 680–682, 2004.

[71] M. Köhn, W. Colitti, P. Gurzì, A. Nowé, and K. Steenhaut, "Multi-layer Traffic Engineering (MTE) in grooming enabled ASON/GMPLS Networks," *Lecture Notes in Computer Science*, vol. 5412, pp. 237–252, 2009.

[72] C. Qiao, C. Xin, Y. Ye, S. Dixit, and C. Qiao, "An integrated lightpath provisioning approach in mesh optical networks," in *Optical Fiber Communications Conference*, p. ThW4, Optical Society of America, 2002.

[73] B. Puype, Q. Yan, D. Colle, S. De Maesschalck, I. Lievens, M. Pickavet, and P. Demeester, "Multi-layer traffic engineering in data-centric optical networks," in *COST266-IST OPTIMIST Workshop on Optical Networks, Budapest, Hungary*, 2003.

[74] J. Comellas, R. Martinez, J. Prat, V. Sales, and G. Junyent, "Integrated IP/WDM routing in GMPLS-based optical networks," *IEEE Network*, vol. 17, no. 2, pp. 22–27, 2003.

[75] M. Kodialam and T. V. Lakshman, "Integrated dynamic IP and wavelength routing in IP over WDM networks," in *In Proceedings of IEEE Infocom 2001*, pp. 358–366, 2001.

[76] T. Cinkler, P. Hegyi, M. Asztalos, G. Geleji, J. Szigeti, and A. Kern, "Multi-layer traffic engineering through adaptive lambda-path fragmentation and de-fragmentation," *Lecture Notes in Computer Science*, vol. 3976, p. 715, 2006.

[77] K. Zhu, H. Zhu, and B. Mukherjee, "Traffic engineering in multigranularity heterogeneous optical WDM mesh networks through dynamic traffic grooming," *IEEE network*, p. 9, 2003.

[78] A. Gencata and B. Mukherjee, "Virtual-topology adaptation for WDM mesh networks under dynamic traffic," *IEEE/ACM Transactions on networking*, vol. 11, no. 2, pp. 236–247, 2003.

[79] K. Sato, N. Yamanaka, Y. Takigawa, M. Koga, S. Okamoto, K. Shiomoto, E. Oki, and W. Imajuku, "GMPLS-based photonic multilayer router (Hikari router) architecture: an overview of traffic engineering and signaling technology," *IEEE Communications Magazine*, vol. 40, no. 3, pp. 96–101, 2002.

[80] N. Yamanaka, M. Katayama, K. Shiomoto, E. Oki, and N. Matsuura, "Multi-layer traffic engineering in photonic-GMPLS-router networks," in *Global Telecommunications Conference*, vol. 3, pp. 2731–2735, Nov. 2002.

[81] F. Glover and M. Laguna, *Tabu Search*. KLUWER ACADEMIC PUBL, 1997.

[82] E. Aarts and J. Lenstra, *Local search in combinatorial optimization*. Princeton Univ Pr, 2003.

[83] G. Lee, S. Xu, and Y. Tanaka, "A logical topology design with tabu search in IP over WDM optical networks," in *Asia-Pacific Conference on Communications, 2006. APCC'06*, pp. 1–5, 2006.

[84] E. Costamagna, A. Fanni, and G. Giacinto, "A tabu search algorithm for the optimisation of telecommunication networks," *European Journal of Operational Research*, vol. 106, no. 2-3, pp. 357–372, 1998.

[85] N. Sengezer, B. Puype, E. Karasan, and M. Pickavet, "A comparative study of single-layer and multi-layer traffic engineering approaches on transparent optical networks," in *9th International Conference on Transparent Optical Networks, 2007. ICTON'07*, vol. 4, 2007.

[86] P. Hegyi, T. Cinkler, N. Sengezer, and E. Karasan, "Traffic engineering in case of interconnected and integrated layers," in *Telecommunications Network Strategy and Planning Symposium, 2008. Networks 2008. The 13th International*, pp. 1–17, 2008.

[87] N. Sengezer and E. Karasan, "An efficient virtual topology design and traffic engineering scheme for IP/WDM networks," in *Proceedings of the 11th international IFIP TC6 conference on Optical network design and modeling*, pp. 319–328, Springer-Verlag, 2007.

[88] T. Cinkler, R. Castro, and S. Johansson, "Configuration and reconfiguration of WDM networks," in *NOC'98: European Conference on Networks and Optical Communications European, Manchester, UK, June 1998.*, 1998.

[89] G. Agrawal, *Fiber-optic communication systems*, ch. 2, pp. 55–59. New York: Wiley.

[90] D. DiGiovanni, D. Jablonowski, and M. Yan, "Optical fiber telecommunications, Volume IIIA," *Optical fiber telecommunications III*, pp. 63–91, 1997.

[91] G. Agrawal, *Lightwave technology: Communication systems*, ch. 9, pp. 351–356. New Jersey, USA: John Wiley & Sons, Inc.

[92] G. Agrawal, *Lightwave technology: Communication systems*, ch. 3, pp. 67–71. New Jersey, USA: John Wiley & Sons, Inc.

[93] Y. Huang, W. Wen, J. Heritage, and B. Mukherjee, "Signal-quality consideration for dynamic connection provisioning in all-optical wavelength-routed networks," *OptiComm 2003: Optical Networking and Communications (Proceedings of the SPIE), Dallas, Texas*, vol. 5285, pp. 163–173, 2003.

[94] G. Agrawal, *Fiber-optic communication systems*, ch. 3, pp. 77–81. New York: Wiley.

[95] G. Agrawal, *Fiber-optic communication systems*, ch. 4, pp. 162–164. New York: Wiley.

[96] C. Cantrell, "Transparent optical metropolitan-area networks," in *LEOS, 16th Annual Meeting*, vol. 2, pp. 608–609, 2003.

[97] W. Winston, *Operations research: Applications and algorithms.* 4 ed., 2004.

[98] "Dynamic Impairment Constraint Network for Transparent Mesh Optical Networks (DICONET) project." `http://www.diconet.eu`.

[99] K. Frazer, "NSFNET: A partnership for high-speed networking, Final Report. 1987-1995. Merit Network," 1995.